2018-01-08

Characterization of Transforming Acidic Coiled Coil Protein Three, a Protein Phosphatase One Binding Protein

Rackel, Brooke

UNIVERSITY OF CALGARY

Characterization of Transforming Acidic Coiled Coil Protein Three, a Protein Phosphatase One Binding Protein

by

Brooke Rackel

A THESIS

SUBMITTED TO THE FACULTY OF GRADUATE STUDIES

IN PARTIAL FULFILMENT OF THE REQUIREMENTS FOR THE

DEGREE OF MASTER OF SCIENCE

GRADUATE PROGRAM IN BIOLOGICAL SCIENCES

CALGARY, ALBERTA

JANUARY, 2018

Abstract

Protein phosphorylation is a key signaling mechanism utilized by cells as a means of regulating various pathways within the cell. Protein phosphatase one (PP1) is a highly conserved enzyme that catalyzes the removal of a phosphate group from serine/threonine residues in eukaryotes. PP1 gains substrate specificity through the binding of regulatory proteins, of which over 200 are currently identified in humans. Most of these subunits dock PP1 via the RVxF binding motif. Transforming acidic coiled coil protein three (TACC3) has been identified as a potential PP1 interactor through quantitative mass spectrometry and also contains an RVxF motif (KVTF). Here, I have validated the TACC3-PP1 interaction, and demonstrated that it occurs via the RVxF motif.

TACC3 is a non-motor spindle assembly protein and plays an important role in the proper segregation of chromosomes during mitosis. Due to its key role in maintaining genomic integrity, it has recently been implicated in a number of cancers. Here, I explore the expression of TACC3 mRNA in 20 cancers and the effect of aberrant TACC3 expression on patient survival from clinical data.

The work presented here increases our knowledge of PP1 and its interaction with the regulatory subunit TACC3, and also provides insight into the role TACC3 is playing in cancer.

Acknowledgements

The completion of my Master's would not have been possible without the amazing people I have in my life. First, to my supervisor and mentor, Dr. Greg Moorhead. I had the pleasure of doing my undergraduate thesis as well as my master's research in his lab and I would not be the scientist I am today if he had not taken a chance on me nearly four years ago. His patience, encouragement and guidance helped bring me to the place where I am today. Thank you for your support and for putting up with my antics throughout this journey. I would also like to thank my committee members Dr. Vanina Zaremberg and Dr. Jennifer Cobb, for pushing me to think outside of my phosphatase box and helping me to see this project in the big picture. Thank you for taking the time to meet with me and answer my relentless emails.

I have been lucky throughout my degree to be surrounded with the best, most supportive lab members both past and present. I would like to thank Dr. Isha Nasa, thank-you from the bottom of my heart for taking me on as an undergraduate and training me. I truly believe I was only able to do this because I learned from the best. I'd also like to thank Sibapriya Chaudhuri for the countless coffee and "coffee" vent sessions and for being my go to rock in the lab. Additionally, Ahmad Vahab, Nic Sieben and Dr. Anne-Marie Labandera, you guys are simply the best. You made coming into the lab everyday a pleasure and I already miss our late-night dominos orders. I also owe a huge thank-you to all the undergraduates who worked in the lab during my time there. Especially Ryan Toth, Paige Grant, Tejinder Gill, Guneet Khosa, and Chris White-Gloria, thanks for casting all the gels I didn't want to. I would also like to thank Kelly Teal and the Turner lab for the use of their lab equipment and the best hallway conversations. Additionally Dr. Pinaki Bose, for asking the question that led to my entire bioinformatics study as well as taking the time to teach me how to process the TCGA data.

Finally, my friends and family. Mom and Dad and Morgan. Seriously, what can I even say. You know, but thank-you. Absolutely none of this would be possible without the immense love and support I have received from you every day. Special thanks to my boyfriend Mathieu for patiently listening to me whine on skype for the past two years. Your support means the world. And the squad. Man, how did I get so lucky to have the best group of friends. Marc, Tessa, Marissa, Karlee, Ashly, Koski, Shawn, Matt Mark, and the rest. You know who you are, let's have some beers and I promise not to bail because I have to do science in the morning.

Dedication

To my family for encouraging me to chase my dreams.

Table of Contents

List of Figures

List of Tables

List of Symbols, Abbreviations and Nomenclature

Symbol	***Definition***
Akt	Protein Kinase B
APC/C	Anaphase Promoting Complex/Cyclosome
ARPP19	cAMP-Regulated Phosphoprotein 19
ATCC	American Type Culture Collection
ATP	Adenosine Triphosphate
AurA	Aurora A
AurB	Aurora B
BLCA	Bladder Urothelial Carcinoma
BME	Beta Mercaptoethanol
BRCA	Breast Invasive Carcinoma
BSA	Bovine Serum Albumin
CAK	CDK-Activating Kinase
CDCxx	Cell Division Cycle
Cdk	Cyclin Dependent Kinase
ch-TOG	Colonic Hepatic Tumor Overexpressed Gene
CHC	Clathrin Heavy Chain
CHOL	Cholangiocarcinoma
CLC	Clathrin Light Chain
COADREAD	Colorectal Adenocarcinoma
DMEM	Dulbecco's Modified Eagle's Medium
DSP	Dual-Specificity Phosphatase
DTT	Dithiothreitol
ECL	Enhanced Chemiluminescence
EDTA	Ethylenediaminetetraacetic Acid
EGF/EGFR	Epidermal Growth Factor/Receptor
EMT	Epithelial–Mesenchymal Transition
ENSA	Alpha-Endosulfine
ESCA	Esophageal Carcinoma
FBS	Fetal Bovine Serum
FCP1	F-Cell Production 1
FGFR	Fibroblast Growth Factor Receptor
GBM	Glioblastoma Multiforme
GBMLGG	Glioma
GFP	Green Fluorescent Protein
GST	Glutathione-S Transferase
GTP	Guanosine Triphosphate
HDACI	Histone Deacetylase Inhibitor
HNSC	Head and Neck Squamous Cell Carcinoma
HRP	Horseradish Peroxidase
Hsp79	Heat Shock Protein 79
KICH	Kidney Chromophobe
KIRC	Kidney Renal Clear Cell Carcinoma
KIRP	Kidney Renal Papillary Cell Carcinoma

Symbol	***Definition***
LB	Lysogeny Broth
LIHC	Liver Hepatocellular Carcinoma
LMWPTP	Low Molecular Weight Protein Tyrosine Phosphatase
LUAD	Lung Adenocarcinoma
LUSC	Lung Squamous Cell Carcinoma
MAP	Microtubule-Associated Protein
MAPK	Mitogen-Activated Protein Kinase
MYPT1	Myosin Phosphatase Target Subunit 1
Myt1	Myelin Transcription Factor 1
Ndel1	Nuclear distribution Protein NudE-Like 1
Nek	Nima-Related Kinase
NIMA	Never-In-Mitosis A
PI3K	Phosphoinositide-3 Kinase
$p21^{WAF}$	Cdk-Interacting Protein 1
PBS	Phosphate Buffered Saline
PCR	Polymerase Chain Reaction
PDB	Protein Data Bank
Phe	Phenylalanine
PLK1	Polo-Like Kinase 1
PMSF	Phenylmethylsulfonyl Fluoride
PP1	Protein Phosphatase 1
PP2A	Protein Phosphatase 2A
PP2C	Protein Phosphatase 2C
PPM	Metallo-Dependent Protein Phosphatases
PPP	Phosphoprotein Phosphatases
PRAD	Prostate Adenocarcinoma
PTEN	Phosphatase and Tensin Homolog
PTP	Protein Tyrosine Phosphatases
READ	Renal Adenocarcinoma
SAC	Spindle Assembly Checkpoint
SDS-PAGE	Sodium Dodecyl Sulfate – Polyacrylamide Gel Electrophoresis
SNX9	Sorting-Nexin 9
STAD	Stomach Adenocarcinoma
STES	Stomach and Esophageal Carcinoma
TACC1/2/3	Transforming Acidic Coiled Coil Protein 1/2/3
TBS	Tris Buffered Saline
TCGA	The Cancer Genome Atlas
THCA	Thyroid Carcinoma
Thr	Threonine
Tyr	Tyrosine
UCEC	Uterine Corpus Endometrial Carcinoma
Val	Valine
γ-TURC	Gamma- Tubulin Ring Complex

Epigraph

You've got to be very careful if you don't know where you are going, because you might not get there. – Yogi Berra

I have no idea what I'm doing. – Science Dog

Chapter One: Introduction

1.1 Post translational modifications and reversible protein phosphorylation

Cell signaling is an important cellular process that provides a means for cells to communicate efficiently within themselves as well as with each other (Morgan 1989). One strategy cells employ during signaling events is to use a variety of post-translational protein modifications. These modifications involve the covalent addition of a ligand to a protein that then causes the protein to function in a modified manner. The change in function of the protein through the modification allows many different cellular processes and pathways to be controlled with either the addition or subsequent removal of a post-translational modification (Mann and Jensen 2003). Dozens of different protein modifications have been identified and include ubiquitination, acetylation, methylation, glycosylation and most commonly, phosphorylation (Khoury, Baliban et al. 2011) (**Figure 1**).

Reversible protein phosphorylation is an important cellular process that serves to regulate many different pathways within the cell. Phosphorylation involves the addition of a phosphate group to a protein from the terminal phosphate of ATP/GTP via a protein kinase. In reverse, the dephosphorylation is the hydrolytic removal of the phosphoryl group by a protein phosphatase (Chen, Plotkin et al. 2005). The addition or removal of a phosphate group acts as a molecular switch thereby altering protein function, changing possible interactors or impacting subcellular localization (Petersen, Lukas et al. 1999, Alvarado-Kristensson, Melander et al. 2004, Mollapour, Tsutsumi et al. 2011). In mammalian cells, this phosphorylation event generally occurs on either a serine, threonine or tyrosine residue within the protein amino acid sequence, with the frequency of phosphorylation on each residue being approximately 86.4%, 11.8%, and

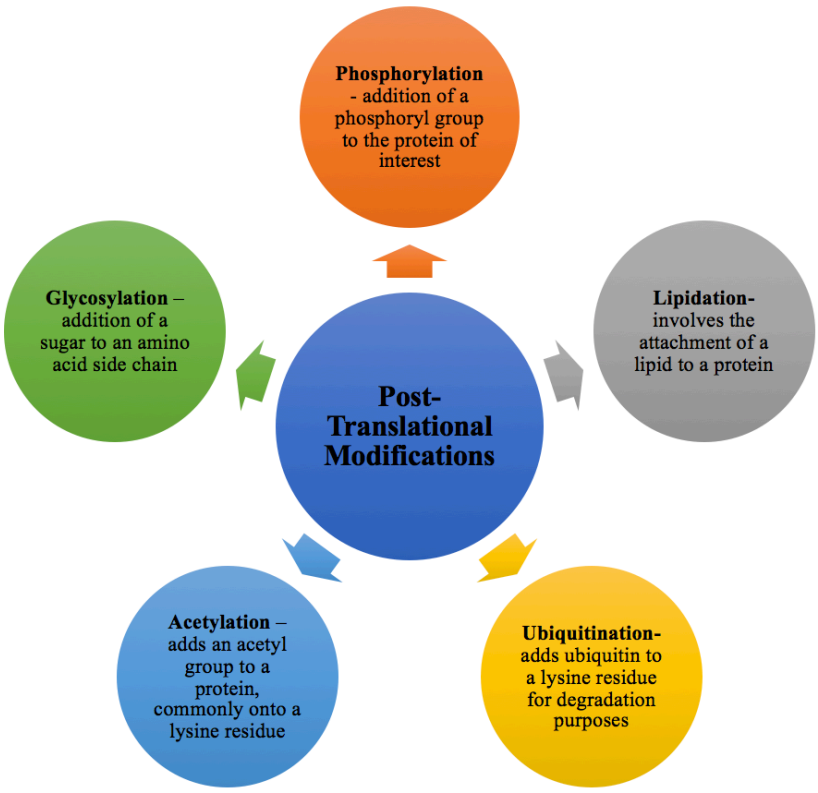

Figure 1.1 Post-translational modifications of proteins.

A selection of types of post-translation modifications commonly found in eukaryotes. Each modification can alter protein function, structure or sub-cellular localization.

1.8% respectively (Olsen, Blagoev et al. 2006, Olsen, Vermeulen et al. 2010, Khandelwal and Wang 2012). The balance of phosphorylation and dephosphorylation events within a cell is crucial. The gain or loss of function of certain protein kinases and protein phosphatases as well as mutations in the phosphorylation sites on key proteins have been found to lead to tumor formation as well as a number of other diseases and disorders (Li, Yen et al. 1997, Fullwood, Zhou et al. 2011, Reimand, Wagih et al. 2013). More than 75% of the human proteome will be

phosphorylated at some point in its lifetime at one or several of the over 100,000 mapped phosphorylation sites within the proteome (Dephoure, Gould et al. 2013, Sharma, D'Souza et al. 2014). Of the vast eukaryotic proteome, studies have shown that between 2-4% of the proteome corresponds to protein kinases and phosphatases, emphasizing the importance of protein phosphorylation as a means of control (Kerk, Templeton et al. 2008).

1.2 Protein phosphatases

1.2.1 Classes of protein phosphatases

Protein phosphatases are a diverse group of proteins with multiple classes or families dividing them based on a number of different properties (Moorhead, De Wever et al. 2009). These proteins catalyze the removal of phosphate groups from specific amino acid residues. The eukaryotic protein phosphatases belong to one of four major families based on several different properties including sequence homology, substrate preference or catalytic signature. The 4 major families are the metallo-dependent phosphatases (PPM), the phospho-tyrosine phosphatases (PTP), the aspartic acid-based phosphatases, and the phosphoprotein phosphatases (PPP) (**Table 1.1**) (Moorhead, De Wever et al. 2009).

The PPM family of protein phosphatases includes members such as PP2C and pyruvate dehydrogenase phosphatase and depend on metal ions (Mg^{2+}/Mn^{2+}) within the active site for catalysis. These phosphatases only dephosphorylate serine and threonine residues, and share 11 conserved motifs and four highly conserved aspartic-acid residues in the active site which are required for coordination of the metal-ions that drive catalysis (Cohen 1997, Andreeva and Kutuzov 2001).

The PTPs are the largest and most diverse group of phosphatases (Alonso, Sasin et al. 2004). They all share a unique catalytic motif, CX_5R, and have a wide variety of substrates including proteins, lipids,

Table 1.1 Classification of protein phosphatases.

Adapted from (Kerk, Templeton et al. 2008). Protein phosphatases as classified into four families: PPP (Phosphoprotein phosphatases), PPM (Mg^{2+}/Mn^{2+}-dependent protein phosphatases), PTP (Protein tyrosine phosphatases) and Asp-based catalysis phosphatases. The table shows the number of genes in humans which encode each type of phosphatase.

Protein Phosphatase Family	***Subclass***	***Human genes***
PPP family	Total	13
	PP1	3
	PP2A	2
	PP2B/PP3	3
	PP4	1
	PP5	1
	PP6	1
	PP7	2
PPM family (PP2C)	Total	20
PTP family	Total	106
Class I PTPs (Classic)	Total	37
	Receptor	20
	Non-receptor	17
Class I PTPs (DSPs)	Total	67
	MAPKP	11
	Slingshots	3
	PRL	3
	Atypical DSP	19
	CDC14	5
	PTEN	7
	Myotubularins	16
	Other	3
Class II PTPs (CDC25)		3
Class III PTPs (LMWPTP)		1
Asp-based catalysis	Total	13
FCP-like		8
Chronophins		1
EYA		4
Total phosphatases		158

complex carbohydrates and mRNA (Fischer, Charbonneau et al. 1991, Guan and Dixon 1991). This group is further divided into three classes based on sequence. Class I PTP's include: the classical PTPs, such as receptor tyrosine phosphatases and non-receptor tyrosine phosphatases which act on phospho-tyrosine residues, and the dual-specificity (DSP) phosphatases, which act on phospho-tyrosine, -serine, and -threonine residues in protein and non-protein substrates. The DSPs include the MAPK phosphatases, Cdc14s, PTENs, myotubularins and atypical DSPs (Moorhead, De Wever et al. 2009). Class II PTPs include only one member, the low molecular mass PTP (LMWPTP), while the Class III PTPs are tyrosine/threonine specific and include the Cdc25s (Bordo and Bork 2002, Bottini, Bottini et al. 2002).

The aspartic-acid based phosphatases earn both their name and classification through the use of aspartic-acid during catalysis, specifically in the highly conserved catalytic motif DXDXT/V (Moorhead, De Wever et al. 2009, Shi 2009). The most prominent member of this family is the RNA polymerase II C-terminal phosphatase (FCP1) (Fuda, Buckley et al. 2012).

The final class of protein phosphatases is the PPP family. This family of phosphatases are serine/threonine specific and share three common motifs (GDXHG-, -GDXVDRG- and –GNHE-) within their catalytic domain (Honkanen and Golden 2002, Wang, Zhang et al. 2008). This family includes the critical cell cycle regulatory proteins PP1 and PP2A, which function by binding additional proteins to aid in specificity, regulation and stability (Cohen 2002). PP1 gains its substrate specificity through the binding of a regulatory subunit, allowing the catalytic subunit to be targeted to many different substrates. Over 200 different regulatory proteins have currently been identified for PP1, which will be discussed in more detail in **Section 1.3**. PP2A binds to a scaffolding (A) subunit as well as one of 26 different regulatory (B) subunits (Cohen, Brewis et al. 1990, Yanagida, Kinoshita et al. 1992). The PPP family of protein phosphatases are considered to be very ancient enzymes and are

widely found across eukaryotes with an impressively high degree of conservation (Moorhead, De Wever et al. 2009).

1.2.2 Evolution of protein phosphatases

One of the key characteristics of protein phosphatase's catalytic subunits is their lack of a conserved substrate targeting sequence (Uhrig, Labandera et al. 2013). This is in direct contrast to the protein kinases that recognize and phosphorylate a unique motif within their substrates (Sharrocks, Yang et al. 2000). The number of protein phosphatases in the cell is markedly lower than the protein kinases, forcing the few protein phosphatases to have a broad substrate specificity in order to dephosphorylate the many substrates of the protein kinases (Moorhead, Trinkle-Mulcahy et al. 2007). Protein phosphatases have evolved to use regulatory subunits or domains as a means to confer their specificity and target them towards their substrates (Ingebritsen and Cohen 1983). The evolution of protein phosphatases, specifically the PPP and PPM families allow us to observe convergent evolution in the real world. These two families, while performing similar functions by strictly dephosphorylating serine/threonine residues, have very little sequence similarity, but structurally share similar folds (Moorhead, De Wever et al. 2009).

1.3 Protein phosphatase one

1.3.1 Protein phosphatase one catalytic subunit and conservation

Protein phosphatase one (PP1) is a member of the PPP family of protein phosphatases and is known to dephosphorylate serine/threonine residues, which account for nearly 98% of the phosphorylated residues within a cell. PP1, along with its PPP family member, PP2A are

responsible for catalyzing approximately 90% of the dephosphorylation reactions from these residues (Sharma, D'Souza et al. 2014). PP1 is a key player in cellular regulation and has been shown to be crucial for many different cellular processes including cell division (Pinsky, Nelson et al. 2009). PP1 itself is considered a catalytic subunit and binds to regulatory subunits in order to form the holoenzyme. This catalytic subunit is encoded by multiple genes in most eukaryotes and has a remarkably high degree of conservation. In humans, there are three different isoforms of PP1: PP1α, PP1β and PP1γ. Each isoform is a separate gene, located at 11q13.2, 2p23.2 and 12q24.11 for α, β, and γ respectively. These isoforms are 90% identical in their amino acid sequences, with slight differences only on the N- and C- termini **(Figure 1.2**). The high level of conservation is not surprising when considering the similarities between catalytic mechanisms and regulation.

1.3.2 Mechanism of catalysis by protein phosphatase one

The mechanism through which the PP1 catalytic subunit carries out the dephosphorylation reaction is, as previously mentioned, highly conserved. As a member of the PPP family of phosphatases, PP1 utilizes metal ions to catalyze the removal of a phosphate group from a serine/threonine residue. The active site on the catalytic subunit is defined by the presence of two metal ions, located between three different clefts, the hydrophobic groove, the acidic groove and the C-terminal groove (Shi 2009). These two metal ions are coordinated by three histidine, two aspartic acid and one asparagine residue that work to actively dephosphorylate the substrate **(Figure 1.3)**. These metal ions interact with the oxygen atoms of a water molecule which then initiates a nucleophilic attack on the phosphorous atom of the phosphate group (Goldberg, Huang et al. 1995, Barford, Das et al. 1998). Other residues located in the active site function to help stabilize the transition state, donate a

Figure 1.2 Conservation of human PP1 isoforms.

The protein sequences of each human PP1 isoform, α, β, and γ (available from NCBI) were aligned using Clustal Omega (Sievers, Wilm et al. 2011). Residues conserved across all three isoforms are indicated by (*), residues with highly similar biochemical properties are indicated by (:), residues with less similar properties are indicated by (.), and residues that are not conserved are indicated by a space. Key active site residues are indicated by red squares.

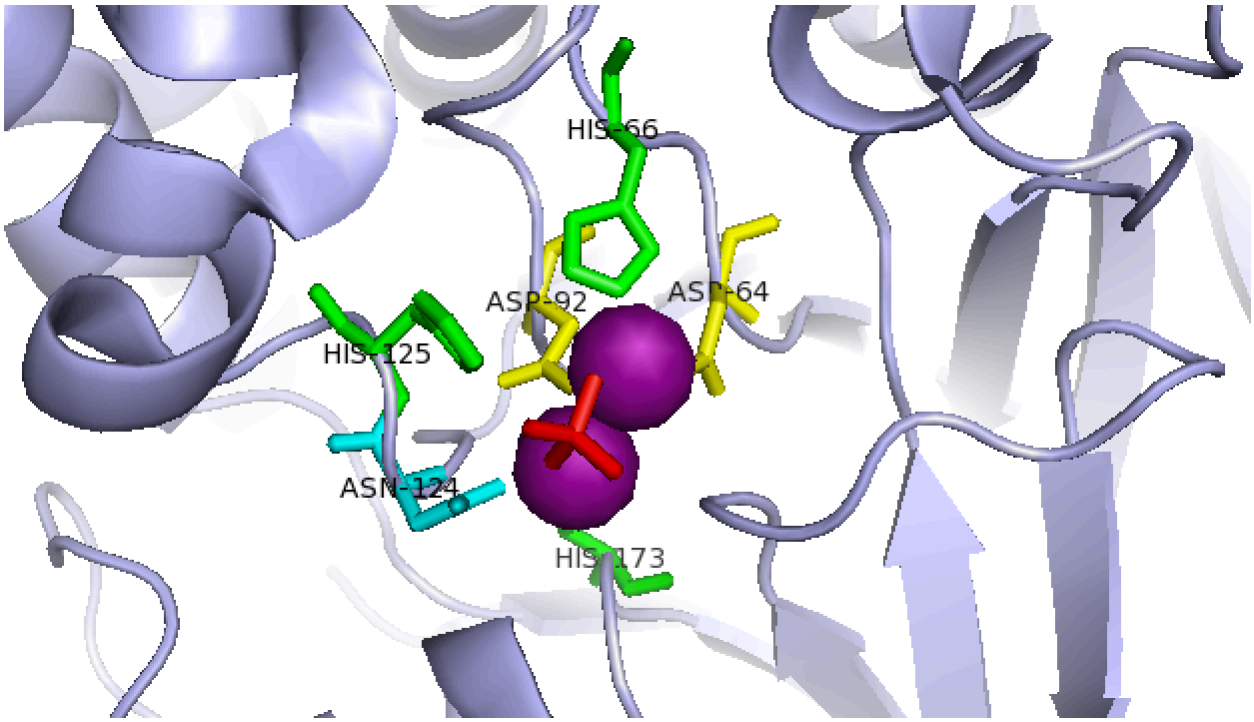

Figure 1.3 Protein phosphatase one active site.

A crystal structure of the active site of PP1. The phosphate molecule (red) is modelled in the active site next to two Mn^{2+} ions (purple) and surrounded by the three histidine residues (green), two aspartic acid residues (yellow) and an asparagine residue (cyan), which are responsible for catalysis. Image was generated from PDB file 4MOV using PyMol (Choy, Hieke et al. 2014, Schrodinger 2015).

proton to the removed phosphate group, and ultimately regenerate the serine/threonine residue.

1.3.3 PP1 regulatory subunits and the RVxF motif

PP1 generally exists *in vivo* as a holoenzyme, consisting of at least two different subunits, the previously discussed catalytic subunit, and a regulatory subunit. Interaction with different regulatory subunits allows PP1 to have multiple substrates and be targeted towards multiple locations at

various time points with only three mammalian isoforms, α, β and γ (Cohen 2002). This demonstrates the importance of the regulatory subunits in diversification of protein phosphatases, especially when considering the discrepancy between the large variety and number of protein kinases in the proteome and the limited number of protein phosphatases available to carry out the subsequent reverse reactions (Moorhead, De Wever et al. 2009). The association of PP1 with one of the over 200 different currently identified regulatory subunits can change the catalytic subunits substrate affinity, sub-cellular localization, or even affect the dephosphorylation capabilities of the enzyme by regulating the activity (Ceulemans, Stalmans et al. 2002, Barr, Elliott et al. 2011).

The majority of these regulatory subunits share a highly conserved, degenerate PP1 docking motif [R/F][X]$_{0-1}$[V/I] {P [F/W], referred to from here on as RVxF (Egloff, Johnson et al. 1997, Bollen 2001, Ceulemans, Stalmans et al. 2002, Wakula, Beullens et al. 2003) **(Figure 1.4A)**. In this motif, the two hydrophobic residues, valine and phenylalanine, are crucial for the docking of this motif to the catalytic subunit of PP1 (Pinheiro, Marsh et al. 2010). They fit into the hydrophobic cleft of the catalytic subunit, located on the back of the protein away from the active site, so as to not interfere with catalytic activity (Gibbons, Weiser et al. 2005) **(Figure 1.4B)**. It has previously been shown through site-directed mutagenesis that mutating the valine and phenylalanine in the RVxF motif disrupts the binding of the catalytic subunit of PP1 with its regulatory subunit and can disrupt PP1 function (Templeton, Nimick et al. 2011). Although the RVxF motif is the most common, several other PP1 regulatory subunit docking motifs do exist such as the G/SILK and MyPhoNE motifs (Uhrig, Labandera et al. 2013). One of the key features of the RVxF motif is the high frequency of a serine or threonine residue in the x position. Serine and threonine are both residues that are frequently phosphorylated. Phosphorylating these residues within the RVxF motif can act as a means of regulating the docking of the RVxF-containing regulatory subunits to PP1. The addition of a phosphate group to a serine/threonine residue in this

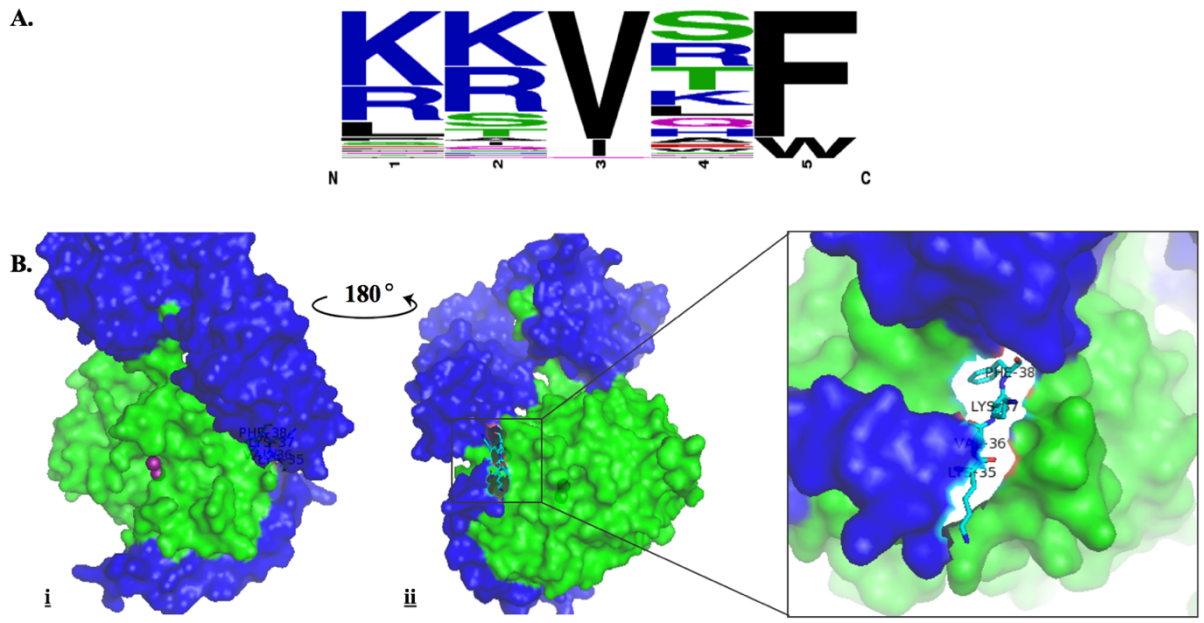

Figure 1.4 Protein phosphatase one and the regulatory subunit docking the RVxF motif. **A.** The consensus sequence for the RVxF motif. The most prevalent residues in each position are shown, based on validated PP1 binding proteins. Motif sequences were taken from (Hendrickx, Beullens et al. 2009) and image created using WebLogo (Crooks, Hon et al. 2004). **B. (i)** Front view of PP1(green) bound to one of its regulatory subunits (MYPT1; blue). The PP1 active site is represented by the 2 purple metal ions. **(ii)** Back view of PP1 bound to MYPT1 showing the conserved RVxF motif (cyan) docking the catalytic subunit of PP1. The valine (VAL-36) and phenylalanine (PHE-38) of the RVxF motif fit into the hydrophobic cleft allowing the regulatory subunit to dock. The hydrophobic cleft is located on the back of the catalytic subunit, away from the active site so as not to interfere with catalysis. Image was manipulated from PDB file 1S70 using PyMol (Terrak, Kerff et al. 2004, Schrodinger 2015).

position will disrupt the interaction of PP1 and the regulatory subunit by preventing the valine and phenylalanine residues from docking to the hydrophobic cleft. The addition of a negative charge from the phosphate group will also act to further abolish binding by repelling the docking site.

1.4 Protein phosphorylation throughout the eukaryotic cell cycle and mitosis

In eukaryotes, the cell cycle is a highly-regulated process that involves time-dependent events with four different stages all functioning to allow the cell to progress through the cycle. The events that take place in the cell cycle such as replication of chromosomes, growth, and cell division are all crucial processes that are required for cells to survive and function properly (Hartwell and Weinert 1989). The four major stages of the cell cycle are: G1-phase, or gap phase 1, where cells grow and prepare for entry into the next stage, S-phase, or synthesis phase, where diploid cells duplicate chromosomes via DNA replication. From S-phase, cells enter another growth stage, referred to as gap 2 phase or, G2-phase. After completing G2, the cell will enter M-phase, or mitosis. It is during this stage in the cell cycle where a parent cell will undergo a cascade of events that leads to the segregation of chromosomes and the generation of a daughter cell (Morgan 2007). There is also an additional quiescent stage G_o, in which a cell will reside until stimuli cause it to enter G1, where it can then progress through the cell cycle. The transition of the cell between these four phases is tightly controlled, largely by the process of reversible protein phosphorylation (Hunt 2002).

1.4.1 Cyclin-dependent kinases as master regulators of the cell cycle

A family of proteins known as the cyclin-dependent kinases (Cdks) and their association with a second family of proteins, the cyclins, are largely considered to be the master regulators of the

cell cycle. The interaction of the Cdks with different members of the cyclins acts as a means of regulating when a cell enters/exits each stage of the cell cycle (Obaya and Sedivy 2002). Cdk's carry out their role as master regulators by controlling mRNA processing, transcription and numerous other cellular events (Morgan 2007). Cdk levels remain fairly constant throughout the cell cycle, while cyclin levels vary depending on the phase. This results in the Cdk activity being regulated via post-translational modifications, mainly phosphorylation, which controls the binding of the appropriate cyclin and the activation of the kinase activity (Morgan 1995). The Cdk-active site is a modified ATP-binding site that is inaccessible to substrate without the docking of a cyclin to the Cdk. Cdks are only active upon formation of the cyclin-Cdk complex (Morgan 2007). Upon cyclin binding, the T-loop of the Cdk undergoes a conformational change, exposing the active site, and allowing ATP to bind. There is a very high degree of specificity controlling which cyclin protein is binding, as the cyclin plays a large role in determining substrate specificity (Morgan 1997). As an additional means of control, Cdk-activating kinases (CAK), phosphorylate Cdks on the T-loop to increase the activity of the complex and allow Cdks to become fully active (Morgan 2007).

In addition to activating kinase activity, phosphorylation at different locations on the Cdks can act to inhibit the kinase activity. Inactivating the Cdks is just as important to proper cell cycle progression as timely activation. By limiting which Cdk is active and when it is activated, the precise timing of the cell cycle is regulated (Morgan 2007) **(Figure 1.5)**.

1.4.2 Mitosis is controlled by phosphorylation

Mitosis is the stage in the cell cycle, where the chromosomes that were previously duplicated during S-phase are divided into two daughter cells. Mitosis itself is divided into four sub-stages: prophase,

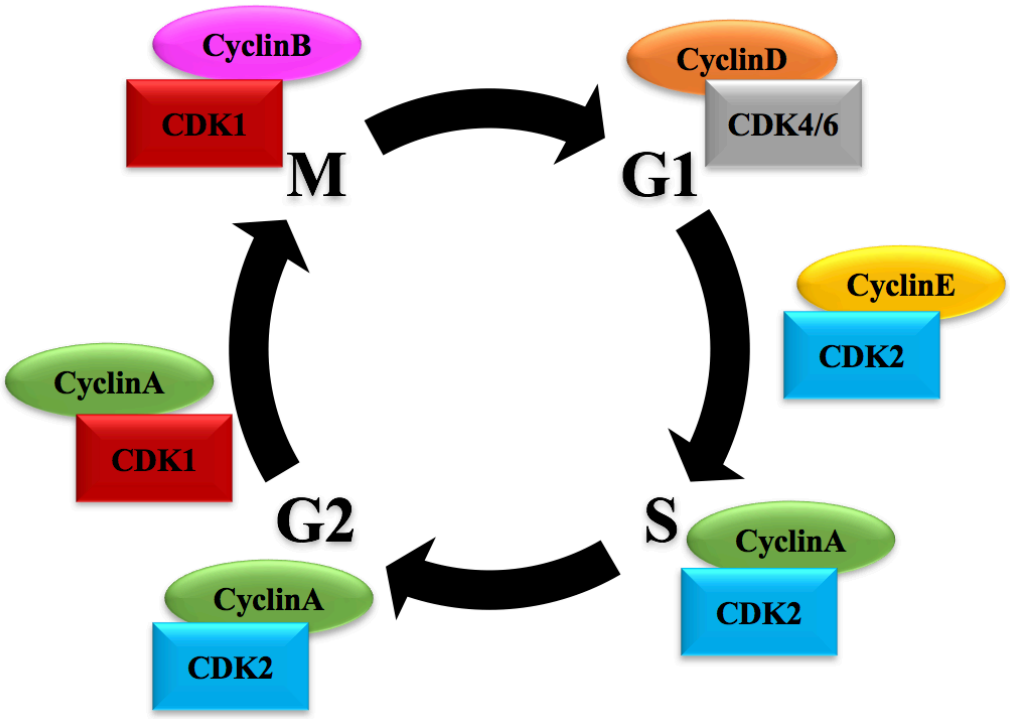

Figure 1.5 The eukaryotic cell cycle is controlled by the cyclin-dependent kinases and the cyclins.

The four major phases of the cell cycle and their associated Cdk/cyclins. Once a cell is stimulated to enter the cell cycle, expression of cyclin D increases and it associates with its binding partners Cdk4/6. The formation of this complex promotes the transcription of genes required for S-phase, including cyclin E. The increased levels of cyclin E allow it to bind Cdk2, resulting in the cell to transition from G1 to S-phase. During S-phase, cyclin A levels rise, and it complexes with Cdk2. The cyclin A/Cdk2 complex regulates the synthesis of a second set of chromosomes and allows the cell to transition to G2-phase. At the G2/M transition, cyclin A associates with Cdk1, promoting the translation of cyclin B, which then forms the cyclin B/Cdk1 complex that is required for mitotic entry. This complex phosphorylates many proteins required for controlling mitotic progression. Upon completion of mitosis, cyclin B is degraded, leading to a decrease in Cdk1 activity and mitotic exit.

metaphase, anaphase and telophase (O'Connor 2008). The process of cell division is tightly regulated through post-translational modifications, specifically, protein phosphorylation. One of the key indicators of the onset of mitosis is a marked increase in the level of protein phosphorylation within the cell. At the onset of mitosis, the serine/threonine mitotic protein kinases, cyclin-dependent kinase 1 (Cdk1), the Auroras (AurA, AurB), the NIMAs (Nek) and the Polos (Plk1) all play major roles in phosphorylating key mitotic players (Nigg 2001, Potapova, Sivakumar et al. 2011).

As previously mentioned, the Cdk1-cyclin B complex is the master regulator of mitosis and is responsible for driving the events required for cell division to occur. Upon mitotic entry and binding to cyclin B, Cdk1 becomes active through the phosphorylation of Thr161 on its T-loop (Enserink and Kolodner 2010). Protein kinases Wee1 and Myt also play a role in regulating Cdk1s activity by phosphorylating Thr14 and Tyr15 residues near the active site (Mueller, Coleman et al. 1995, O'Farrell 2001). These protein kinases prevent Cdk1 from becoming active prior to the G2/M transition until CDC25 dephosphorylates these residues fully activating Cdk1 and allowing mitosis to begin (Russell and Nurse 1986, O'Farrell 2001). The balance of regulation mechanism between the protein kinases and the protein phosphatases is crucial for the proper timely progression of the mitotic events (Nigg 2001). The fully active Cdk1 then begins to phosphorylate key mitotic players including Polo-like kinase 1 (Plk1), Greatwall kinase and the Aurora kinases to activate numerous downstream pathways and drive mitotic progression forward (Dephoure, Zhou et al. 2008, Olsen, Vermeulen et al. 2010). Protein phosphatase activity is crucial outside of mitosis to prevent early mitotic entry, but must be inhibited for the cell to fully enter mitosis. PP1 is inactivated by phosphorylation of Thr320 by Cdk1, while PP2A is inhibited by both ENSA and ARPP19, which, interestingly, are activated by Greatwall kinase, one of Cdk1's substrates (Lindqvist, Rodriguez-Bravo et al. 2009, Wu, Guo et al. 2009, Gharbi-Ayachi, Labbe et al. 2010, Mochida, Maslen et al. 2010).

As the cell progresses through mitosis and more downstream effects are felt, eventually mitotic kinase activity begins to decrease. At the metaphase/anaphase transition, the formation of the APC/C complex allows the proteolytic degradation of cyclin B by this complex. With decreased cyclin B levels, Cdk1 activity drops, and the ~700 residues that were phosphorylated by the mitotic kinases must be dephosphorylated for mitotic exit to occur (Potapova, Sivakumar et al. 2011). It is at this point that the protein phosphatases, specifically PP1 and PP2A play a critical role and begin to dephosphorylate the large number of phospho-serine/threonine residues and return the cell back to an interphase level of phosphorylation (Potapova, Sivakumar et al. 2011). With the declining activity of Cdk1, PP1 is able to auto-dephosphorylate at Thr320 and partially activate until it can dephosphorylate and dissociate from its inhibitory binding partner, inhibitor-1. This then allows PP1 to fully activate and begin actively dephosphorylating the large number of proteins and allow mitotic exit (Wu, Guo et al. 2009).

1.4.3 The mitotic spindle and the spindle assembly checkpoint

The mitotic spindle is a highly dynamic structure found within dividing eukaryotic cells and is essential for the separation of sister chromatids between daughter cells during anaphase. The mitotic spindle is a cytoskeletal structure composed of hundreds of different proteins, the majority of which are tubulin, forming microtubules (Walczak and Heald 2008). Microtubules are composed of α and β tubulin heterodimers, that arrange to form the cylindrical, hollow microtubule structure. A third type of tubulin, γ, is a specialized variant that forms the γ-tubulin ring complex (γ-TURC), which acts as a nucleation site for microtubule formation (Zheng, Wong et al. 1995, Nogales, Whittaker et al. 1999). Of these microtubules, there are three distinct types which all serve unique functions for the mitotic spindle. Microtubules have plus and minus ends, with the plus ends growing much more rapidly. The astral microtubules (i) radiate into the cytoplasm from centrosomes. These microtubules are present

during interphase, and at the onset of mitosis, they shorten in length. As the astral microtubules shorten, many more microtubules are nucleated from the centrosomes. Some of these microtubules become kinetochore microtubules (ii) and connect the poles to the kinetochores, which are attached to the sister chromatids and help to hold them together. These microtubules bundle together in parallel to form K-fibers (O'Connell and Khodjakov 2007). The remaining microtubules are polar microtubules (iii), which also originate from the spindle poles at the centrosome and overlap in an anti-parallel manner at the spindle equator, interacting with the free arms of the chromosomes (Karsenti and Vernos 2001). The polymerization and subsequent de-polymerization of microtubules drives their dynamic nature. As the asymmetrical microtubules lengthen and shorten, their bipolar nature creates an opposing tension force on the kinetochores from the opposite poles of the cell. This results in the alignment of the sister chromatids at the cellular equator(Nogales and Ramey 2009). Once the chromosomes are properly aligned and pass through the spindle assembly checkpoint (SAC), the microtubules retract and pull the sister chromatids apart to opposite poles of the cell, progressing mitosis from metaphase to anaphase (Walczak and Heald 2008).

Many different proteins called MAPs (microtubule associated proteins) enhance the stability of the microtubules and assist in their dynamic nature. Dyenin and kinesin are two MAP motor proteins, that recognize the spindle structure and polarity and move different microtubules, associated protein complexes, and even chromosomes along the anti-parallel spindles (Saxton, Stemple et al. 1984, Wittmann, Hyman et al. 2001). In addition to the tubulins and motor proteins, many kinase complexes are recruited to the centrosomes to phosphorylate and assist in regulating the dynamic cell cycle. Many proteomic studies have identified a high level of spindle proteins are phosphorylated during mitosis, implying once again that the mitotic kinases are crucial in driving mitosis and overall cell cycle progression (Doxsey, Zimmerman et al. 2005, Nousiainen, Sillje et al. 2006, Walczak and Heald 2008).

Proper segregation of chromosomes is crucial for cell cycle progression and a healthy, functional cell post-mitosis. One way that the cell ensures proper separation occurs is through the alignment of the chromosomes at the metaphase plate by the mitotic spindle. Improper alignment of chromosomes can lead to cells that are multinucleated, have aneuploidy or have supernumerary centrosomes leading to the cells later being arrested in G1 at the post-mitotic checkpoint. For this reason, the metaphase-anaphase transition has its own checkpoint, the Spindle Assembly Checkpoint (SAC) that ensures the chromosomes are properly aligned and that the spindle is properly functioning prior to the progression to anaphase.

Phosphorylation once again, acts as a regulatory mechanism for the SAC. AurB has been identified as the mitotic protein kinase responsible for this event. It is important to note that AurB localizes to the centrosome during metaphase and performs this key role by phosphorylating the SAC proteins, turning the checkpoint "on", and arresting the cell in metaphase. AurB can sense the tension in the centrosomes that is generated by the microtubules being properly attached to the chromosomes at the metaphase plate. Without the presence of tension, AurB promotes the recruitment of several SAC proteins to the kinetochores to aid in proper attachment of the chromosomes and ultimately the proper alignment. These proteins inhibit the APC/C, delaying the onset of anaphase (Krenn and Musacchio 2015).

Once the kinetochores are properly attached, and the chromosomes are aligned, the SAC must be turned "off" to allow progression into anaphase. PP1 is targeted to the kinetochores by several associated proteins allowing it to reverse the phosphorylation events initiated by AurB (Lesage, Qian et al. 2011). CASC5, a kinetochore associated protein and known RVxF containing regulatory subunit of PP1, is one of the proteins responsible for the recruitment of PP1 to the kinetochores to perform this action. Interestingly, it has been shown that mutations within the conserved binding motif can lead to prolonged activation of the SAC and delay the onset of anaphase. With proper alignment of the

chromosomes and increased tension on the centrosomes, AurB is pulled away from its substrates, allowing PP1 to dephosphorylate the SAC proteins and drive mitotic progression (Liu, Vleugel et al. 2010, Rosenberg, Cross et al. 2011).

1.5 Transforming acidic coiled coil protein 3 and the TACC family of proteins

1.5.1 The transforming acidic coiled coil (TACC) proteins

Transforming acidic coiled coil protein 3 (TACC3) is a member of the TACC family of proteins. This group of proteins consists of three members, TACC1, TACC2 and TACC3. They are named for their acidic nature and the presence of a C-terminal coiled coil domain now known as the TACC domain (**Figure 1.6**) (Still, Hamilton et al. 1999, Still, Vince et al. 1999, Peset and Vernos 2008). This domain is the signature of the family and shows a high level of conservation. Although all three TACC proteins share this conserved C-terminal domain, they have very diverse N-terminal domains, suggesting that the TACC domain is crucial to the functionality of this family of proteins (Gergely 2002, Still, Vettaikkorumakankauv et al. 2004, Peset and Vernos 2008). TACC proteins are present in many different eukaryotic organisms from yeast to mammals, with lower organisms having one homolog, and mammals having three (Gergely 2002).

All members of the TACC family are associated with regulation of chromosome integrity, centrosome-dependent assembly of microtubules and mitotic spindle stability during mitosis (Schneider, Essmann et al. 2008). They also function as microtubule plus-end tracking proteins that regulate microtubule dynamics (Nwagbara, Faris et al. 2014). These ideas have gained-widespread support through different experimental studies. The TACC proteins have all been shown to localize to the centrosome during cell division, but in slightly different ways. TACC2

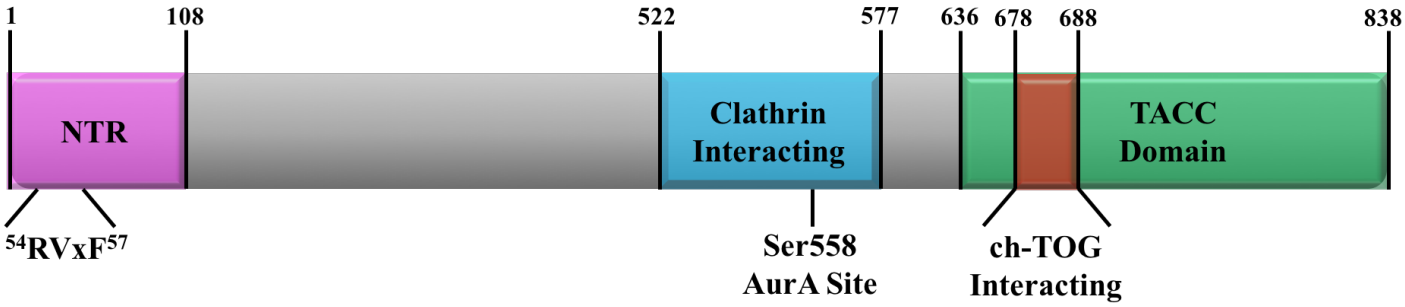

Figure 1.6 The domain architecture of TACC3.

The domain structure of TACC3 with select key features highlighted. N-terminal region (NTR; pink), residues 1-108; Clathrin interacting domain (blue), residues 522-577; ch-TOG interacting region (orange), residues 678-688; TACC domain (green), residues 636-838. The RVxF motif and a key AurA phosphorylation site are also indicated(Burgess, Peset et al. 2015).

localizes to the centrosome throughout the cell cycle, whereas TACC1 and TACC3 only localize to the centrosome during mitosis, with TACC3 covering a much larger area. This suggests that these proteins have similar, yet non-overlapping functions. Although more studies need to be done, it is likely TACC1 and TACC3 localize to the cytoplasm during interphase, but there is also some evidence they may remain in the perinuclear region (Gergely, Karlsson et al. 2000, Piekorz, Hoffmeyer et al. 2002, Peset and Vernos 2008). It has also been shown that the coiled-coil TACC domain is required to localize these proteins to the centrosomes and microtubules (Gergely, Karlsson et al. 2000, Piekorz, Hoffmeyer et al. 2002).

The TACC proteins first emerged as a group of proteins implicated in cancer due to their genes being found in genomic regions frequently rearranged in various cancers. Specifically,

TACC1 was first identified as being located within a genomic region amplified in breast cancer. The expression of the TACC proteins is altered in numerous different cancers (Still, Hamilton et al. 1999, Gergely, Karlsson et al. 2000, Peset and Vernos 2008). Interestingly, all three TACC genes are located near an FGFR gene. It is believed that the TACC family and the FGFR family likely arose from an ancestral FGFR/TACC gene pair. TACC3 maps close to FGFR3, and the fusion products of these two proteins have been implicated in a handful of different cancers (Still, Vince et al. 1999, Stewart, Thompson et al. 2004, Parker, Annala et al. 2013, Capelletti, Dodge et al. 2014, Yuan, Liu et al. 2014). All 3 TACC proteins are known to interact with ch-TOG, a cytoskeleton associated protein, however the function of this interaction has only been determined with TACC3 (Peset and Vernos 2008).

1.5.2 Transforming acidic coiled coil 3

TACC3 is a non-motor microtubule associated protein (MAP), that is known to play a major role in the formation of the mitotic spindle (Peset and Vernos 2008). As previously mentioned, it is localized to the centrosomes and microtubules of the mitotic spindle. Depletion of TACC3 has been linked to numerous defects including: triggering the SAC, partially destabilized microtubule content, defects in chromosome alignment, decreased microtubule density, increased duration of mitotic events, aneuploidy, chromosomal instability, $p21^{WAF}$ mediated G_o/G_1 phase arrest, or even apoptosis. Studies in mice have shown that the absence of TACC3 can lead to embryonic lethality, suggesting that TACC3 is essential for embryonic development and cell division (Piekorz, Hoffmeyer et al. 2002, Gergely, Draviam et al. 2003, Schneider, Essmann et al. 2007, Schneider, Essmann et al. 2008). In contrast, overexpression of TACC3 causes an accumulation at the spindle poles, and increased microtubule length (Gergely, Karlsson et al. 2000, Peset, Seiler et al. 2005, Peset and Vernos 2008).

TACC3 is required to allow the cell to pass through the SAC and transition from metaphase to anaphase, allowing proper mitotic progression (Schneider, Essmann et al. 2007). Due to its role in mitosis, TACC3 protein levels must be tightly regulated to ensure proper progression of the cell cycle. It has been reported that TACC3 levels are elevated during G2/M phase and that the levels are regulated via a proteasome dependent pathway (Piekorz, Hoffmeyer et al. 2002, Jeng, Lin et al. 2009). TACC3 protein levels follow a trend similar to that seen for typical mitotic markers such as Cyclin B1, Cdh1 and Cdc20. It has been shown that TACC3 interacts with the APC/C activating protein Cdh1, and this interaction controls TACC3 levels by mediating the interaction of TACC3 for ubiquitination and ultimately proteasome-dependent degradation (Jeng, Lin et al. 2009).

TACC3 is expressed in relatively few adult tissues with the exception being high levels in lung, testes, ovaries, and hematopoietic lineages such as bone marrow, liver, thymus and spleen. It has also been found in all stages of embryonic development, particularly in proliferating tissues, again implicating its important in cell division and overall development. Embryonic lethality, decreased cell number, widespread cell death and mitotic defects have been observed in TACC3 deficient mice (Piekorz, Hoffmeyer et al. 2002, Yao, Natsume et al. 2007, Peset and Vernos 2008).

Given its importance in maintaining genomic integrity in the cells, TACC3 has also previously been associated with many different types of cancers, which will be discussed further in **Section 1.5.4** (Lauffart, Vaughan et al. 2005, Cerami, Gao et al. 2012, Gao, Aksoy et al. 2013, Yao, Kondoh et al. 2014).

1.5.3 TACC3 and its role in mitosis

TACC3, as previously mentioned, plays a role in mitotic spindle assembly and chromosome alignment during mitosis. As a member of the TACC family, it localizes to the centrosomes and

microtubules of the mitotic spindle, specifically co-localizing with α-tubulin on the spindles and γ-tubulin at the centrosome (Gergely, Karlsson et al. 2000, Piekorz, Hoffmeyer et al. 2002, Peset, Seiler et al. 2005). Emerging evidence suggests TACC3 is involved in the regulation of centrosome-mediated microtubule nucleation by impacting γ-tubulin ring complexes. These complexes play a key role in the control of microtubule nucleation. Depletion of TACC3 affected the assembly of the γ-TURC and reduced the localization of the γ-TURC proteins to the centrosome, ultimately affecting chromosome integrity (Kollman, Polka et al. 2010, Singh, Thomas et al. 2014, Suhail, Singh et al. 2015).

It has been shown that TACC3 forms a 1:1 complex with colonic hepatic tumor overexpressed gene (ch-TOG), a cytoskeleton associated protein and microtubule polymerase that is essential to the stabilization of microtubules (Kinoshita, Noetzel et al. 2005, Brouhard, Stear et al. 2008). The interaction between these two proteins is conserved across evolution and occurs via the TACC domain. This strengthens the idea that the TACC domain is crucial for promoting microtubule assembly (Lee, Gergely et al. 2001, Kinoshita, Noetzel et al. 2005, O'Brien, Albee et al. 2005, Peset, Seiler et al. 2005, Peset and Vernos 2008). The formation of this complex is important for the function of both proteins. In TACC3 depleted cells, ch-TOG localization to the centrosomes and microtubules is impaired, while overexpression of TACC3 recruits more ch-TOG to the spindle poles. This implies that TACC3 is crucial for the correct localization and recruitment of ch-TOG (Lee, Gergely et al. 2001, Kinoshita, Noetzel et al. 2005, Peset and Vernos 2008). Ch-TOG does have a function independent of TACC3. At the centrosomes, it promotes microtubule assembly and growth, is a known microtubule plus-end tracking protein that binds the ends of microtubules, and helps to contribute to spindle bipolarity (Gergely, Draviam et al. 2003, Holmfeldt, Stenmark et al. 2004, Barr and Gergely 2008, Akhmanova and Steinmetz 2010, Hood and Royle 2011). There is mounting evidence that TACC3 may also behave

as a plus-end tracking protein as it has been observed in human cells with ch-TOG mediating the interaction between TACC3 and the microtubule plus-ends. The formation of the TACC3-ch-TOG complex is required for TACC3 to track the ends, suggesting ch-TOG may be responsible for bringing TACC3 to the plus-ends, as it is still able to track the ends in the absence of TACC3.

Clathrin is a protein formed through the association of three clathrin heavy chains (CHC) that interact via their C-termini, with each CHC tightly associating with a clathrin light chain (CLC). The N-terminus of the CHC is a globular domain that allows the protein to localize to the mitotic spindle (Royle, Bright et al. 2005, Royle 2006, Royle and Lagnado 2006). A protein generally associated with membrane-trafficking, a small sub-set of clathrin has also been shown to form a complex at the microtubules with TACC3 and ch-TOG (Tanenbaum, Vallenius et al. 2010, Hood and Royle 2011, Royle 2012). This TACC3-ch-TOG-clathrin complex works to stabilize K-fibers within the mitotic spindle by forming physical cross-linking bridges between adjacent microtubules, and possibly reducing the rates of microtubule catastrophe (Cheeseman, Booth et al. 2011, Hood and Royle 2011). The complex also appears to contribute towards the stability of centrosomal tubulin as loss of the complex results in γ-tubulin dispersion and centrosome fragmentation (Foraker, Camus et al. 2012). It is important to note that this complex is different from the TACC3-ch-TOG complex as when non-clathrin binding TACC3 mutants were studied, they were still able to complex with ch-TOG and track the microtubule plus-ends (Gutiérrez-Caballero, Burgess et al. 2015). These bridges were first seen many years ago through electron microscopy that showed the presence of density between the microtubules of K-fibers (Wilson 1969). It is only in recent years that the composition of these bridges has been discovered and models have been proposed. The bridges are an interconnected network that can contact multiple microtubules within the K-fiber forming a mesh-like structure.

Clathrin was first identified as a TACC3 interacting partner through a quantitative proteomics study and has the same microtubule distribution pattern as TACC3 and ch-TOG, but only during mitosis, suggesting it is a binding partner only during mitosis (Hubner, Bird et al. 2010, Booth, Hood et al. 2011). Interestingly, the depletion of clathrin, specifically the CHC during mitosis has similar effects as TACC3 depletion, including less bridges between K-fibers and decreased microtubule density. The depletion of both proteins did not cause more severe defects, which implies the proteins belong to the same complex. The TACC3-ch-TOG-clathrin complex may also prevent the loss of microtubules from the K-fibers through the cross-linking or ch-TOG polymerase activity (Gergely, Draviam et al. 2003, Royle, Bright et al. 2005, Lin, Hu et al. 2010, Booth, Hood et al. 2011). Clathrin itself is unable to bind the microtubules and requires TACC3-ch-TOG to perform its role at the K-fibers (Booth, Hood et al. 2011). The stabilizing effects of this complex on the spindle suggests TACC3 has a role in mitosis as an adaptor that brings proteins together into complex on the microtubule to hold K-fibers together. It is still unclear whether this complex also interacts with inter-polar microtubules, and how/if it gains specificity for kinetochore microtubules. The order of recruitment of these proteins to the K-fibers also requires more study, but phosphorylation of TACC3 by mitotic kinase AurA has been shown to play a key role.

Aurora A (AurA) interacts with all the TACC proteins via one or more consensus motifs. The interaction between AurA and TACC3 is important for TACC3's localization and function at the centrosome, which has been supported in several different systems. It has been shown that the inhibition of AurA prevents TACC3 from localizing to the centrosome in humans, suggesting that phosphorylation by this kinase serves as a means of regulating TACC3 recruitment and by association, ch-TOG and clathrin (Conte, Delaval et al. 2003, Kinoshita, Noetzel et al. 2005, LeRoy, Hunter et al. 2007, Booth, Hood et al. 2011). AurA phosphorylates TACC3 at Ser-558. It is possible that this causes

a conformational change that allows TACC3 to bind the microtubules. This phosphorylation event by AurA allows the direct interaction between CHC and TACC3, forming the TACC3-ch-TOG-clathrin complex. This entire complex is loaded onto the spindles and recruits additional proteins for spindle assembly. Further studies are required to understand how the phosphorylation of TACC3 on Ser-558 influences its association with microtubules (Albee and Wiese 2008, Lin, Hu et al. 2010).

Currently, there are multiple theories on how the TACC3-ch-TOG-clathrin complex forms and localizes itself to the kinetochore microtubules. The current leading theory suggests that TACC3 in complex with ch-TOG at the centrosomes is phosphorylated by AurA at Ser-558 causing it to localize to the microtubules. Phosphorylated TACC3 is then able to recruit clathrin to the spindle where it is able to bind multiple TACC3 proteins forming the microtubule bridges and generating the mesh structure **(Figure 1.7)**. Many different studies have provided evidence for this proposed model. It has been shown that the overexpression of TACC3 increases the amount of the TACC3-ch-TOG-clathrin complex on the K-fibers. This caused the chromosome to take more time to align at the metaphase plate, suggesting that mitosis is very sensitive to TACC3 levels, and making TACC3 a likely candidate for controlling the formation of the TACC3-ch-TOG-clathrin complex at the K-fibers (Nixon, Gutiérrez-Caballero et al. 2015). Further evidence for TACC3 as the primary factor recruiting the remaining complex components was gained through the depletion of each of the three complex members. The depletion of TACC3 or ch-TOG greatly reduced the amount of clathrin recruited to the spindle. Depleting TACC3 or clathrin also decreased the binding of ch-TOG to the microtubules. In contrast, depleting ch-TOG seems to have little to no effect on TACC3 localization, where clathrin depletion results in a small but significant decrease in TACC3 spindle localization (Booth, Hood et al. 2011). These experimental results strongly suggest that TACC3 is the first protein of the complex to be recruited to the kinetochore microtubules, in an AurA-dependent manner (Booth, Hood et al. 2011).

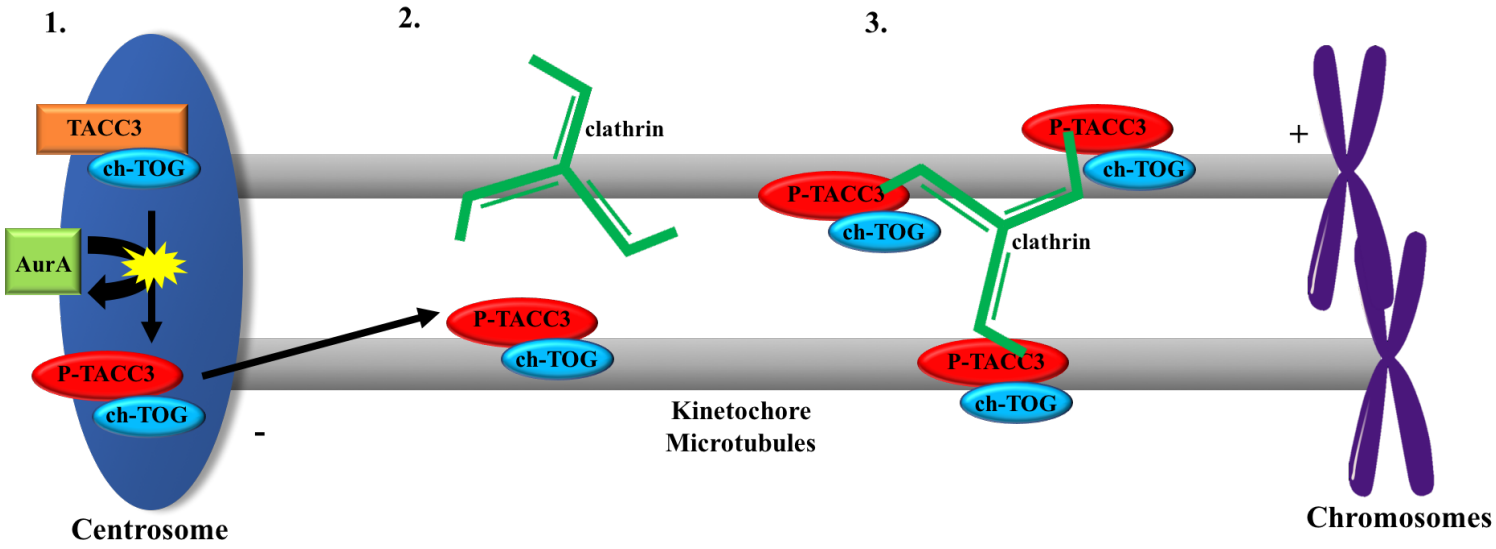

Figure 1.7 Phosphorylated TACC3 forms a complex with ch-TOG and clathrin to help stabilize K-fibers.

One possible model for the formation and localization of the TACC3-ch-TOG-clathrin complex at the kinetochore microtubules. First (1.), TACC3 already bound to ch-TOG at the centrosome is phosphorylated at Ser-558 by AurA. The phosphorylated TACC3-ch-TOG complex then moves to the microtubules and recruits clathrin (2.) The triskelion clathrin is then able to bind multiple p-TACC3-ch-TOG complexes forming the final complex and stabilizing the K-fibers (Booth, Hood et al. 2011, Hood and Royle 2011, Royle 2012, Thakur, Singh et al. 2013).

Increasing numbers of studies into TACC3 have identified several other protein binding partners, although the function of their interactions is less clear at this time. NDEL1, an AurA substrate may be required for TACC3 recruitment to the centrosomes, potentially serving to connect TACC3 and AurA(Mori, Yano et al. 2007). SNX9 and Hsp72 have both been implicated in the recruitment and assembly of TACC3-ch-TOG- clathrin complex at the K-fibers (Ma, Robinson et al. 2013, O'Regan,

Sampson et al. 2015). It is clear that TACC3 alone and in complex plays an important role in mitosis. More research is necessary to fully understand the molecular mechanisms taking place at the mitotic spindle. As more and more information is uncovered implicating TACC3 in cancers, understanding the role TACC3 is playing at the molecular level will allow researchers to develop new strategies.

1.5.4 TACC3 and cancer

TACC3 is emerging as an interesting target in cancer. In the past year alone 14 papers on TACC3 and its expression or role in cancer cells have been published. The TACC3 gene maps to 4p16, which is within a translocation breakpoint region. Its aberrant expression has been detected in various cancers leading to numerous mitotic defects. However whether it is functioning as an oncogene or tumor suppressor is still unclear (Ding, Huang et al. 2017). It has been shown to be upregulated in many different cancers including lung, prostate, glioma, cholangiocarcinoma, colorectal and gastric. Interestingly, it has been shown to be downregulated in thyroid and ovarian cancers (Peters, Kudla et al. 2005, Ulisse, Baldini et al. 2007, Yun, Rong et al. 2015, Du, Liu et al. 2016, He, Yao et al. 2016, Jiang, Kuang et al. 2016, Ding, Huang et al. 2017, Li, Ye et al. 2017, Sun, Tian et al. 2017). Understanding the mechanism of TACC3 in cancer may help to target cancer cells and mitotic processes without impacting the microtubule activity in non-dividing cells (Ding, Huang et al. 2017).

An FGFR3-TACC3 fusion protein has been identified in many cancers, with the TACC domain remaining highly conserved, leading to increased levels of fibroblast growth factor receptor 3 (FGFR3) activation, which then turns on other signaling pathways such as the key ERK and PI3K/Akt pathways (Yuan, Liu et al. 2014). The fusion product localizes to spindle poles and moves to the mid-body in late mitosis, which is different than TACC3 alone (Singh,

Chan et al. 2012). EGF/EGFRs are inducers of the epithelial-mesenchymal transition (EMT), which plays a major role in metastasis of cancer cells. Depletion of TACC3 in cancer cells has been shown in cervical cancer to abolish EGF-mediated EMT, decreasing the chance the cell will undergo metastasis (Ha, Kim et al. 2013, Petschnigg, Kotlyar et al. 2017).

In prostate cancer, the expression of TACC3 is significantly upregulated compared to normal tissue and is associated with poor prognosis. Downregulating TACC3 in these cells repressed prostate cancer cell migration and invasion. This study by Li, *et al*. found a direct correlation between the mRNA expression level of TACC3 and the aggressiveness of the prostate cancer. They also found that the increased expression led to significantly shorter survival times in patients with lower TACC3 expression. The Wnt/β-catenin signaling pathway is a pathway that when activated contributes to metastasis and is frequently activated in prostate cancer. Silencing TACC3 in prostate cancer cells reduced the expression of β-catenin, suggesting that the overexpression of TACC3 may play a role in activating this pathway and therefore inducing metastasis. This makes TACC3 an attractive target for preventing metastasis in prostate cancer cells (Li, Ye et al. 2017).

A study by Sun *et al*. 2017 looked at the expression of TACC3 in glioma. They found that increased TACC3 expression was associated with higher grade tumors, mutations in isocitrate dehydrogenase and more. They believe TACC3 may impact DNA repair in addition to the cell cycle and that TACC3 has the potential to be predictive marker for chemo- and radiotherapy. Consistent with the study done in prostate cancer, this study also found that higher expression levels of TACC3 led to decreased prognosis and survival time. Specifically, they identified TACC3 as an independent prognostic factor for overall survival (Sun, Tian et al. 2017).

A study of TACC3 in cholangiocarcinoma by He *et al*. 2016 found that TACC3 may be an anti-cancer molecular drug target of histone deacetylase inhibitors (HDACIs). They found that TACC3 mRNA was downregulated in cells treated with HDACIs, and that TACC3 protein levels were increased in untreated cholangiocarcinoma cells (He, Yao et al. 2016). This is consistent with the above studies, strongly implicating increased TACC3 expression with cancer.

From this small sample of the many studies of TACC3 and its role in various cancers, it is clear to see that more research must be done to understand TACC3's role and how we can use it as a potential anti-cancer target.

1.6 Project objectives and hypothesis

With limited knowledge of TACC3 and its many roles in the cell as well as its implication in many cancers, there is much to explore with regards to this protein. We hypothesize that TACC3 is a regulatory subunit of PP1, binding through the RVxF motif, and serves to either regulate or be regulated by PP1. It is also hypothesized that PP1 interacts with TACC3 specifically during mitosis, potentially impacting the spindle associated function of TACC3. Additionally, since aberrant TACC3 expression has been implicated in many different cancers, we also believe it may be a potential biomarker, prognostic marker or therapeutic target in cancer treatment.

1.6.1 Specific research objectives

- Confirm that the interaction between TACC3 and PP1 is direct and occurs through the conserved RVxF motif both *in vivo* and *in vitro* using various biochemical techniques.
- Investigate whether the binding of TACC3 and PP1 is dependent on the phosphorylation status of the RVxF motif or other phosphorylation sites of TACC3.

- Gain insight into the timing of the TACC3-PP1 interaction, specifically whether the interaction is mitosis specific.
- Explore the link between TACC3 and cancer using a bioinformatics approach.

Chapter Two: TACC3 and PP1 interact specifically through the RVxF motif

2.1 Introduction

Protein phosphorylation, as previously discussed, is a key post-translational modification, crucial for the regulation of many different cellular processes. Identifying the kinases and phosphatases responsible for these modifications and how they interact with different proteins is key to understanding the vast signaling network of reversible protein phosphorylation.

Previous work has been done to identify new PP1 regulatory subunits. TACC3 was first identified as a novel PP1 regulatory subunit by Nasa (2016). Utilizing U2OS cells stably expressing GFP-tagged PP1 α, β, γ or GFP- alone, she performed a GFP-Trap experiment to pull out PP1 and any interacting proteins. These potential interacting proteins were then sent to the Kettenbach lab at Dartmouth for mass spectrometry analysis. Her work identified 173 asynchronous and 78 mitotic potential PP1 interactors. One of the potential PP1 interacting proteins was identified as TACC3. Since this protein is known to be involved in mitosis and has been implicated in cancer we chose to explore the interaction between TACC3 and PP1. Here, we characterize that TACC3-PP1 interact both *in vitro* and *in vivo,* and is mediated through the highly conserved RVxF motif.

2.2 Materials and methods

2.2.1 Cloning and site directed mutagenesis of TACC3

A pGEX-6p-1 plasmid containing the TACC3 gene with GST- on the N-terminus and -His6 on the C-terminus was obtained through Addgene. The GST-TACC3-His6 was a gift from Stephen Royle (Addgene plasmid # 69106) (Nixon, Gutiérrez-Caballero et al. 2015). The putative PP1

binding motif and/or the proximal Cdk1 consensus site, KVTFQTP (TACC3-WT) within the TACC3 gene in the plasmid was mutated to generate four different mutants: $_{54}$KATAQTP$_{60}$ (TACC3-KATA), $_{54}$KVDFQTP$_{60}$ (TACC3-KVDF), $_{54}$KVTFQEP$_{60}$ (TACC3-EP) and $_{54}$KVDFQTP$_{60}$ (TACC3-KVDFQEP), via site directed mutagenesis. Purified GST-TACC3-His6 plasmid (100ng) was mixed with the respective mutant primer, designed using the QuikChange Primer Design System (Agilent Technologies) and mutated using the QuikChange Lightning Multi Site-Directed Mutagenesis Kit (Agilent Technologies) and PCR (95°C; 2min, [95°C; 20s, 55°C; 30s, 65°C; 225s]$_{30}$, 65°C; 5min. 4°C; forever). The PCR product was then incubated with Dpn1 at 37°C for 5 min. The digestion product was transformed into XL10-gold *E. coli* cells and plated on 100mg/mL ampicillin-LB agar plates and incubated (overnight) O/N at 37°C. Mutated colonies were validated by sequencing through Eurofin MWG Operon LLC sequencing. Plasmids were then transformed into *E. coli* CPRIL BL21 for protein expression.

2.2.2 Sequence alignment of WT TACC3 and RVxF mutants

TACC3 and the RVxF mutant proteins (WT, KATA, KVDF, KVDFQEP, KVDFQEP) sequences were obtained through sequencing (Eurofin). Sequences were aligned using Clustal Omega (Sievers, Wilm et al. 2011).

2.2.3 Expression and purification of wild-type human GST-TACC3-His6 and its four KVTFQTP mutants

E. coli CPRIL BL21 cells containing the WT or mutant TACC3 plasmids were seeded into LB cultures O/N with 100µg/mL ampicillin at 37°C and 200RPM. The saturated cultures were then sub-cultured (1:100) into 1L LB media with 100µg/mL ampicillin. Cultures were then incubated at 37°C with shaking (200RPM) until the OD_{600} reached 0.4, at which time expression was

induced with 0.1mM isopropyl-thio-β-D-galactopyranoside (IPTG). Induction occurred O/N (not to exceed 16h) at 21°C with shaking (200RPM). Following induction, the *E. coli* cells were collected via centrifugation at 5000RPM for 20 min. Cells were then re-suspended in GST lysis buffer (50mM Tris-HCl pH 7.5; 150mM NaCl; 3mM DTT; 0.05% (v/v) NP-40; 1mM benzamidine and 1mM PMSF) and lysed using sonication at level 14 for 7 cycles of 30s pulses. Lysed cells were spun down at 14,000RPM for 40 minutes. The supernatant was removed and filtered through a double layer of miracloth. The filtered lysate was then incubated with 1 mL of Glutathione-Sepharose beads (GE Life Sciences) at 4°C for 1-1.5h. The lysate and beads were then placed in a gravity column and allowed to settle. The beads were washed with 200 column volumes (CV) of GST-wash buffer A (25mM Tris-HCl pH7.5; 750mM NaCl; 1mM DTT; 0.1% (v/v) NP-40) followed by washing with 50CV of GST-wash buffer B (25mM Tris-HCl pH7.5; 150mM NaCl; 1mM DTT). TACC3 proteins were then eluted using GST-elution buffer (25mM Tris-HCl pH 7.5; 150mM NaCl; 1mM DTT; 30mM reduced Glutathione – pH to 8.0). 2mL of elution buffer was added to the column and allowed to incubate with the beads for 5 min then collected. This was repeated 5 times for a total elution volume of 10mL. Eluted TACC3 proteins were then concentrated down to ~300μL using a 30kDa Centricon. Concentrated proteins were then dialyzed O/N into GST-pulldown assay buffer (25mM Tris-HCl pH 7.5; 150mM NaCl; 5% glycerol). Dialyzed proteins were assayed using Bradford reagent with BSA as a standard to determine the concentration and either used immediately, or stored at -80°C. TACC3 has an expected molecular weight of 140kDa. With the addition of the N-terminal GST tag (26kDa) and the C-terminal His6 tag (1kDa) the GST-TACC3-His6 protein was an expected molecular weight of approximately 170kDa. The presence of full-length protein was confirmed through Western

blotting with three different antibodies, Anti-GST (N-terminal tag), Anti-TACC3 (protein of interest) and Anti-His6 (C-terminal tag) (**Figure 2.1**).

2.2.4 Western blotting and antibodies

Samples for immunoblotting were run on SDS-PAGE, transferred onto nitrocellulose membranes for 200V/h and then probed with the appropriate antibodies. Antibodies and their dilutions used in this study: Anti-GST (RGST-45A-Z, ICL, 1:500), Anti-PP1/Anti-PP1α (SC7482, Santa Cruz, 1:500), Anti-PP1β (Ab53315, AbCam, 1:50000), Anti-PP1γ (in-house, 1:500), Anti-TACC3 (8069, Cell Signaling Technology, 1:1000), Anti-His6 (MHIS-45ALY-Z, ICL, 1:10000), and Anti-GFP (11814460001, Roche Diagnostics, 1:1000). Following incubation with the primary antibodies, membranes were washed (3x5min) with TBS+ 0.1% (v/v) Tween-20 and then incubated with HRP-conjugated goat anti-mouse or goat anti-rabbit (Thermo-Fisher Scientific, 1:5000). Membranes were again washed (3x5min) with TBS+ 0.1% (v/v) Tween-20 and developed with enhanced chemiluminescence (ECL; Perkin-Elmer).

2.2.5 Expression and purification of human PP1 isoforms

PP1 (α, β, γ) was expressed and purified as described in Moorhead *et al.* 1994(Moorhead, MacKintosh et al. 1994). In summary, *E. coli* CPRIL BL21 cells containing pCW-PP1 plasmid (α, β, γ) were seeded into LB cultures overnight (O/N) with 100μg/mL ampicillin at 37°C and 200RPM. Saturated cultures were sub-cultured (1:100) into 1L LB media with 100μg/mL ampicillin. Cultures were then incubated at 28°C with shaking (200RPM) until the OD_{600} reached 0.4, at which time expression was induced with 0.3mM IPTG. Induction occurred O/N (not to exceed 16h) at 28°C with shaking (200RPM). Following induction, the *E. coli* cells wer

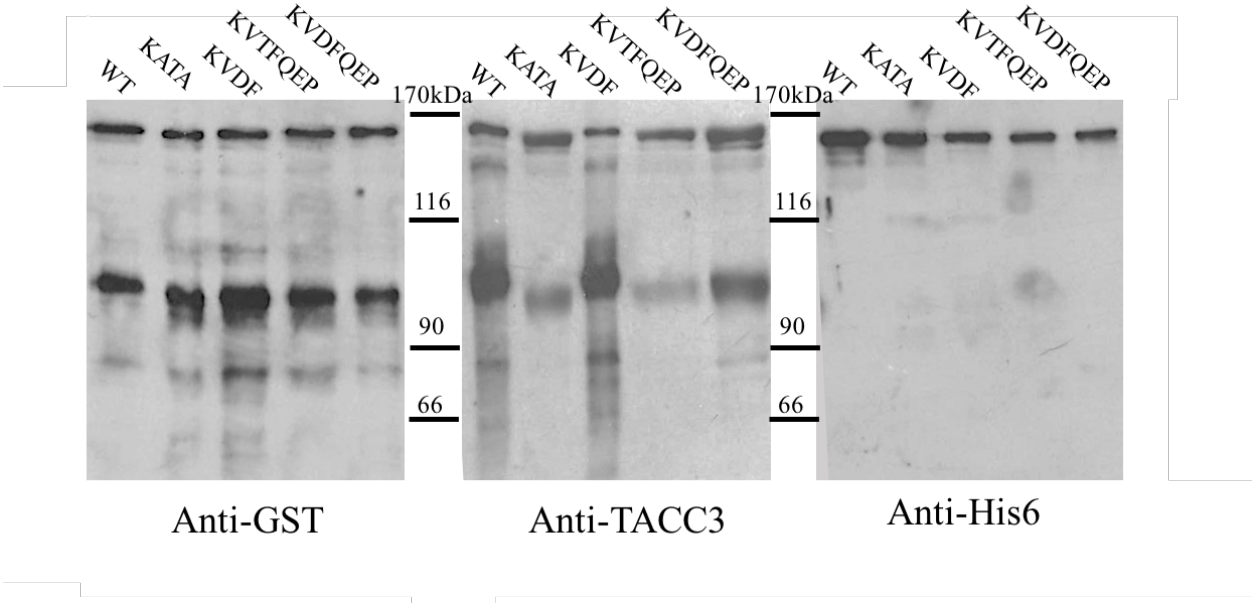

Figure 2.1 Confirmation of full-length GST-TACC3-His6.

BL21 *E. coli* cells expressing one of five versions of GST-TACC3-His6 (WT, KATA, KVDF, KVTFQEP or KVDFQEP) were collected and lysates were incubated with Glutathione Sepharose beads (GST purification). To confirm the protein purified was full-length TACC3 with both the N-terminal GST tag and the C-terminal His6 tag, purified protein was separated using SDS-PAGE and analyzed using western blotting. Expected molecular weight for full-length GST-TACC3-His6 is approximately 170kDa (n=3).

collected via centrifugation at 5000RPM for 20 min. Cells were then re-suspended in PP1 resuspension buffer (50mM HEPES pH 7.5; 100mM KCl; 1mM EDTA; 2mM $MnCl_2$; 5% (v/v) glycerol; 0.1% (v/v) BME and 0.1mM PMSF) and lysed using sonication at level 14 for 7 cycles of 30s pulses. Lysed cells were spun down at 14,000RPM for 40 minutes. The supernatant was

removed and filtered through a double layer of miracloth. The filtered lysate was then incubated with 1 mL of Sepharose beads covalently linked with microcystin-LR at 4°C for 1.5h. The lysate and beads were then placed in a gravity column and allowed to settle. Beads were then washed with 200CV of PP1 wash buffer A (50 mM Tris-HCl pH 7.5; 0.5M NaCl; 0.1 mM EGTA; 5% (v/v) glycerol; 1 mM $MnCl_2$; 0.1% (v/v) BME) followed by washing with 50CV of PP1 wash buffer B (50 mM Tris-HCl pH 7.5; 0.1 mM EGTA; 5% (v/v) glycerol; 1 mM $MnCl_2$; 0.1% (v/v) BME). The PP1 isoforms were then eluted using PP1 wash buffer B with an additional 3M NaSCN. 5 mL of the elution mixture was added to the column and allowed to incubate for 30 minutes. The 5mL was then collected and the column was washed with an additional 5mL of the elution mixture. Eluted PP1 proteins were dialyzed O/N into dialysis buffer 1 (PBS; 0.2M KCl and 0.1% (v/v) BME). Dialyzed proteins were then concentrated down to ~500µL using a 10kDa centricon and the concentrated PP1 proteins were dialyzed once more O/N into dialysis buffer 2 (PBS; 0.2M KCl and 0.1% (v/v) BME and 50% glycerol). Dialyzed proteins were then assayed using Bradford reagent with BSA as a standard to determine the concentration and either used immediately, or stored at -80°C. Each isoform of PP1 (α, β, γ) has an expected molecular weight of 37kDa. Isoform specific antibodies were used to identify each isoform through western blotting purified protein (**Figure 2.2**).

2.2.6 In-vitro PP1 binding assay

Glutathione Sepharose beads (50µL) were blocked with 5% (w/v) BSA in assay buffer (25mM Tris-HCl pH 7.5; 150mM NaCl) for 30min at 4°C. Blocked beads were washed (1x5min) with assay buffer. TACC3 was purified as described in **Section 2.2.3**, added to the beads along with

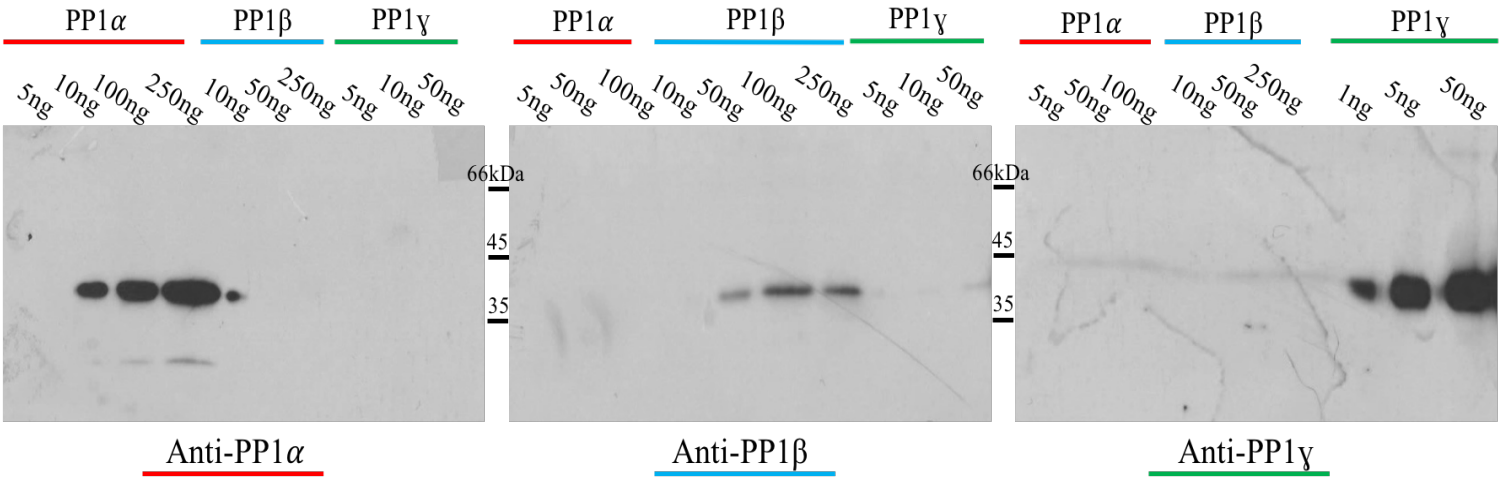

Figure 2.2 Validation of isoform specific PP1 antibodies.

BL21 *E. coli* cells expressing either PP1α, β, or γ were collected purified using microcystin sepharose. To confirm the protein purified was the correct isoform and that the antibodies were not cross-reacting, purified protein was separated using SDS-PAGE and analyzed using western blotting. Expected molecular weight for all PP1 isoforms is 37kDa (n=3).

assay buffer to a total volume of 500µL, and incubated end-over-end (EOE) for 30min at 4°C. Purified PP1 (as described in **Section 2.2.5**) was added, and the mixture was allowed to incubate EOE for another 2h at 4°C. Beads were then washed (3x5min) with wash buffer (25mM Tris-HCl pH 7.5; 150mM NaCl; 0.01% (v/v) NP-40) and eluted by boiling (10min) with 2X SDS buffer. Eluates were analyzed by western blotting (**Section 2.2.4**).

2.2.7 HeLa cell culture, mitotic cell synchronization, cell cycle synchronization and cell lysate collection

HeLa cells obtained from ATCC were cultured in DMEM and supplemented with 10% (v/v) FBS and 10U/mL penicillin-streptomycin. To obtain mitotic cell populations, cells were arrested in pro-metaphase with 40ng/mL nocodazole. After 12-16h of arrest, cells were released into fresh media for 30min to ensure they entered mitosis. To synchronize cells for cell cycle collection, cells were arrested with 2mM thymidine for 17h followed by 7h release. Following release, cells were blocked in prometaphase with 40 ng/mL nocodazole. After 9 h arrest, the cells were released into fresh media and harvested at different time points within a 24 h cycle. All cells (asynchronous, mitotic, cell cycle) were collected in the same manner. Cells were washed with PBS and either scraped (asynchronous and cell cycle) or shook-off (mitotic) into lysis buffer (10mM Tris-HCl pH 7.5; 150mM NaCl, 5mM EDTA and 0.5% (v/v) NP-40). Lysates were sonicated at level 7 for 3 rounds of 30s pulses and spun down (14000RPM at 4°C for 10 min) to remove cellular debris. Protein concentration was determined using the Bradford assay with BSA as a standard. Lysates were either used immediately, or stored at -80°C.

2.2.8 GST-TACC3-His6 pulldown of PP1 in HeLa cells

Glutathione Sepharose beads (50μL) were blocked with 5% (w/v) BSA in assay buffer (25mM Tris-HCl pH 7.5; 150mM NaCl; 1mM EDTA) for 30min at 4°C. Beads were then washed (1x5min) with assay buffer. TACC3 was purified as described in **Section 2.2.3**, was added to the beads along with assay buffer to a total volume of 500μL, and incubated EOE for 30min -1h at 4°C. Following the incubation, beads were spun down and the supernatant removed. HeLa cell lysates (described in **Section 2.2.7**) were added to the beads and incubated EOE for an additional

1-1.5h at 4°C. Beads were washed (3x5min) with wash buffer (25mM Tris-HCl pH 7.5; 150mM NaCl; 1mM EDTA; 0.1% (v/v) NP-40) and eluted by boiling (10min) with 2X SDS buffer. Eluates were analyzed by western blotting (**Section 2.2.4**) (n=3).

2.2.9 U2OS cell culture, mitotic cell synchronization and cell lysate collection

U2OS cells expressing GFP-alone or one of three GFP-tagged isoforms (GFP-C, GFP-PP1α, GFP-PP1β and GFP-PP1γ) were a generous gift from Dr. Laura Trinkle-Mulcahy, University of Ottawa (Trinkle-Mulcahy, Chusainow et al. 2007). When these stable cell lines were generated, they were specifically selected for cells expressing GFP-tagged PP1α, β, and γ at endogenous levels. The cells were cultured in DMEM and supplemented with 10% (v/v) FBS and 400μg/mL gentecin (G418; Gold Biotechnology). To obtain mitotic cell populations, cells were arrested in pro-metaphase with 40ng/mL nocodazole. After 12-16h of arrest, cells were released into fresh media for 30min to ensure the cells entered mitosis. Mitotic and asynchronous cells were collected. Cells were washed with PBS and either scraped (asynchronous) or shook-off (mitotic) into GFP-Trap lysis buffer (10mM Tris-HCl pH 7.5; 150mM NaCl, 0.5mM EDTA and 0.5% (v/v) NP-40). Lysates were sonicated at level 7 for 3 rounds of 30s pulses and spun down (14000RPM at 4°C for 10 min) to remove cellular debris. Protein concentration was determined using the Bradford assay with BSA as a standard. Lysates were either used immediately, or stored at -80°C. Endogenous TACC3 has an expected molecular weight of 140kDa. With the addition of the N-terminal GFP tag (27kDa), the GFP-TACC3 protein has an expected molecular weight of approximately 170kDa.

2.2.10 GFP-Trap using U2OS GFP-tagged PP1 cells

Mitotic and asynchronous U2OS cell lysates (as described in **Section 2.2.9**) were incubated with GFP-Trap_A beads (Chromotek) for 1h at 4°C. Following incubation, the beads were washed (3x5min) with GFP-Trap wash buffer A (10mM Tris-HCl pH 7.5; 150mM NaCl; 0.5mM EDTA and 0.5% (v/v) NP-40) then with GFP-Trap wash buffer B (10mM Tris-HCl pH 7.5; 150mM NaCl and 0.5mM EDTA). Bound proteins were eluted with 2X SDS buffer and eluates were analyzed by western blotting (**Section 2.2.4**) (n=4).

2.2.11 Transfection of HeLa cells with GFP-TACC3

A pBrain plasmid containing the TACC3 gene with GFP- on the N-terminus and an shRNA site to knockdown endogenous TACC3 was obtained through Addgene. The pBrain-GFP-TACC3KDP-shTACC3 was a gift from Stephen Royle (Addgene plasmid #59356)(Booth, Hood et al. 2011). The presence of the sh-RNA site will function to knock down the endogenous TACC3 in the HeLa cells so only knock-down proof GFP-tagged TACC3 will be expressed. HeLa cells were cultured in antibiotic-free DMEM, supplemented with 10% (v/v) FBS and grown to 60-70% confluency. GFP-TACC3 plasmid was diluted with Opti-MEM reduced serum media (Thermo-Fisher Scientific) while Lipofectamine® 2000 (Thermo-Fisher) was also diluted with Opti-MEM. Both solutions were allowed a short incubation (5min) at room temperature and then were combined and again allowed to incubate for 5min at room temperature. The plasmid-Lipofectamine mixture was then added drop-wise to HeLa cells and allowed to react at 37°C for 48h. Cells were either collected (as previously described in **Section 2.2.7**) or placed under selective pressure using DMEM supplements with 10% (v/v) FBS, 10U/mL penicillin-

streptomycin and 400μg/mL Geneticin (G418; Gold Biotechnology). Collected cells were analyzed through western blotting (**Section 2.2.4**) (n=5).

2.3 Results and discussion

2.3.1 TACC3 sequence analysis

Following the identification of TACC3 as a potential PP1 interactor through mass spectrometry, we searched the protein sequence for the presence of a PP1 binding motif. We identified an RVxF motif with sequence KVTF at residues 54-57 in the N-terminal region of the protein. The perfect PP1 binding RVxF motif as well as the presence of a threonine residue in the x position makes TACC3 an excellent candidate for a PP1 regulatory subunit. Threonine is a polar amino acid and accounts for approximately 12% of the protein phosphorylation events within the proteome. As previously mentioned, the presence of a serine or threonine residue in the x position of the RVxF motif acts a means of regulating PP1 docking to the regulatory subunits. The large phosphoryl group blocks the Val and Phe residues from docking into the hydrophobic binding groove on the PP1-catalytic subunit. Since TACC3 contains an RVxF motif with sequence KVTF, it seems probable that TACC3 interacts with PP1 via this sequence and that the binding is controlled through the phosphorylation of Thr-56. Threonine-56 has been reported as being phosphorylated in several data sets and studies (Kettenbach, Schweppe et al. 2011, Klammer, Kaminski et al. 2012). Although the kinase and phosphatase responsible have yet to be identified, the literature supports the idea that the TACC3-PP1 interaction is regulated through phosphorylation of the RVxF motif. Interestingly, there is a Cdk1 phosphorylation site (S/TP) located only two residues downstream of the RVxF motif within the N-terminal region of

TACC3. The TP site (residues 59-60) has been reported as phosphorylated in over 60 data sets and studies (Yu, Zhu et al. 2007, Miller, Brunak et al. 2010, Kettenbach, Schweppe et al. 2011, Klammer, Kaminski et al. 2012, Mertins, Qiao et al. 2013, Mertins, Yang et al. 2014, Sharma, D'Souza et al. 2014, Mertins, Mani et al. 2016). With the proximity to the RVxF motif, it is possible that the phosphorylation of Thr-59 may also prevent PP1 docking to TACC3, and one or both phosphorylated threonine residues may regulate the PP1-TACC3 interaction. The phosphorylation site of a nearby TP site has been previously shown to regulate PP1 docking to the RVxF in other cases such as NIPP-1 (Beullens, Van Eynde et al. 1999).

In order to explore that TACC3 and PP1 are interacting through the RVxF motif, and that the interaction is regulated through the phosphorylation of Thr-56 and/or Thr-59 we successfully generated a series of four TACC3-RVxF mutants: TACC3-$_{54}$KATA$_{57,}$ the non-binding mutant missing the key valine and phenylalanine residues required for PP1 docking; TACC3-$_{54}$KVDF$_{57}$, the RVxF phospho-mimetic mutant with aspartic acid in the x position to mimic a state of constant phosphorylation; TACC3-$_{59}$EP$_{60}$, the TP phospho-mimetic mutant to again mimic a constant state of phosphorylation; and the TACC3-$_{54}$KVDFQEP$_{60}$ mutant, mimicking constant phosphorylation at both the RVxF motif and the TP site. The mutants were generated through site-directed mutagenesis and validated with sequencing (**Figure 2.3**). The wild-type TACC3 protein and the four TACC3 RVxF/TP mutant proteins were expressed and purified from *E. coli* cells (**Figure 2.4**). The purification was performed with Glutathione-Sepharose, and as can be seen in the colloidal stains (**Figure 2.4, A-E**) there are some degradation products present in the final eluates, however, the presence of the full-length protein was validated through western blotting (**Figure 2.4, F**).

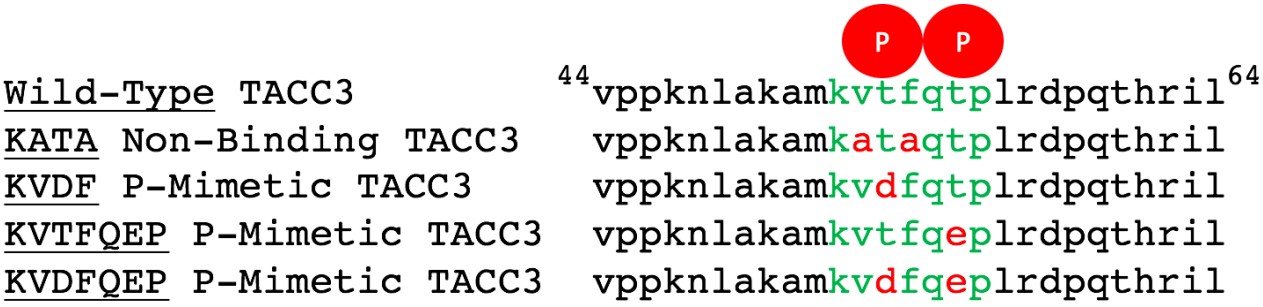

Figure 2.3 Alignment of wild-type TACC3 and four RVxF TACC3 mutants.
The partial protein sequences (residues 44-64 of 838) of human TACC3 and four RVxF TACC3 mutants. Full protein is 838 amino acids. Partial sequences were aligned using Clustal Omega. The conserved RVxF docking site (residues 54-57) and the Cdk1 TP phosphorylation site (residues 59-60) are indicated in green. Mutated residues are indicated for each mutant in red. The red circles represent phosphorylation of the threonine residues (T56/T59) and how access to the key docking residues (V55/F57) would be restricted when the motifs are phosphorylated.

2.3.2 TACC3 protein levels are decreased outside of mitosis

Previous studies have indicated that TACC3 levels are reduced outside of mitosis via a proteasome-dependent pathway (Jeng, Lin et al. 2009). We confirmed this result through a cell cycle experiment. Our results support the previously published work (**Figure 2.5**). HeLa cells were synchronized and collected as described in **Section 2.2.9**. The blot shows that the TACC3 levels follow that same pattern as known mitotic markers CyclinB1 and H3S10, with protein levels peaking at 1-2 hours and beginning to decrease after mitosis (3h).

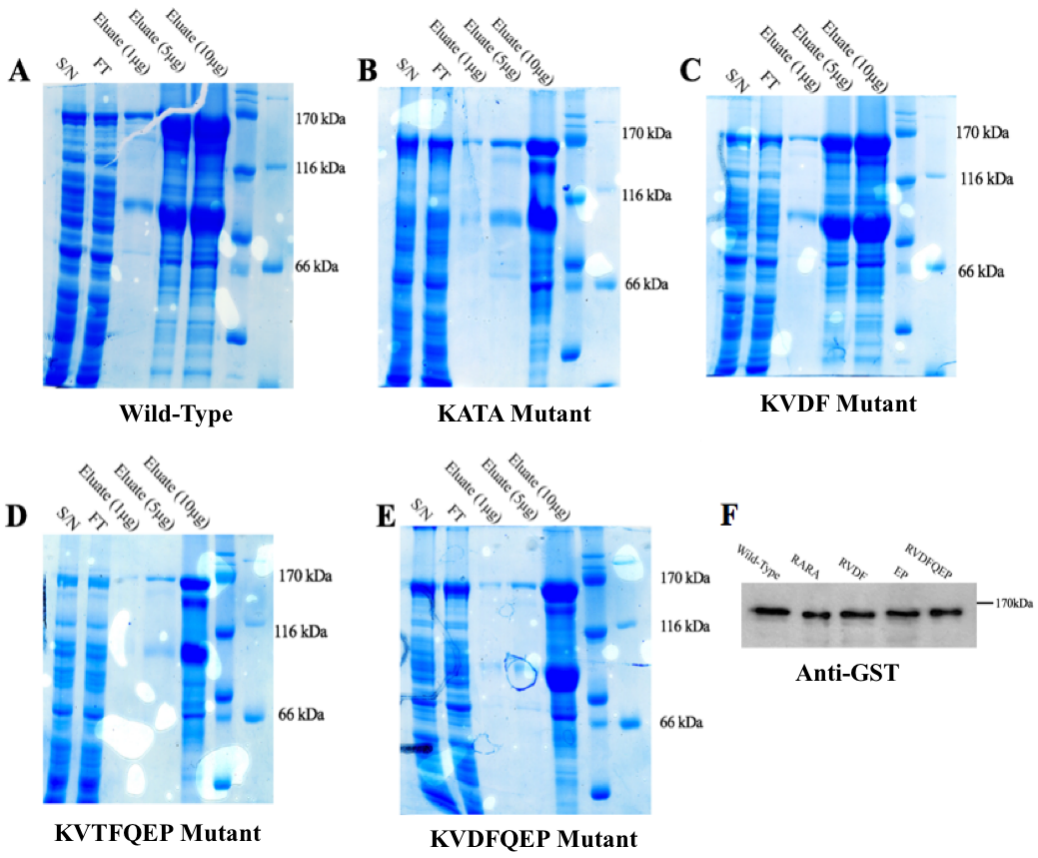

Figure 2.4 Expression and purification of wild-type GST-TACC3-His6 and RVxF mutants from *E.coli* BL21 cells.

BL21 *E. coli* cells expressing one of five versions of GST-TACC3-His6 (WT, KATA, KVDF, KVTFQEP or KVDFQEP) were collected and lysates were incubated with Glutathione Sepharose beads (GST purification). Panels **A-E.** Colloidal stain of the expression and purification procedure. **A.** Wild-type TACC3 protein. **B.** KATA - non-binding mutant protein. **C.** KVDF - phospho-mimetic mutant protein. **D.** KVTFQEP - phospho-mimetic protein. **E.** KVTFQEP - double phospho-mimetic protein. **F.** Western blot confirming the identity of the WT and 4 RVxF mutant proteins as GST-TACC3-His6. Blot was probed with Anti-GST antibody (ICL Labs). Molecular weight markers are indicated on the right (n=15).

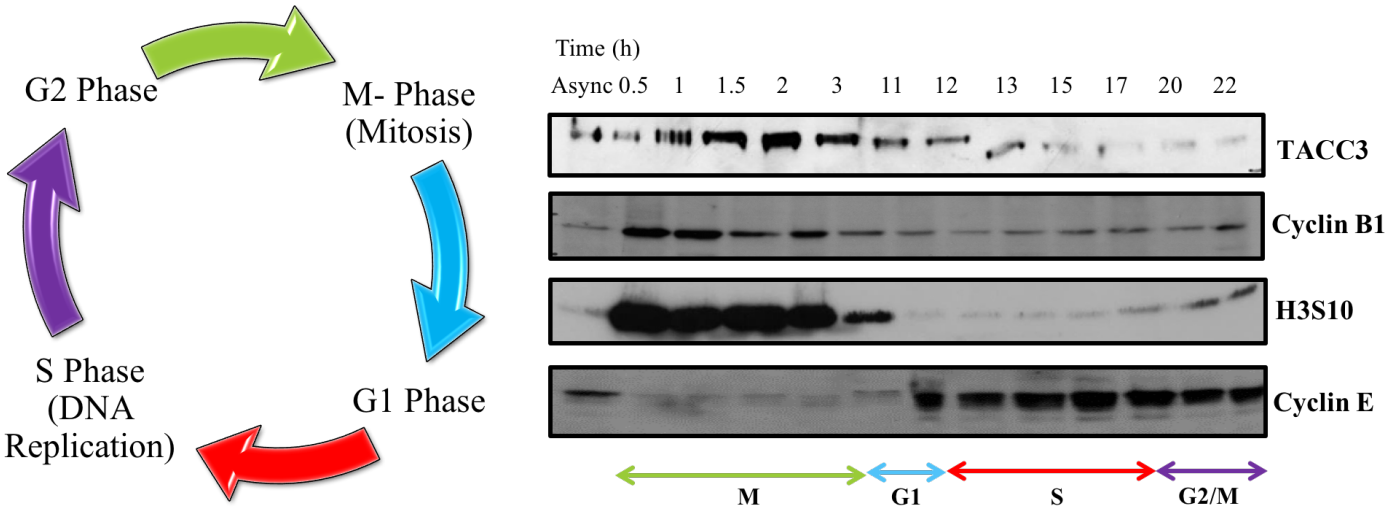

Figure 2.5 TACC3 protein levels are decreased outside mitosis

HeLa cells were synchronized in G2/M phase following an incubation with thymidine/nocodazole. Cells were collected every hour and cell lysate proteins were separated using SDS-PAGE. Membranes were probed for the presence of TACC3 (Cell Signalling) or known cell cycle markers: CyclinB1 – mitotic marker, H3S10 – mitotic marker, and CyclinE – interphase marker (n=2).

2.3.3 TACC3 binds PP1 in vitro

The mass-spectrometry data showed that TACC3 interacted with PP1 in mitotic and asynchronous eluates. To determine if the interaction between TACC3 and PP1 is direct, an *in vitro* PP1 binding assay using partially purified full-length TACC3 and PP1 was performed and the eluates were western blotted for the presence of PP1. The blot shows the presence of PP1 in the TACC3, as compared to the control with GST alone, suggesting the interaction between the two proteins is direct (**Figure 2.6**).

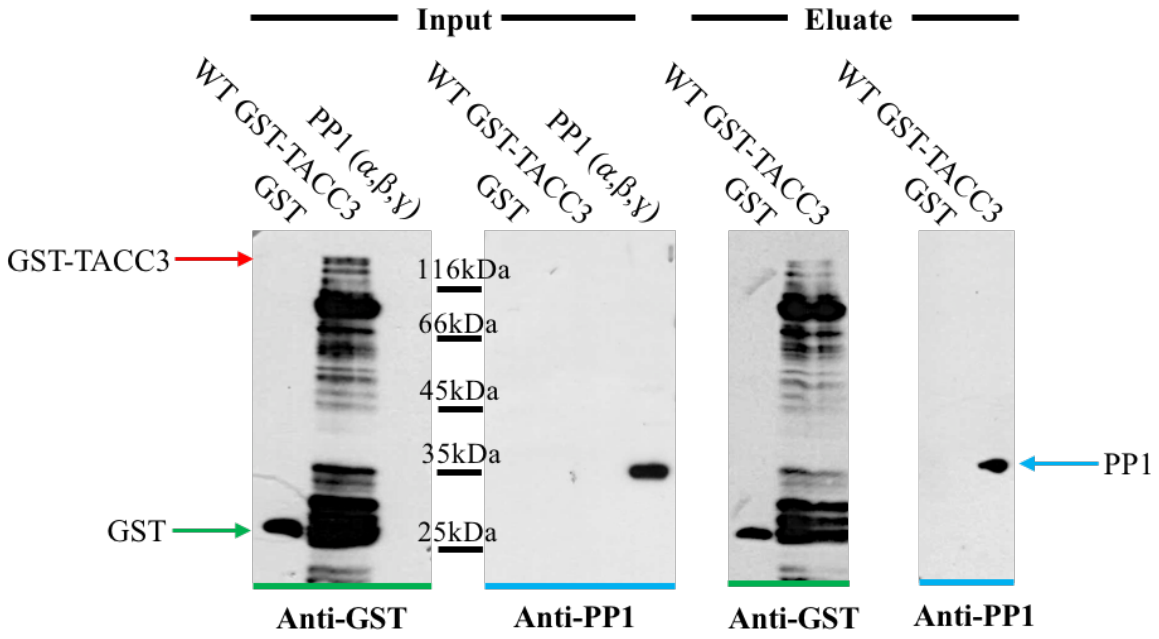

Figure 2.6 GST-TACC3-His6 binds recombinant PP1 *in vitro*.

Glutathione Sepharose beads were incubated with purified wild-type GST-TACC3-His6, or GST protein alone. Purified human PP1 (α, β, ɣ) and protein complexes were eluted from the resin using 2X-SDS buffer and separated using SDS-PAGE. Membranes were probed for the presence of PP1 in the eluates with Anti-PP1 (Santa-Cruz), and controls were probed with Anti-GST (ICL Labs) (n=6).

2.3.4 TACC3 binds PP1α, β, and γ via the RVxF motif in vitro

TACC3 has a perfect PP1 RVxF motif with sequence KVTF, making it an ideal PP1 interacting partner. With the confirmation that TACC3 and PP1 are binding *in vitro* we set out to validate that the interaction between the two proteins is occurring via the RVxF motif. Additionally, we wanted to explore the role of phosphorylation either within the RVxF motif

and/or at the Cdk1 site to regulate the docking of TACC3 to PP1. The *in vitro* PP1 isoform binding assay was performed using wild-type TACC3 and the previously discussed TACC3 mutants. The TACC3 proteins were incubated with each of the three isoforms of PP1 (α, β, γ) to see if the proteins showed a preference for a specific isoform. Western blot analysis was performed on eluates from the experiment and probed for the presence of PP1α, PP1β or PP1γ. The blots show the presence of all three PP1 isoforms in the wild-type at similar levels, as compared to the GST control alone, suggesting that the interaction between the two proteins is not isoform specific (**Figure 2.7**). Due to the high degree of similarity between the three PP1 isoforms, it is not surprising that TACC3 is able to bind all of them. Looking at the TACC3-KATA mutant, or the non-binding mutant, we observe a reduction in PP1 signal to below the levels of detection (**Figure 2.7**). This result supports the idea that the RVxF is important for interaction with PP1, and emphasizes the key roles of the valine and phenylalanine for docking. With regards to the role of phosphorylation as a means of regulating the TACC3-PP1 interaction, we see slightly different results between the three isoforms of PP1. PP1α is present with the TACC3-KVDF mutant as well as the TACC3-KVDFQEP mutant, but is not present with the TACC3-EP mutant (**Figure 2.7**). It is important to note that the amount of PP1 present in the TACC3-KVDF and TACC3-KVDFQEP mutants is less when compared to the wild-type TACC3. The presence of PP1 with the TACC3-KVDF and lack of PP1 with the TACC3-EP suggest that phosphorylation of the Cdk1 site may be responsible for the regulation of PP1 docking to the TACC3 RVxF motif, however, the presence of a band in the TACC3-KVDFQEP mutant suggests phosphorylation of these two motifs does not control PP1 binding. In comparison, PP1β is present with the TACC3-EP and TACC3-KVDFQEP mutants but not with

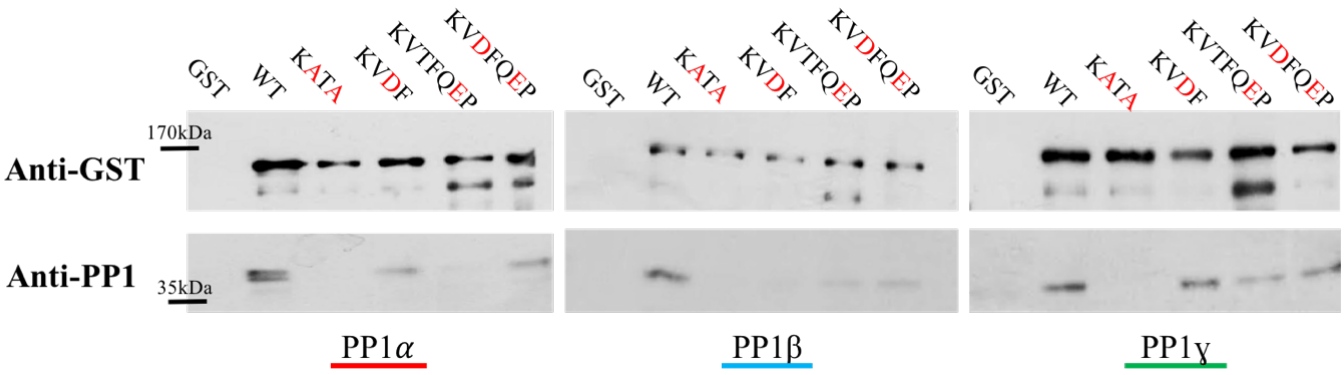

Figure 2.7 GST-TACC3-His6 binds all isoforms of recombinant PP1 *in vitro* through the RVxF motif.

Glutathione Sepharose beads were incubated with purified wild-type GST-TACC3-His6 as well as with the four TACC3 mutants. Purified human PP1 (α, β, or γ) was added and complexes were eluted from the resin using 2X-SDS buffer and run on SDS-PAGE. Membranes were probed for the presence of PP1 in the eluates with Anti-PP1 (lower panels; α, Santa-Cruz; β, AbCam γ, in-house), and controls were probed with Anti-GST (upper panels; ICL-Labs) (n=4).

the TACC3-RVDF (**Figure 2.7**). The presence of PP1β with the TACC3-EP and not the TACC3-RVDF would suggest that phosphorylation of the RVxF is regulating PP1 docking, but like PP1α, the presence of PP1β with the TACC3-KVDFQEP would suggest neither phosphorylation site is responsible. Similar to PP1α, less PP1β appears with the RVDF-EP and PP1-RVDFQEP mutants. Finally, PP1γ is present with TACC3-KVDF, TACC3-EP and TACC3-KVDFQEP (**Figure 2.7**). This result suggests that phosphorylation of the RVxF motif and/or the Cdk1 site is not controlling PP1 docking to the TACC3 RVxF motif.

The results of the *in vitro* PP1 isoform binding assay confirm that TACC3 interacts with all three isoforms of PP1 through the RVxF docking motif. The role of phosphorylation of the RVxF motif and/or the Cdk1 site as a means of regulating the interaction is still unclear. PP1 is still present with the TACC3 phospho-mimetic mutants, but less than is present with the wild-type TACC3. The result obtained suggests that phosphorylation at one or both phosphorylation sites may contribute to regulating binding, but there are likely additional factors playing a role in the overall regulation. One possibility that should be noted is the possibility that the phospho-mimetic residues are not in fact mimicking the effect of phosphorylation in this position. To explore this possibility, a peptide pulldown could be performed using synthetic peptides phosphorylated at Thr56, Thr59 or both.

2.3.5 TACC3 binds PP1 in vivo

Following the validation of the TACC3-PP1 interaction *in-vitro*, we set out to confirm the interaction of these proteins in mammalian systems. Purified wild-type TACC3 and the RVxF mutants were incubated with either asynchronous or mitotic HeLa cell lysate and western blot analysis was performed on the pulldown eluates, probing for the presence of PP1. The blot shows the presence of PP1 with the wild-type TACC3 in both the mitotic and asynchronous experiments, with a much stronger band in the mitotic sample (**Figure 2.8**). No PP1 was found with the GST-only control or any of the TACC3 mutants. The greater amount of PP1 found in the mitotic eluate is expected as it is hypothesized TACC3 and PP1 interact primarily during mitosis. The absence of PP1 with TACC3-KATA further indicates that the TACC3-PP1 interacting is occurring via the RVxF motif. The lack of PP1 with TACC3-KVDF, TACC3-EP and TACC3-KVDFQEP would suggest that phosphorylation at both sites results in abolishment

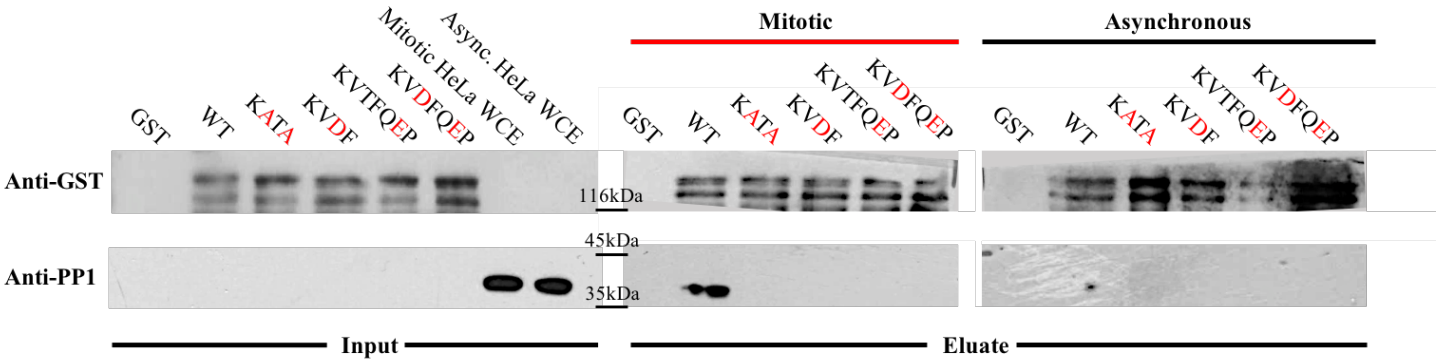

Figure 2.8 GST-TACC3-His6 binds PP1 in HeLa cells.

Glutathione Sepharose beads were incubated with purified wild-type GST-TACC3-His6 as well as with four TACC3 mutants, or GST protein alone. HeLa whole cell lysates (mitotic or asynchronous) were added and complexes were eluted from the resin using 2X-SDS buffer and run on SDS-PAGE. Membranes were probed for the presence of PP1 in the eluates with Anti-PP1 (lower panels; Santa-Cruz) and controls were probed with Anti-GST (upper panels; ICL Labs) (n=3).

of the TACC3-PP1 interaction. It is interesting that no PP1 binding is seen with the phospho-mimetic mutants in the HeLa lysate pulldown, while some binding was seen with the *in vitro* binding assay. Since most cellular proteins are present in the HeLa lysate, it strengthens the idea that additional factors may be contributing to regulating the TACC3-PP1 interaction, and that phosphorylation of these sites alone is not sufficient to completely abolish binding. Another possibility as to why we see no binding of PP1 with these mutants is the possibility of PP1 being bound by endogenous TACC3 still present in the cell lysates. To ensure the results we are seeing

are true, and that the mutants are really not binding PP1, the pulldown should also be done using HeLa cells with endogenous TACC3 knocked down.

To further explore the interaction of TACC3 and PP1 *in vivo*, a GFP-Trap experiment using GFP-tagged PP1 (α, β, γ) expressing U2OS cells showed an enrichment of TACC3 in the mitotic eluates of all three PP1 isoforms, as compared to the GFP control (**Figure 2.9**). Looking at the intensity of the TACC3 bands, it appears TACC3 may prefer binding PP1β, then PP1α and then PP1γ. However, it is important to note that the levels of PP1 in each of the three isoform cell lines corresponds to endogenous levels. PP1β has the highest level of expression, followed by PP1α and finally PP1γ. The blots do show the presence of TACC3 with all three isoforms of PP1 in the asynchronous eluates, however, they are comparable in intensity to the band found with the GFP control. Since cellular levels of TACC3 levels are reduced outside of mitosis (**Figure 2.5**), this result is consistent with the expected result (Jeng, Lin et al. 2009). The results from the GFP-Trap experiment further validate the TACC3-PP1 interaction *in vivo*, and that it is specifically occurring during mitosis. It also provides insight into the possibility that TACC3 may preferentially bind certain isoforms of PP1 *in vivo.*

2.3.6 Transfection of HeLa Cells with GFP-TACC3

To further explore the TACC3-PP1 interaction *in vivo*, we set out to develop a stable HeLa cell line expressing GFP-tagged TACC3, with endogenous TACC3 knocked down. To do this we successfully transfected a plasmid containing the GFP-TACC3 gene into HeLa cells (**Figure 2.10**). The blot shows the presence of the GFP-tagged TACC3 as well as the endogenous TACC3. It has been reported in one recent studies that TACC3 may have several splice variants,

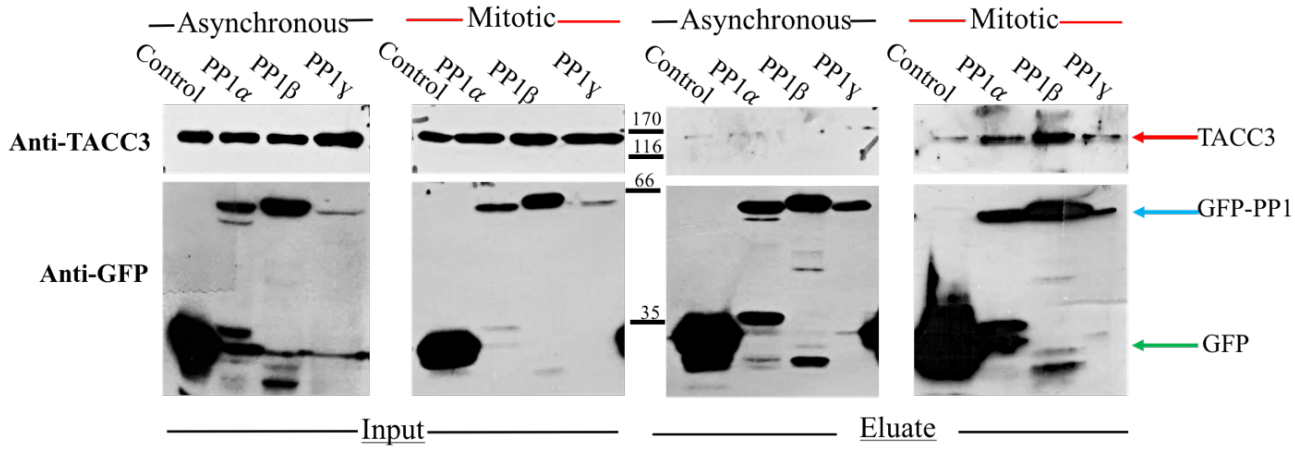

Figure 2.9 GFP-PP1 preferentially binds TACC3 during mitosis in U2OS cell lysates. Asynchronous or mitotic U2OS cell lysates with the GFP-tagged PP1 isoforms were incubated with GFP-Trap beads and allowed to incubate. Elutes were run on SDS-PAGE. Membranes were probed with Anti-TACC3 (upper panels, Cell Signaling), and controls were probed with Anti-GFP (lower panels, Roche) (n=4).

TACC3-001 is the full-length protein at 838 amino acids and 140kDa. The other six variants are all considerable smaller ranging from 16-25kDa. It is possible a dimer of these splice variants may account for the bands seen at the bottom of the transfection blot (Ezkurdia, Juan et al. 2014). To fully develop the stable cell line and fully knock-down the endogenous TACC3, the transfected cells must be placed under selective pressure to remove any un-transfected cells. Once the cells are selected, we would expect to only obtain the top band, and no longer see the endogenous TACC3 expressed.

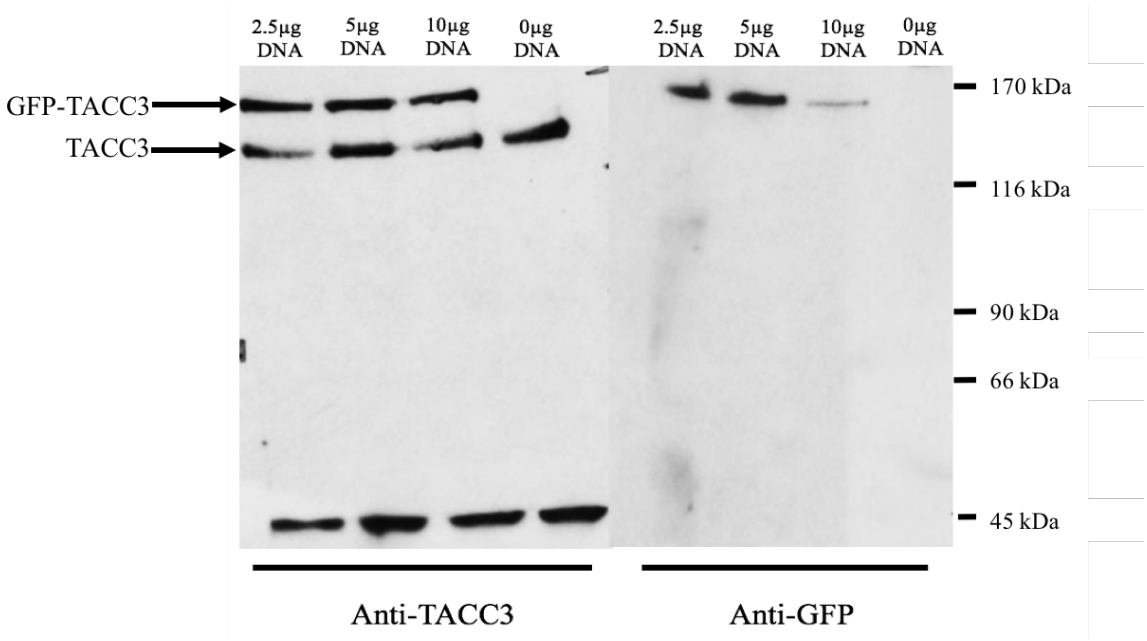

Figure 2.10 Transfection of HeLa cells with pBrain-GFP-TACC3KDP-shRNA.
Purified plasmid was successfully transfected into HeLa cells using Lipofectamine 2000 reagent and Opti-MEM media. Cells were collected and lysed. Membranes were probed with Anti-TACC3 (Cell Signalling) or Anti-GFP (Roche) antibodies (n=5).

2.4 Conclusions

The results presented here confirm the mass spectrometry results, which first identified a potential interaction between TACC3 and PP1. This interaction occurs via the highly conserved RVxF motif with sequence KVTF in TACC3. My results also demonstrate that the Val and Phe are crucial for docking to PP1 and that the mutation of these residues abolishes the interaction. The role of phosphorylation as a means of regulating the interaction still requires more study. *In vitro*, binding is still observed between TACC3 and PP1 when the RVxF and/or Cdk1 site

($_{54}$KVTFQTP$_{60}$) are phosphorylated, although it appears reduced. *In vivo*, binding of the two proteins appears to be abolished upon phosphorylation of one or both motifs. These results suggest that phosphorylation of these motifs is likely playing a role in regulating the TACC3-PP1 interaction but that additional factors are required to fully abolish binding. The *in vitro* and *in vivo* results both show that TACC3 can bind all three isoforms of PP1, however it may prefer PP1β *in vivo.*

2.5 Future directions

With the data presented above, we have confirmed the mass spectrometry data that first detected the TACC3-PP1, and validated that it occurs via the conserved RVxF motif, but we have also raised several questions that require more study. First, understanding the role of phosphorylation of the RVxF and/or Cdk1 site as a means of regulating the TACC3-PP1 interaction requires additional work. Our results here indicate that phosphorylating these motifs may play a role, but further studies are needed to fully understand these events.

The KVTF sequence within TACC3 has been identified as being phosphorylated, but the kinase responsible is still unknown. Identification of the kinase responsible will provide insight into when during the cell cycle this motif is phosphorylated, and ultimately on the function of the TACC3-PP1 interaction. Additionally, very little is known with regards to the phosphatases responsible for dephosphorylating TACC3. Thr-56 and Thr-59, both implicated above as playing a part in affecting the TACC3-PP1 interaction do not yet have a phosphatase associated with their dephosphorylation. The phosphatase responsible for dephosphorylating the key AurA

phosphorylation site Ser-558 is also yet to be identified. Identifying the phosphatases responsible for these events will provide insight into TACC3-PP1 interaction.

Finally, upon the successful generation of the GFP-TACC3 HeLa stable cell line, the role of the TACC3-PP1 interaction *in vivo* can be explored more closely. Specifically, the effect of abolishing the interaction on mitotic spindle assembly, chromosome segregation and overall mitotic rate using the TACC3-KATA mutant. Since TACC3 and PP1 both play important roles in mitosis and mitotic progression, it will be interesting to fully understand the role these proteins are playing together.

Chapter Three: TACC3 expression and cancer

3.1 Introduction

Cancer is the leading cause of death in Canada, causing over 75,000 or 30% of deaths in 2013 (StatisticsCanada). To combat this deadly group of diseases, we must understand the underlying molecular mechanisms that lead to tumorgenesis and metastasis. The loss of cell cycle control through the activation of oncogenes or inactivation of tumor suppressor genes leads to genomic instability and is recognized as one of the hallmarks of cancer (Hanahan and Weinberg 2000). Fundamentally, cancer is a disease of tissue growth regulation. TACC3, as previously discussed is involved in mitotic spindle assembly and chromosome alignment during mitosis. Due to its importance in cell division and ensuring the proper segregation of chromosomes to maintain genomic integrity, it is not surprising that TACC3 is emerging as a growing target for cancer research. Overexpression of TACC3 in cells has been shown to cause disorder in the organization of K-fibers, reducing the spacing of the microtubules causing them to be more tightly packed (Nixon, Gutiérrez-Caballero et al. 2015). Overexpression has also been linked to mitotic defects such as an increase in the length and number of microtubules and cancers (Lee, Gergely et al. 2001, Ha, Kim et al. 2013).

The Cancer Genome Atlas (TCGA) is a public database containing patient data for both tumor and normal tissues as well as clinical data for genomic changes in 33 types of cancer. Available in this database is mRNA sequencing data, which provides insight into the quantity of mRNA transcripts for thousands of proteins. Here, using this database we explore the mRNA levels of TACC3 in 20 different cancers and the effect of these mRNA levels on patient survival.

3.2 Materials and methods

3.2.1 TCGA datasets and Broad GDAC Firehose

Patient samples were collected and analyzed through the TCGA. The TCGA collects and analyzes high-quality tumor samples and makes the data publicly available. The data is passed through several different groups for various types of analysis before being added to the public database. Clinical and mRNA datasets utilized in this study were accessed through the Broad GDAC Firehose, which provides TCGA data and analyses for immediate algorithmic analysis. Datasets used in this study are: Bladder urothelial carcinoma (BLCA), Breast invasive carcinoma (BRCA), Cholangiocarcinoma (CHOL), Colorectal adenocarcinoma (COADREAD), Esophageal carcinoma (ESCA), Glioblastoma multiforme (GBM) Glioma (GBMLGG), Head and neck squamous cell carcinoma (HNSC), Kidney chromophobe (KICH), Kidney renal clear cell carcinoma (KIRC), Kidney renal papillary cell carcinoma (KIRP), Liver hepatocellular carcinoma (LIHC), Lung adenocarcinoma (LUAD), Lung squamous cell carcinoma (LUSC), Prostate adenocarcinoma (PRAD), Rectum adenocarcinoma (READ), Stomach adenocarcinoma (STAD), Stomach and esophageal carcinoma (STES), Thyroid carcinoma (THCA) and Uterine corpus endometrial carcinoma (UCEC). Special thanks to Dr. Pinaki Bose (University of Calgary) for introducing me to these databases and taking the time to teach me how to analyze the vast amount of information present within them.

3.2.2 TACC3 mRNA expression plots

Box and whisker plots were generated from mRNA sequencing normalized gene data sets using Microsoft Excel. Statistical significance was calculated using an unpaired two-sided Student's t-test. $P<0.05$ was considered statistically significant.

3.2.3 Kaplan-Meier survival curves

Kaplan-Meier survival curves were generated from mRNA sequencing normalized gene data sets and clinical data sets using Cutoff Finder (Budczies, Klauschen et al. 2012). It is important to note that the data used in these curves are the same as those in the cancer expression graphs and that the TACC3 expression data has been matched to the patient clinical information. The most significant cut-off was determined using a log-rank test to compare the hazard estimate of the two groups with regards to survival. The log-rank test is a non-parametric test done by looking at all observed and expected events (our event = death) in each group at each observed time point and generating an overall summary across all time points(Harrington 2005). It accomplishes this through the comparison of hazard ratios, which are the conditions of two levels of the event. These ratios are obtained through regression models. These ratios can be interpreted as the chance of the event occurring in group one, versus the chance of the event occurring in group two of a study (Spruance, Reid et al. 2004, Brody 2016). The cut-off values represent the TACC3 mRNA expression level where either above or below, survival rates are most significantly decreased. $P<0.05$ was considered statistically significant.

3.3 Results and discussion

3.3.1 Increased TACC3 mRNA levels in cancer tissues correlates with decreased patient survival

First, we wanted to explore the expression of TACC3 in both cancer and normal tissues using mRNA sequencing data from the TCGA. we explored the mRNA levels of TACC3 in both tumor and normal tissue samples. We generated box and whisker plots for each of these data sets. Upon

analysis of data sets from 20 different cancers, we grouped the cancers into three separate groups based on the mRNA expression levels and the correlation of patient survival as determined from Kaplan-Meier plots to those mRNA levels.

The first group of cancers all have significantly increased TACC3 mRNA levels in cancer tissues compared with normal tissues. These ten cancers also have significantly decreased patient survival with increased TACC3 mRNA levels (**Figures 3.1, 3.2, 3.3, 3.4, 3.5**). Looking at each cancer individually, we can see a definite trend in the data for this group. LUAD had TACC3 mRNA expression levels that were significantly increased in cancer tissues versus normal tissues (**Figure 3.1A**). Interestingly, a Kaplan-Meier survival analysis using the data obtained from the TCGA dataset, shows that patients with high TACC3 expression had survival outcomes decreased to levels that were significant compared to patients with low TACC3 expression (**Figure 3.1B**). This data suggests that the upregulation of TACC3 might contribute to the progression of LUAD and a poor clinical outcome. Additionally, we looked to see if any other factors such as age, race, cancer stage or whether the patient underwent radiation treatment contributed to TACC3 mRNA expression level and/or patient prognosis in LUAD. Of the 515 cancer patients, there was no correlation with any of these factors. Male and female patients ranged in age from 38-88 years of age with 388 identifying as Caucasian, 52 as Black/African American, 8 as Asian, 1 as American Indian/Alaska Native and 66 had no race data available. TACC3 mRNA expression levels and patient prognosis was evenly distributed throughout the genders, ages and races. All four cancer stages were also identified within the 515 patients with the majority (269 patients) being either 1A or 1B. However, there once again appeared to be no correlation between the cancer stage and TACC3 expression or patient survival. The same was

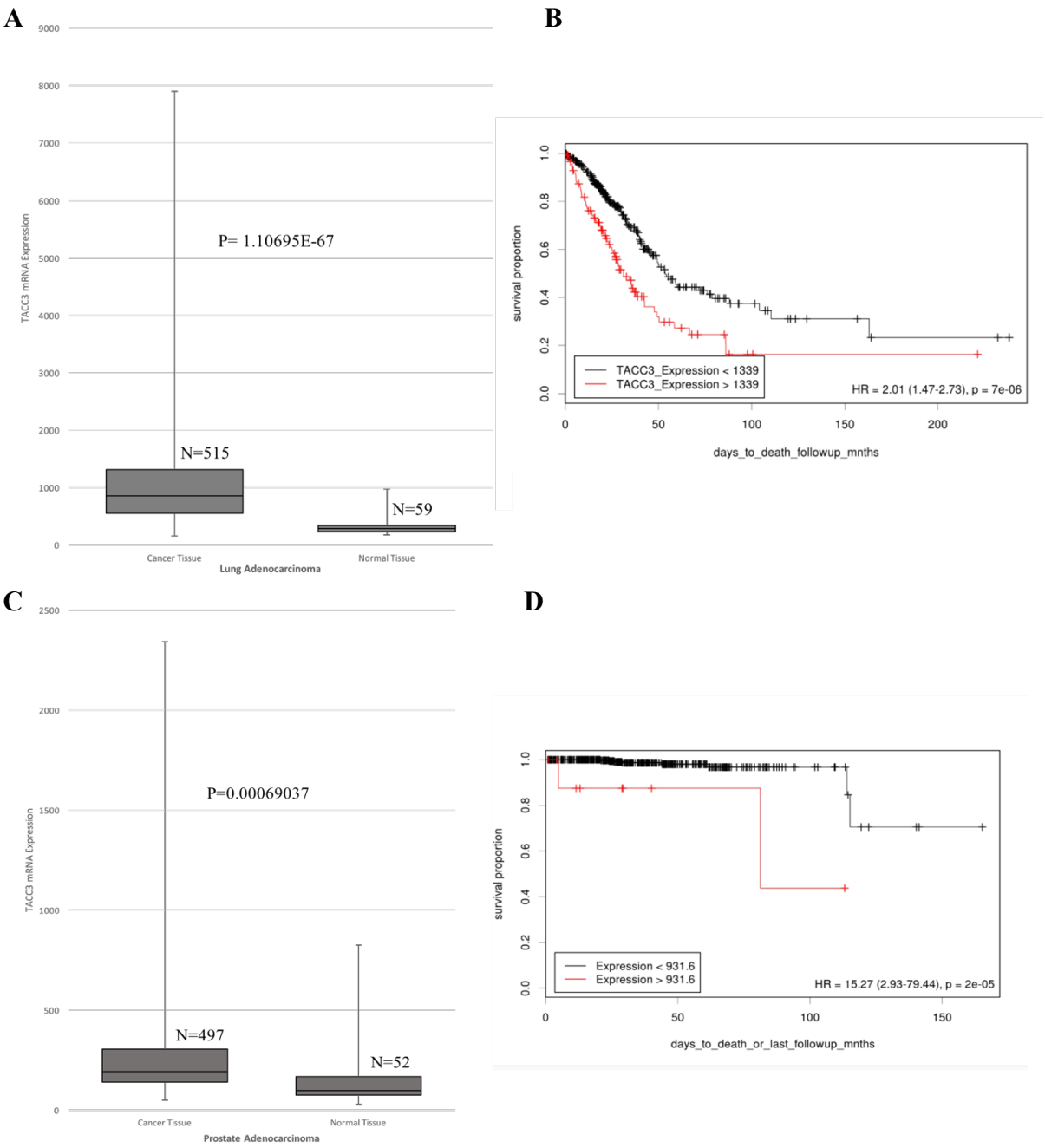

Figure 3.1 TACC3 is upregulated in lung adenocarcinoma and prostate adenocarcinoma tissues, and survival rates are decreased with high TACC3 expression.

A. TACC3 mRNA expression levels in LUAD (TCGA, Normal n=59; Tumor n=515) **B**. Kaplan-Meier analysis of TACC3 mRNA levels for LUAD patients (TCGA; Cutoff Finder, Charite) **C**. TACC3 mRNA expression levels in PRAD (TCGA, Normal n=52; Tumor n=497) **D**. Kaplan-Meier analysis of TACC3 mRNA levels for PRAD patients (TCGA; Cutoff Finder, Charite).

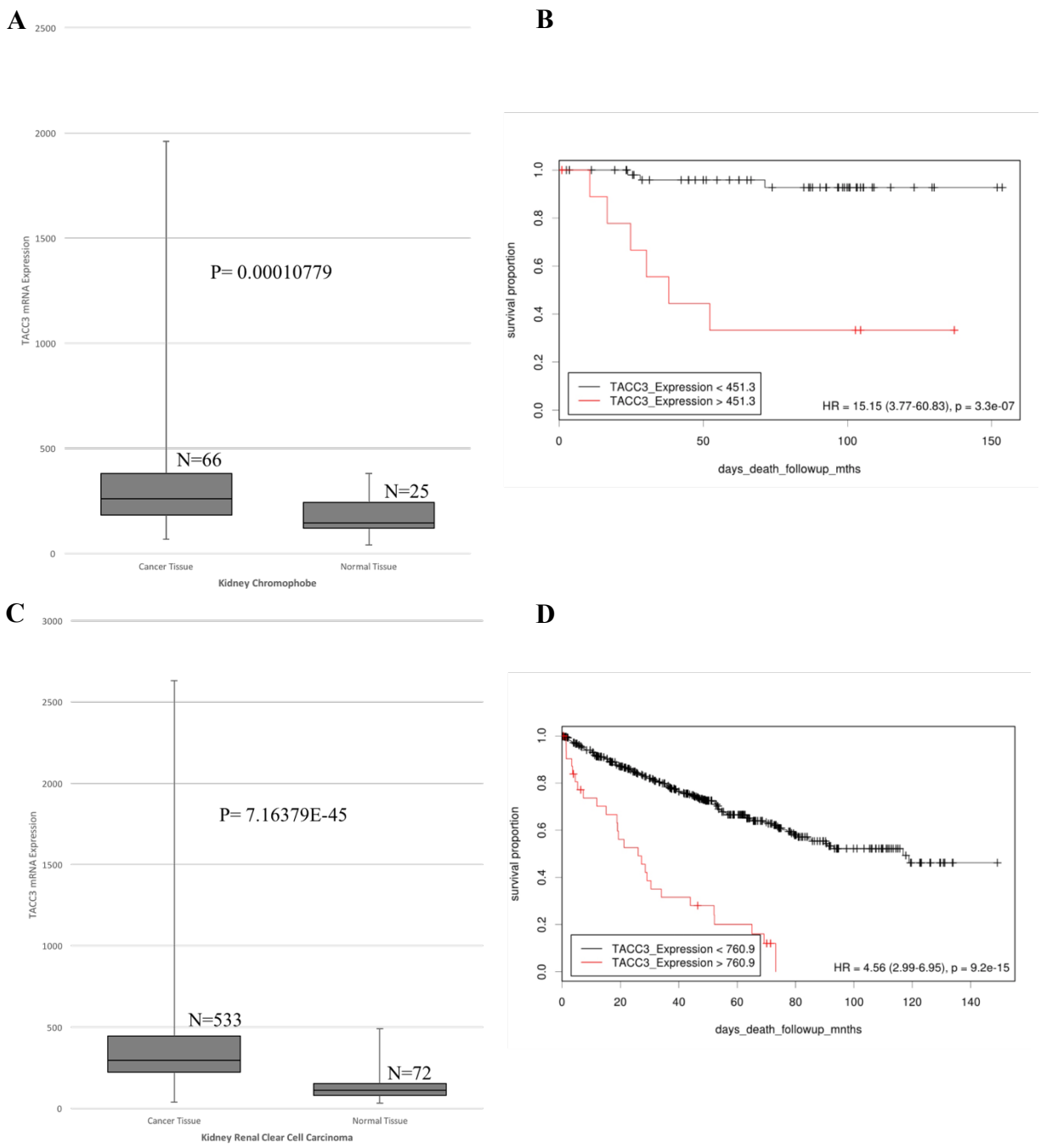

Figure 3.2 TACC3 is upregulated in kidney chromophobe and kidney renal clear cell carcinoma tissues, and survival rates are decreased with high TACC3 expression.

A. TACC3 mRNA expression levels in KICH (TCGA, Normal n=25; Tumor n=66) **B**. Kaplan-Meier analysis of TACC3 mRNA levels for KICH patients (TCGA; Cutoff Finder, Charite) **C**. TACC3 mRNA expression levels in KIRC (TCGA, Normal n=72; Tumor n=533) **D**. Kaplan-Meier analysis of TACC3 mRNA levels for KIRC patients (TCGA; Cutoff Finder, Charite).

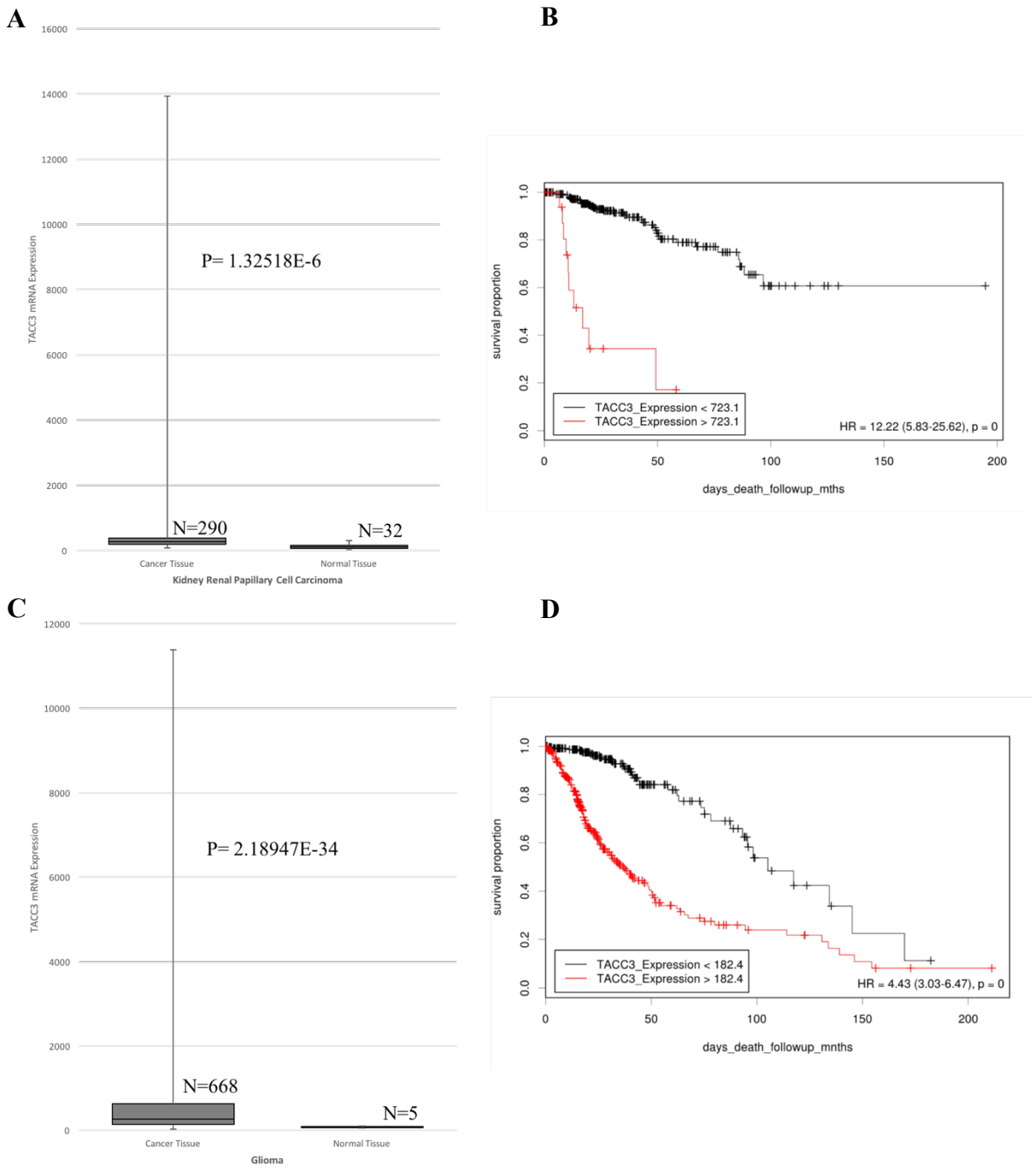

Figure 3.3 TACC3 is upregulated in kidney renal papillary cell carcinoma and glioma tissues, and survival rates are decreased with high TACC3 expression.

A. TACC3 mRNA expression levels in KIRP (TCGA, Normal n=32; Tumor n=290) **B**. Kaplan-Meier analysis of TACC3 mRNA levels for KIRP patients (TCGA; Cutoff Finder, Charite) **C**. TACC3 mRNA expression levels in GBMLGG (TCGA, Normal n=5; Tumor n=668) **D**. Kaplan-Meier analysis of TACC3 mRNA levels for GBMLGG patients (TCGA; Cutoff Finder, Charite).

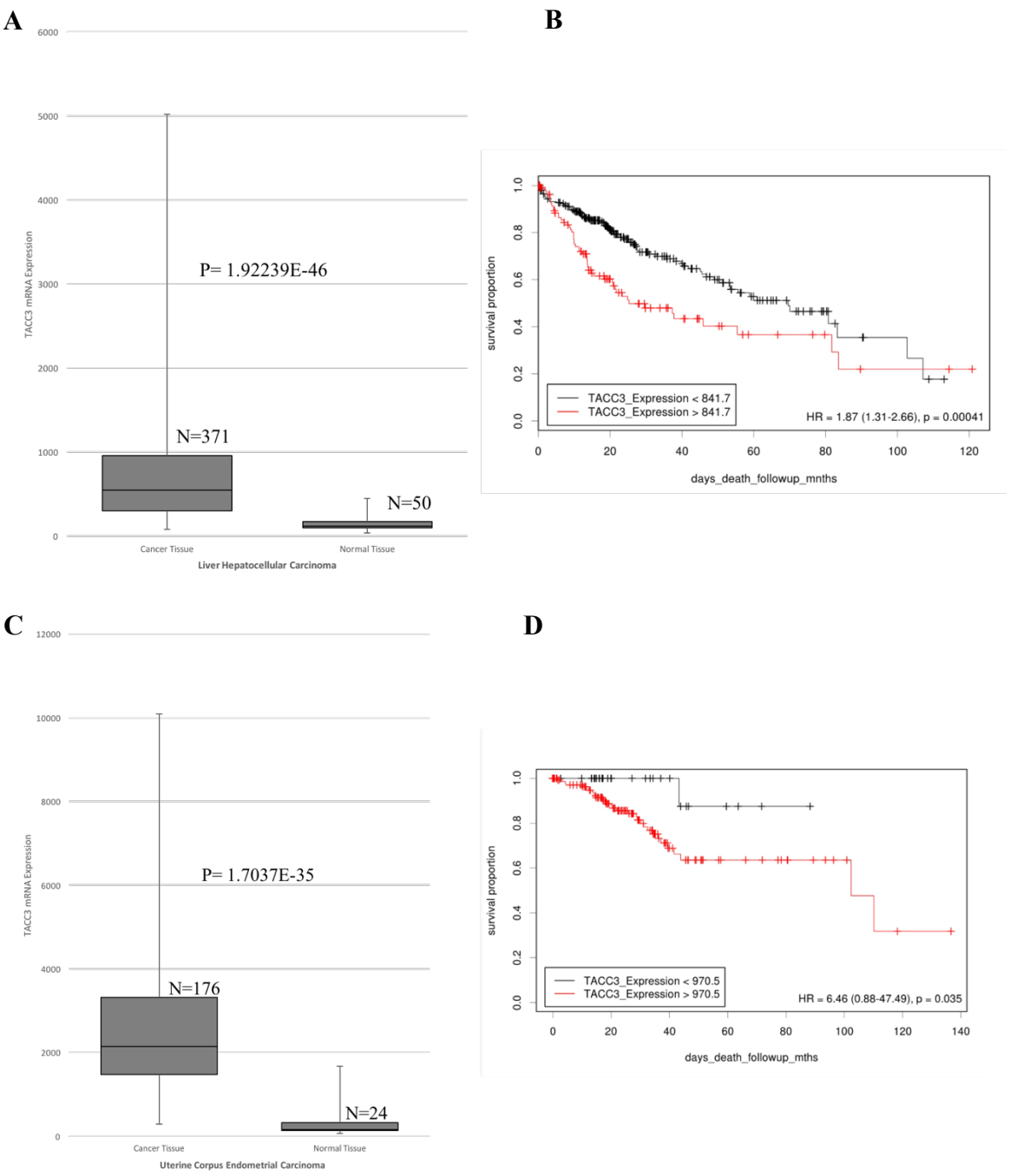

Figure 3.4 TACC3 is upregulated in liver hepatocellular carcinoma and uterine corpus endometrial carcinoma tissues, and survival rates are decreased with high TACC3 expression.

A. TACC3 mRNA expression levels in LIHC (TCGA, Normal n=50; Tumor n=371) **B**. Kaplan-Meier analysis of TACC3 mRNA levels for LIHC patients (TCGA; Cutoff Finder, Charite) **C**. TACC3 mRNA expression levels in UCEC (TCGA, Normal n=24; Tumor n=176) **D**. Kaplan-Meier analysis of TACC3 mRNA levels for UCEC patients (TCGA; Cutoff Finder, Charite).

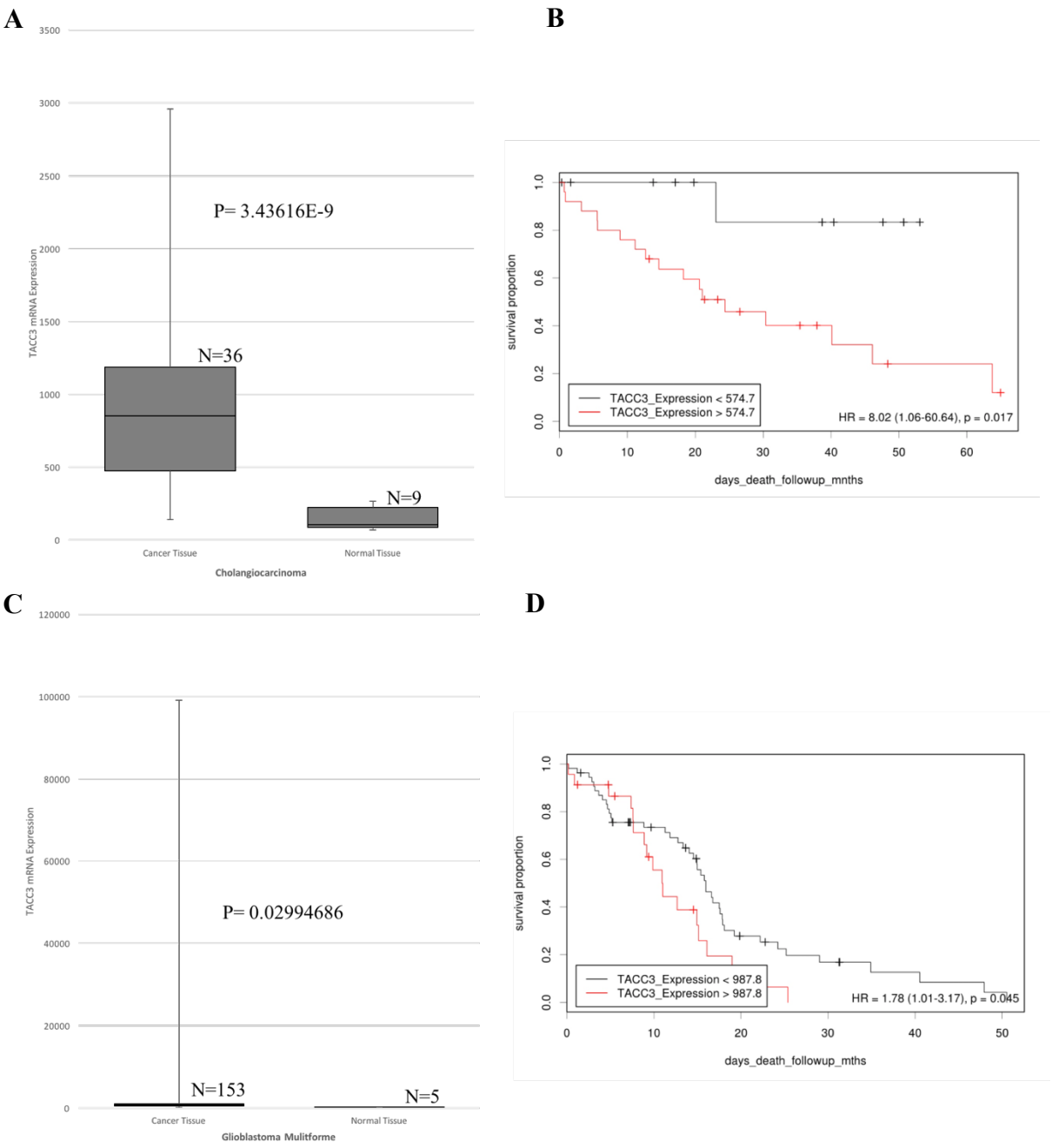

Figure 3.5 TACC3 is upregulated in cholangiocarcinoma and glioblastoma multiforme tissues, and survival rates are decreased with high TACC3 expression.

A. TACC3 mRNA expression levels in CHOL (TCGA, Normal n=9; Tumor n=36) **B**. Kaplan-Meier analysis of TACC3 mRNA levels for CHOL patients (TCGA; Cutoff Finder, Charite) **C**. TACC3 mRNA expression levels in GBM (TCGA, Normal n=5; Tumor n=153) **D**. Kaplan-Meier analysis of TACC3 mRNA levels for GBM patients (TCGA; Cutoff Finder, Charite).

true for radiation. Only 61 of the 515 patients had undergone radiation treatment, which did not appear to contribute to the level of TACC3 mRNA expression or survival.

In addition to LUAD, six other cancer datasets (PRAD, **Figure 3.1C-D**; KICH, **Figure 3.2A-B**; KIRC, **Figure 3.2C-D**; KIRP, **Figure 3.3A-B**; GBMLGG, **Figure 3.3C-D**; and LIHC, **Figure 3.4A-B**) had TACC3 mRNA expression levels that were significantly increased in cancer tissues versus normal tissues, and significantly decreased patient survival outcomes with high TACC3 expression. Two cancer datasets (UCEC, **Figure 3.4C-D**; and CHOL, **Figure 3.5A-B**) had significantly increased TACC3 mRNA expression in cancer, and significantly decreased patient survival outcomes with high TACC3 expression and finally, one data set (GBM, **Figure 3.5C-D**) had significantly increased TACC3 mRNA expression in cancer tissues, and significantly decreased patient survival outcomes with high TACC3 expression. These ten cancers account for 50% of the datasets explored in this study. Together, these datasets suggest that TACC3 is upregulated in cancer, and that increased TACC3 mRNA expression leads to decreased survival rates.

3.3.2 TACC3 mRNA levels are increased in cancer tissues but does not correlate with patient survival

Utilizing the same data analysis techniques as for the first group of cancers, the second group of cancers studied were also identified as having significantly increased TACC3 mRNA levels in cancer tissues compared with normal tissues. However, in contrast to the first group, these eight cancers had poor patient survival when TACC3 expression was below the significant cut-off (**Figures 3.6, 3.7, 3.8, 3.9**). All the cancers in this group share the same trend of increased TACC3 expression in cancer tissues, but six show decreased survival with lower TACC3

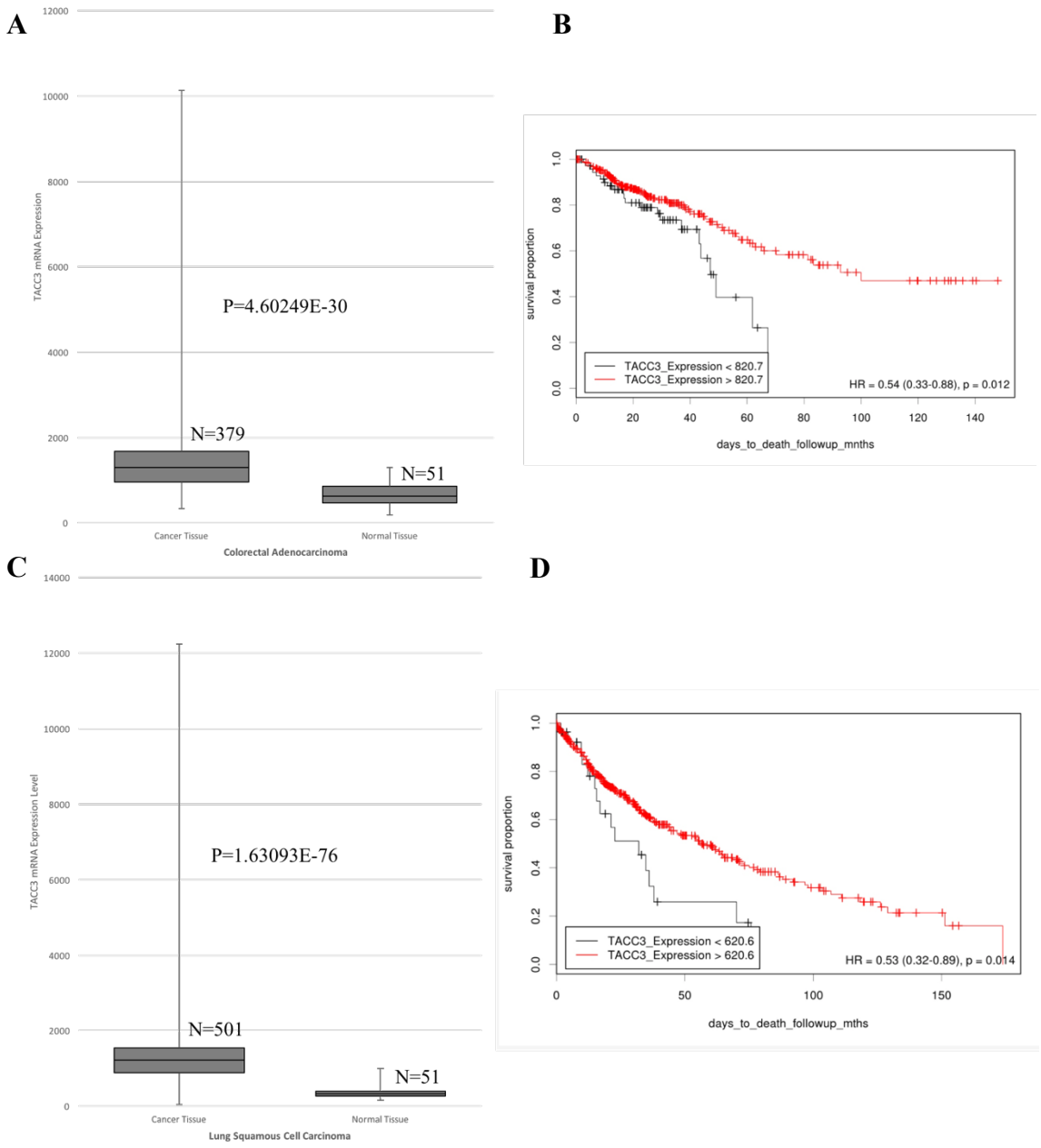

Figure 3.6 TACC3 is upregulated in colorectal adenocarcinoma and lung squamous cell carcinoma tissues, but survival rates are decreased with low TACC3 expression.

A. TACC3 mRNA expression levels in COADREAD (TCGA, Normal n=51; Tumor n=379) **B**. Kaplan-Meier analysis of TACC3 mRNA levels for COADREAD patients (TCGA; Cutoff Finder, Charite) **C**. TACC3 mRNA expression levels in LUSC (TCGA, Normal n=51; Tumor n=501) **D**. Kaplan-Meier analysis of TACC3 mRNA levels for LUSC patients (TCGA; Cutoff Finder, Charite).

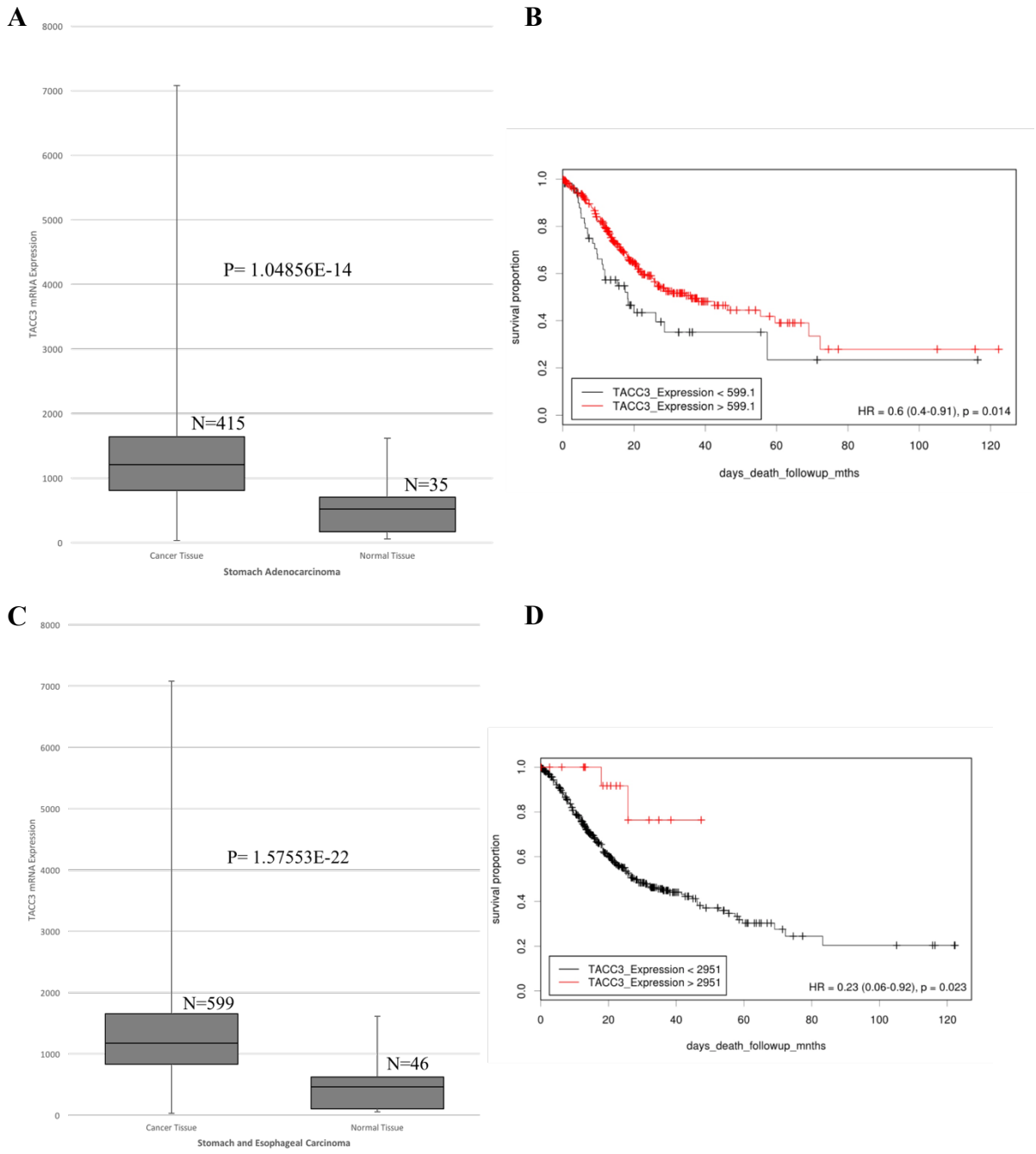

Figure 3.7 TACC3 is upregulated in stomach adenocarcinoma and stomach and esophageal carcinoma tissues, but survival rates are decreased with low TACC3 expression.

A. TACC3 mRNA expression levels in STAD (TCGA, Normal n=35; Tumor n=415) **B**. Kaplan-Meier analysis of TACC3 mRNA levels for STAD patients (TCGA; Cutoff Finder, Charite) **C**. TACC3 mRNA expression levels in STES (TCGA, Normal n=46; Tumor n=599) **D**. Kaplan-Meier analysis of TACC3 mRNA levels for STES patients (TCGA; Cutoff Finder, Charite).

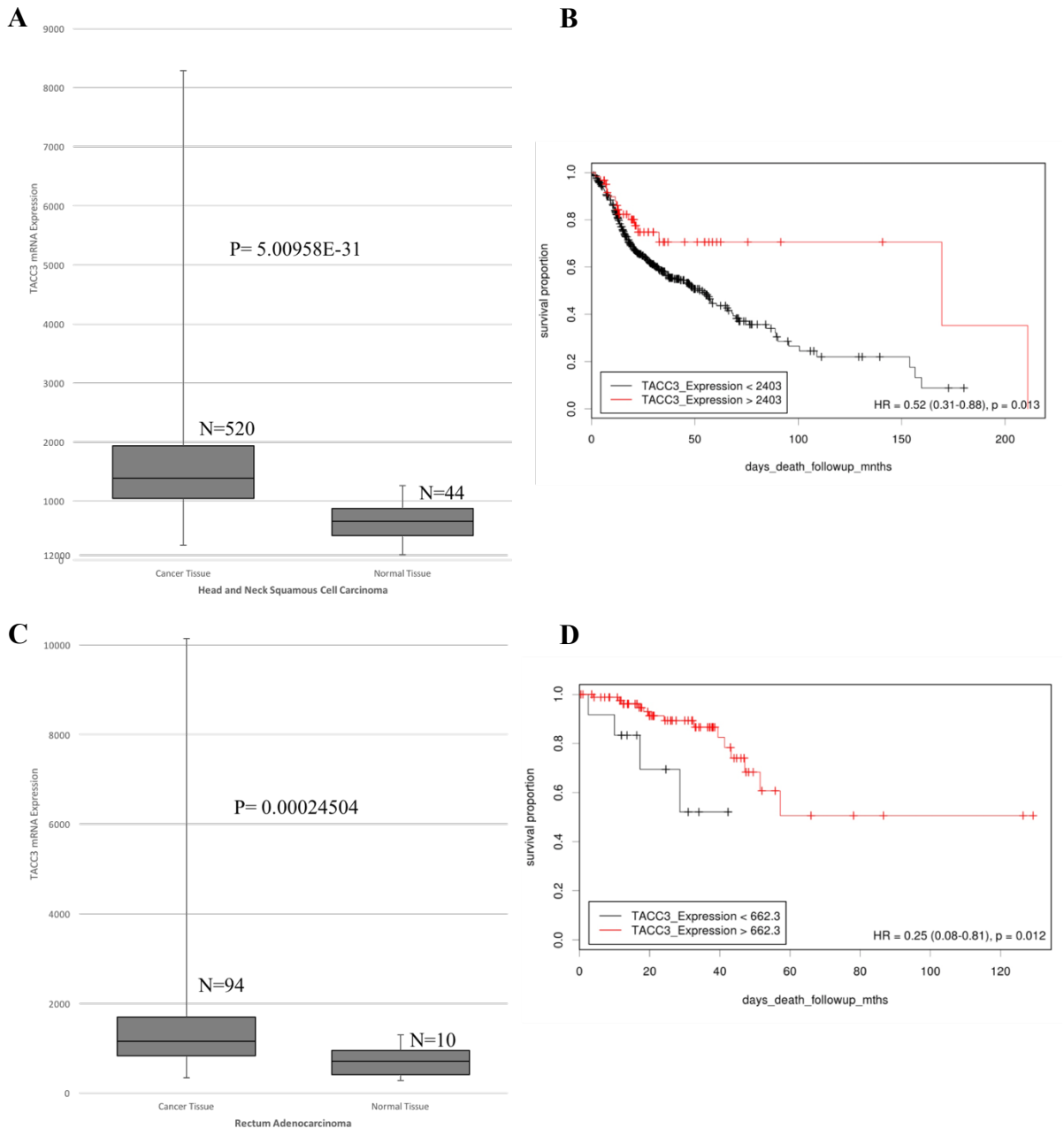

Figure 3.8 TACC3 is upregulated in head and neck squamous cell carcinoma and rectum adenocarcinoma tissues, but survival rates are decreased with low TACC3 expression.

A. TACC3 mRNA expression levels in HNSC (TCGA, Normal n=44; Tumor n=520) **B**. Kaplan-Meier analysis of TACC3 mRNA levels for HNSC patients (TCGA; Cutoff Finder, Charite) **C**. TACC3 mRNA expression levels in READ (TCGA, Normal n=10; Tumor n=94) **D**. Kaplan-Meier analysis of TACC3 mRNA levels for READ patients (TCGA; Cutoff Finder, Charite).

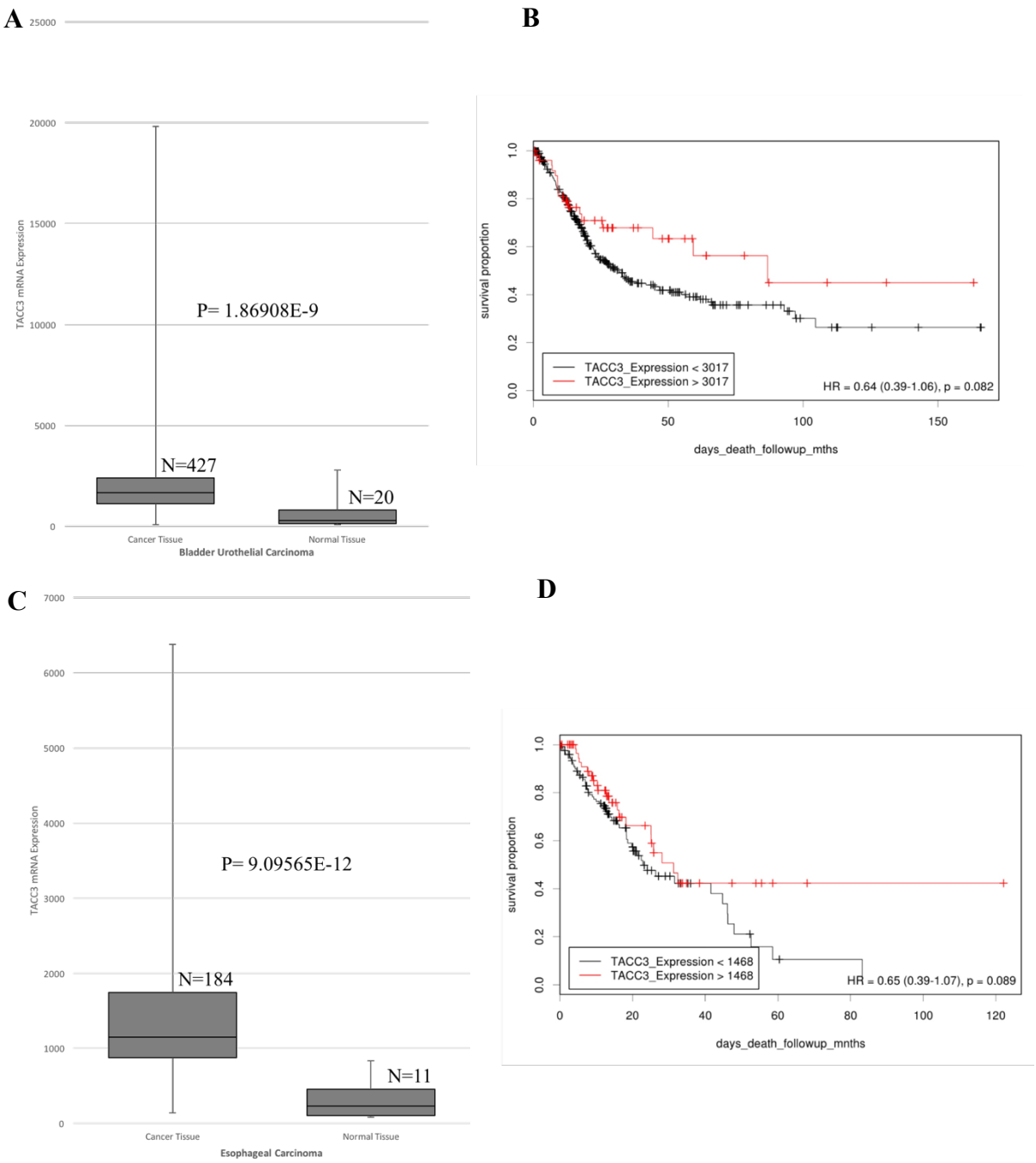

Figure 3.9 TACC3 is upregulated in bladder urothelial carcinoma and esophageal carcinoma tissues, and decreased survival rates are not significant.

A. TACC3 mRNA expression levels in BLCA (TCGA, Normal n=20; Tumor n=427) **B**. Kaplan-Meier analysis of TACC3 mRNA levels for BLCA patients (TCGA; Cutoff Finder, Charite) **C**. TACC3 mRNA expression levels in ESCA (TCGA, Normal n=11; Tumor n=184) **D**. Kaplan-Meier analysis of TACC3 mRNA levels for ESCA patients (TCGA; Cutoff Finder, Charite).

expression and two show no significance with regards to patient survival and TACC3 expression.

COADREAD has TACC3 mRNA expression levels that were significantly increased in cancer tissues versus normal tissues (**Figure 3.6A**). In contrast to the previous group, a Kaplan-Meier survival plot showed that patients with lower TACC3 expression had a significantly decreased survival outcome than patients with low TACC3 expression (**Figure 3.6B**). This data raises some questions as to whether the upregulation of TACC3 is contributing to COADREAD progression and a poor clinical outcome. In addition to COADREAD, five other cancer datasets (LUSC, **Figure 3.6C-D**; STAD, **Figure 3.7A-B**; STES, **Figure 3.7C-D**; HNSC, **Figure 3.8A-B**; and READ, **Figure 3.8C-D**) had TACC3 mRNA expression levels that were significantly increased in cancer tissues versus normal tissues and had significantly decreased patient survival outcomes with low TACC3 expression. Two cancer datasets (BLCA, **Figure 3.9A-B**; and ESCA, **Figure 3.9 C-D**) also had significantly increased TACC3 mRNA expression in cancer, but patient survival with decreased TACC3 levels was not significant.

Looking at these eight cancers as well as the ten cancers from group one, it appears that TACC3 is upregulated in cancers. 18 of the 20 (90%) cancer datasets in this study have significantly increased TACC3 mRNA expression in cancer tissues. The survival data is less clear at this time. In this group of eight cancers, six had significantly decreased patient survival with decreased TACC3 expression, but it is important to note that the significant cut-off values for high and low expression in these cancers, especially STES and HNSC, were well above most of the normal tissue expression levels. Connecting the upregulation of TACC3 mRNA expression levels in cancer and patient survival outcomes will require more study.

3.3.3 TACC3 mRNA levels are not increased in cancer tissues

Finally, the last group of cancers we studied did not have significantly increased TACC3 mRNA levels in cancer tissue compared to normal tissues, and did not follow the trends of the first two groups. The first, THCA did not have significantly increased TACC3 mRNA levels in cancer tissues, but survival was significantly decreased when TACC3 expression was high (**Figure 3.10A-B**). Interestingly, the second cancer in this group appears to have an opposite trend from all the other cancer datasets studied. BRCA had significantly decreased TACC3 expression in cancer tissues when compared to normal tissues (**Figure 3.10C**). The Kaplan-Meier survival analysis for BRCA also correlated with the expression data, with decreased patient survival rates seen with low TACC3 expression, although the significant cut-off value was well below the bulk of the expression data. (**Figure 3.10D**). Both cancers in this group do not fit with the trends seen for the other 18 cancer datasets analyzed in this study. THCA does not appear to have increased TACC3 mRNA levels and in BRCA it appears TACC3 may be downregulated. Additionally, the patient survival outcomes for these two groups do not fit with the trends seen with the other 18 cancer datasets. Further analysis and additional data is needed to draw conclusions as to the role of TACC3 expression in cancer and its effect on patient survival.

3.3.4 Clathrin and ch-TOG mRNA levels are also significantly increased in lung adenocarcinoma

With 90% of the cancers analyzed having significantly increased levels of TACC3 mRNA, we next explored whether two of TACC3's binding partners, clathrin and ch-TOG, also had increased mRNA levels. We chose to look at lung adenocarcinoma (LUAD), a cancer in which

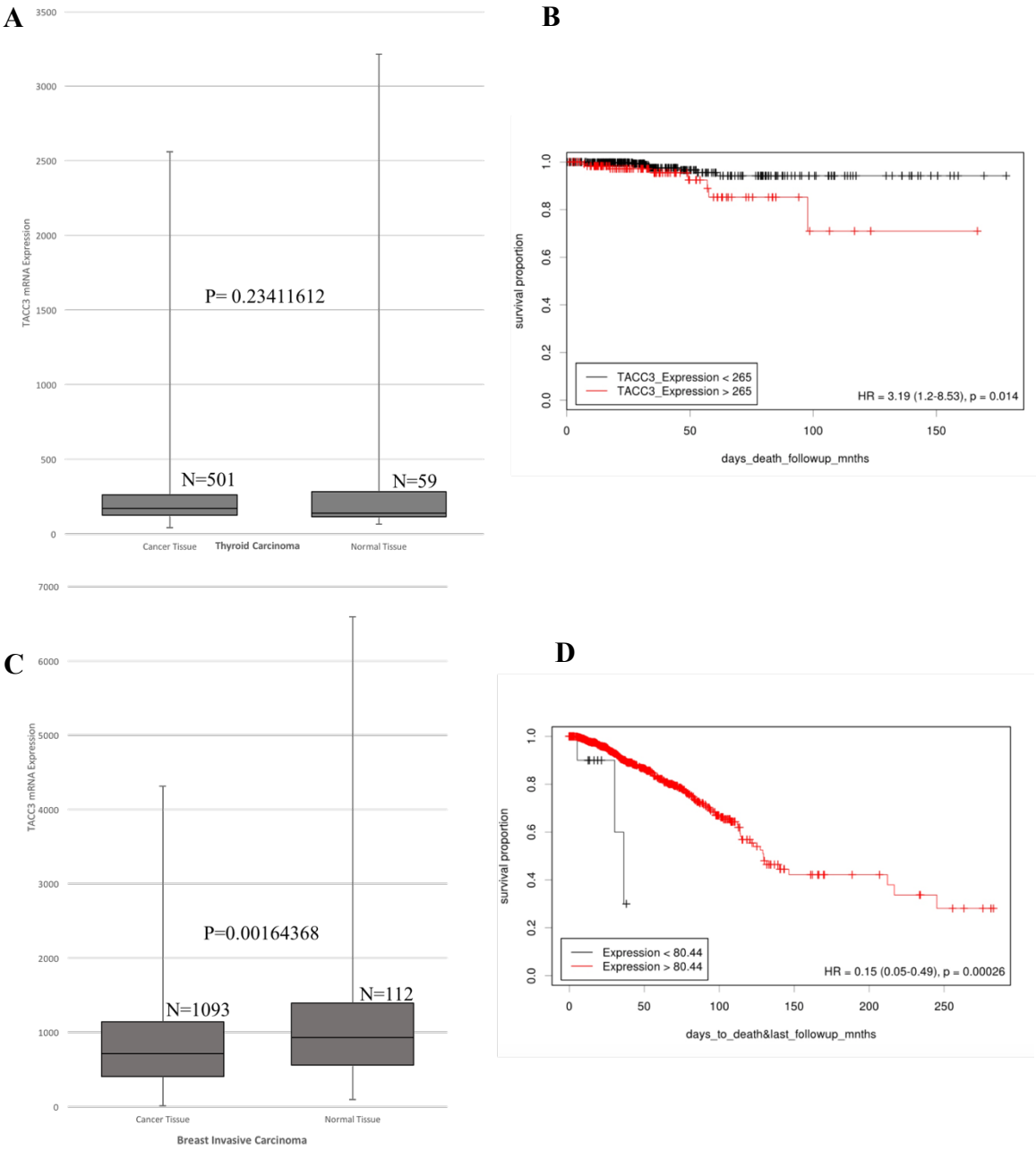

Figure 3.10 TACC3 is not upregulated in thyroid carcinoma and is downregulated in breast invasive carcinoma tissues.

A. TACC3 mRNA expression levels in THCA (TCGA, Normal n=59; Tumor n=501) **B**. Kaplan-Meier analysis of TACC3 mRNA levels for THCA patients (TCGA; Cutoff Finder, Charite) **C**. TACC3 mRNA expression levels in BRCA (TCGA, Normal n=112; Tumor n=1093) **D**. Kaplan-Meier analysis of TACC3 mRNA levels for BRCA patients (TCGA; Cutoff Finder, Charite).

TACC3 mRNA levels were significantly increased, and poor patient survival was also found to be significantly increased. We generated box and whisker plots for both of these data sets using mRNA sequencing data from the TCGA, in the same manner as with TACC3. It is important to note that these are the same LUAD patient samples and data as used in the TACC3 mRNA analysis.

Upon analysis of the data sets, we found that both clathrin and ch-TOG have significantly increased mRNA levels in LUAD cancer tissues compared with normal tissues (**Figure 3.11**). This result is consistent with what was seen with TACC3 mRNA levels in LUAD. Since all three of these proteins are known to form a complex that plays a role in mitosis and genome integrity it is interesting to see them following the same trends. Whether the upregulation of TACC3, clathrin or ch-TOG is contributing to the upregulation of the others, or whether an entirely different factor is causing these high mRNA levels remains to be determined. It seems likely that since these proteins are involved in the same complex, there is a yet to be determined factor causing the overexpression of TACC3, chTOG, and clathrin mRNAs. High levels of these proteins would lead to increased numbers of the complex on the mitotic spindle, which is known to cause K-fibers to pack more tightly and cause issues with the stability of the spindle.

3.4 Conclusions

The analysis of 20 cancer datasets has suggested that TACC3 is upregulated in some cancers. In 90% of the cancers, TACC3 was significantly increased when compared to normal tissue mRNA expression. In 50% of the cancers, high TACC3 expression led to decreased patient survival outcomes, suggesting a role for TACC3 in decreasing patient prognosis. TACC3 was also identified as being downregulated in BRCA, with low TACC3 expression leading to poor

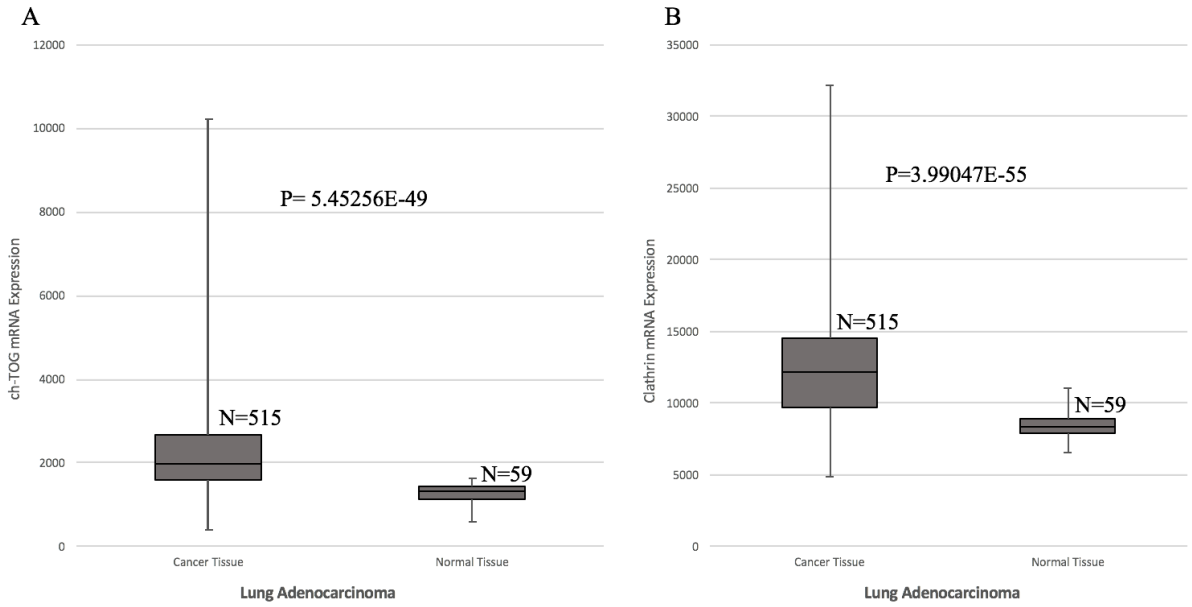

Figure 3.11 ch-TOG and clathrin are both upregulated in lung adenocarcinoma tissues. **A**. ch-TOG mRNA expression levels in LUAD (TCGA, Normal n=59; Tumor n=515) **B**. Clathrin mRNA expression levels in LUAD (TCGA, Normal n=59; Tumor n=515).

patient survival (**Table 3.1**). This is in direct contrast with the majority or the data, but implies that TACC3 may be playing a different role in BRCA. The expression data we obtained for LUAD, PRAD, GBMLGG, CHOL, COADREAD and BRCA is all consistent with previously reported studies, strengthening our results (Du, Liu et al. 2016, He, Yao et al. 2016, Jiang, Kuang et al. 2016, Ding, Huang et al. 2017, Li, Ye et al. 2017, Sun, Tian et al. 2017). Additionally, we also found that ch-TOG and clathrin mRNA levels are also significantly increased in LUAD, following the same trend we saw with TACC3.

Table 3.1 Summary of TACC3 mRNA expression plots and Kaplan-Meier survival curves.

TACC3 mRNA expression levels in 20 different cancer types compared with TACC3 mRNA expression in normal tissues and grouped together based on significance. The expression data was matched to patient clinical survival data. The table summarizes the data presented.

Cancer Type	*Cancer mRNA Expression Range*	*Normal mRNA Expression Range*	*Expression Significance*	*Patient Survival Outcome*	*mRNA Expression Cut-off and Significance*
LUAD	156-7906	174-972	1.106E-67	Decreased with *high* TACC3 expression	1339/p=7E-6
PRAD	50-2342	30-826	6.904E-4		932/p=2E-5
KICH	67-1959	42-381	1.078E-4		451/p=3.3E-7
KIRC	38-2630	32-488	7.164E-45		761/p=9.2E-15
KIRP	58-13944	57-312	1.325E-6		723/p=0
GBMLGG	32-11389	52-99	2.189E-34		182/p=0
LIHC	79-5017	41-449	1.922E-46		842/p=4.1E-4
UCEC	289-10086	75-1682	1.704E-35		971/p=3.5E-1
CHOL	141-2960	68-266	3.436E-9		575/p=1.7E-2
GBM	81-99057	52-99	2.995E-2		988/p=4.5E-2
COADREAD	337-10136	193-1294	4.602E-30	Decreased with *low* TACC3 expression	821/p=1.2E-2
LUSC	49-12244	157-996	1.631E-76		621/p=1.4E-2
STAD	34-7081	61-1616	1.049E-14		599/p=1.4E-2
STES	34-7081	16-1616	1.576E-22		2951/p=2.3E-2
HNSC	257-8294	90-1265	5.010E-31		2403/p=1.3E-2
READ	337-10136	284-1294	2.450E-4		662/p=1.2E-2
BLCA	89-19817	79-2786	1.869E-9		3017/p=8.2E-2
ESCA	143-6380	83-834	0.096E-12		1468/p=8.9E-2
THCA	40-2560	65-3215	2.341E-1	Decreased with *high* TACC3 expression	256/p=1.4E-2
BRCA	13-1413	99-6593	1.644E-3	Decreased with *low* TACC3 expression	80/p=2.6E-4

With the conflicting role of TACC3's expression in cancer, it is still unclear what the effects of the protein are on cancer cells. It is important to note that this expression data is based on mRNA sequencing counts, not protein. Although mRNA and protein and closely linked, there is no clear relationship between mRNA transcripts and the protein present in the cell. Many cellular processes such as translation rates, protein transport and protein degradation can all influence the amount of protein in the cell and cause it to differ from mRNA levels and these processes are often disrupted in cancer (McManus, Cheng et al. 2015, Liu, Beyer et al. 2016). There are currently no technologies available to correctly predict the protein concentration based solely from mRNA transcript level. To accurately determine protein levels, measurements must rely on antibody techniques such as Western blotting or quantitative mass spectrometry. To determine whether the results of this bioinformatics study have clinical applications, the actual protein levels present with these transcripts must be determined. A study by He *et al*. 2016, found that in CHOL, protein levels were increased, and did correlate with the mRNA sequencing data (He, Yao et al. 2016). Additional biochemical studies should be done to determine if the protein levels are increased in the remaining cancers and confirm that TACC3 is upregulated.

3.5 Future directions

With the data presented above, we have found that TACC3 mRNA is upregulated in some cancers, and high levels appear to contribute to poor patient survival, raising several questions that require further study. First, determining the actual protein level present in these tissues will be crucial in understanding this mRNA data. As previously mentioned, mRNA levels do not always directly indicate protein levels (Liu, Beyer et al. 2016). To ensure that the protein levels in these tissues correlate with the mRNA levels, patient tissue samples could be western blotted

for the presence and level of TACC3 in both normal and cancer tissues. Although western blotting is powerful, quantitative mass spectrometry could also be used to compare TACC3 levels in tumorigenic versus normal tissue (Kettenbach, Schweppe et al. 2011).

Another important study that should be done with this data is to correlate it with other mRNA transcripts commonly under/over expressed in cancers. We have already done this with ch-TOG and clathrin in LUAD, and it would be interesting to see if the results are consistent between the three proteins across the 20 cancers in this study. By identifying other proteins that are up/downregulated in these cancers in a manner similar to TACC3, we may be able to gain further insight into the role of TACC3 in the cancer cells. Additionally, by correlating with other mRNAs, such as known TACC3 interactors, we may be able to see how these proteins are connected within cancer cells and begin to get a clearer picture of what is happening at the molecular level, and how it differs from normal cells.

Currently 213 TACC3 mutations have been identified in 161 cancer samples (Cerami, Gao et al. 2012). Of these mutations, the majority are missense, with the remainder being truncating, either through fusion or splicing, and in-frame mutations. No mutations have currently been identified within TACC3's RVxF motif or the downstream TP site ($_{54}$KVTFQTP$_{60}$), however, exploring the currently identified mutations may provide insight into TACC3's role in cancer cells. By mapping the TACC3 mutations to potential phosphorylation or protein binding sites, trends may begin to emerge to help us understand the impact of these mutations.

Finally, and most importantly is linking this bioinformatics data to clinical applications. Understanding how the expression and mutations of TACC3 are affecting cancer cells will potentially allow researchers to use it as a biomarker for cancer, in diagnosis and/or prognosis. Additionally, upon understanding the molecular role TACC3 is playing, researchers may be able

to utilize it as a drug target for preventative or therapeutic purposes. In conclusion, understanding the expression of TACC3 in cancer might provide new directions for utilizing this protein as a therapeutic target.

Chapter Four: Final Conclusions and Directions

TACC3 is a non-motor microtubule associated protein with a key role in the formation of the mitotic spindle. Depletion and overexpression of this protein has been shown to cause multiple different mitotic and chromosomal defects. Recently TACC3 has been implicated in several different cancers. The main goal of this thesis was to characterize the interaction between TACC3 and PP1 *in-vitro* (**Chapter 2**) and explore the link between TACC3 and cancer through bioinformatics (**Chapter 3**). Here we present that TACC3 interacts with PP1 through the RVxF motif, and that the interaction is mitosis specific. We also show that TACC3 mRNA levels are significantly increased in 18 of 20 cancers and that high levels of TACC3 mRNA correlate with decreased patient prognosis.

As an RVxF containing protein we have shown a novel interaction between TACC3 and PP1 via the RVxF motif. The regulation of this interaction still requires more study to fully uncover the mechanism. Our results indicate that phosphorylation of the motif may contribute to the abolishment of the interaction, but that additional factors are likely required. We believe TACC3 binding to PP1 may be regulated through multiple contact points between the proteins, not just the RVxF motif. This has been shown in other known regulatory proteins such as NIPP1, inhibitor-2, and spinophilin (Hurley, Yang et al. 2007, Carmody, Baucum et al. 2008, O'Connell, Nichols et al. 2012). In this proposed model, we believe the RVxF site is required to help bring TACC3 into contact with PP1 and that there likely exist other contact points or motifs where TACC3 and PP1 also bind. Upon phosphorylation on the RVxF motif or the TP site, the interaction between the two proteins begins to decrease, however it is not fully abolished due to the other docking sites on the proteins. These other contact points have yet to be identified and

further studies are required to fully understand how the docking of these proteins is regulated. Fully understanding how these two proteins interact and identifying the kinases and phosphatases associated with regulating the interaction will help to provide insight into the mechanistic effects of the interaction.

The role these two proteins are playing as a pair within the cell has also yet to be determined. Through the generation of stable HeLa cell lines, their cellular effects on mitotic spindle assembly, chromosome segregation and overall mitotic progression can be explored.

With TACC3 emerging as a new target of study in cancer research we looked at TCGA data for TACC3 mRNA expression in 20 different cancer tissues vs normal tissues. We found that TACC3 mRNA levels were significantly increased in 90% of the cancers when compared with normal tissue mRNA expression. Additionally, we found that high TACC3 mRNA expression correlated with significantly decreased patient survival.

Understanding the implication of this result requires further study. First, this study was performed using mRNA sequencing data, which does not always correlate with total protein levels. To determine whether these results have any potential clinical applications, true protein levels should be determined.

We also explored the mRNA expression of ch-TOG and clathrin, two known TACC3 interactors, in lung adenocarcinoma. Both were found to be significantly upregulated in cancer versus normal tissues. It would be interesting to explore if the trend remains true across the remaining cancers in the study. Exploring levels of the PP1 isoforms within the cancers could also provide insight into what is happening at the molecular level. Understanding how TACC3 and PP1 expression is linked within cancer cells may provide mechanistic insight into the implication of this interaction in both normal and cancer cells.

Through the biochemical exploration of the TACC3-PP1 interaction *in vivo* and its potential downstream consequences, we may be able to use the bioinformatics results from this study and gain insight into what is happening within cancer cells.

TACC3 is a protein implicated in both cancer and mitosis, and PP1 is known to play a key role in cell cycle control. It seems likely that the interaction of these two proteins plays a role in proper mitotic progression and cell division. Since the hallmarks of cancer include genetic instability and mutations, improper cell division can help cancer cells to proliferate. Understanding the interaction of these two proteins and their expression within cancer cells may provide a potential biomarker for diagnosis/and or prognosis or even a therapeutic target. In conclusion, understanding the interaction of PP1 and TACC3 may provide insight into the cell cycle progression and its effects on cancer.

References

Akhmanova, A. and M. O. Steinmetz (2010). "Microtubule+ TIPs at a glance." J Cell Sci **123**(20): 3415-3419.

Albee, A. J. and C. Wiese (2008). "Xenopus TACC3/maskin is not required for microtubule stability but is required for anchoring microtubules at the centrosome." Molecular biology of the cell **19**(8): 3347-3356.

Alonso, A., J. Sasin, N. Bottini, I. Friedberg, I. Friedberg, A. Osterman, A. Godzik, T. Hunter, J. Dixon and T. Mustelin (2004). "Protein tyrosine phosphatases in the human genome." Cell **117**(6): 699-711.

Alvarado-Kristensson, M., F. Melander, K. Leandersson, L. Rönnstrand, C. Wernstedt and T. Andersson (2004). "p38-MAPK signals survival by phosphorylation of caspase-8 and caspase-3 in human neutrophils." Journal of Experimental Medicine **199**(4): 449-458.

Andreeva, A. V. and M. A. Kutuzov (2001). "PPP family of protein Ser/Thr phosphatases: two distinct branches?" Mol Biol Evol **18**(3): 448-452.

Barford, D., A. K. Das and M. P. Egloff (1998). "The structure and mechanism of protein phosphatases: insights into catalysis and regulation." Annu Rev Biophys Biomol Struct **27**: 133-164.

Barr, A. R. and F. Gergely (2008). "MCAK-independent functions of ch-Tog/XMAP215 in microtubule plus-end dynamics." Molecular and cellular biology **28**(23): 7199-7211.

Barr, F. A., P. R. Elliott and U. Gruneberg (2011). "Protein phosphatases and the regulation of mitosis." J Cell Sci **124**(Pt 14): 2323-2334.

Beullens, M., A. Van Eynde, V. Vulsteke, J. Connor, S. Shenolikar, W. Stalmans and M. Bollen (1999). "Molecular determinants of nuclear protein phosphatase-1 regulation by NIPP-1." Journal of Biological Chemistry **274**(20): 14053-14061.

Bollen, M. (2001). "Combinatorial control of protein phosphatase-1." Trends in Biochemical Sciences **26**(7): 426-431.

Booth, D. G., F. E. Hood, I. A. Prior and S. J. Royle (2011). "A TACC3/ch-TOG/clathrin complex stabilises kinetochore fibres by inter-microtubule bridging." The EMBO journal **30**(5): 906-919.

Bordo, D. and P. Bork (2002). "The rhodanese/Cdc25 phosphatase superfamily. Sequence-structure-function relations." EMBO Rep **3**(8): 741-746.

Bottini, N., E. Bottini, F. Gloria-Bottini and T. Mustelin (2002). "Low-molecular-weight protein tyrosine phosphatase and human disease: in search of biochemical mechanisms." Arch Immunol Ther Exp (Warsz) **50**(2): 95-104.

Brody, T. (2016). Clinical trials: study design, endpoints and biomarkers, drug safety, and FDA and ICH guidelines, Academic press.

Brouhard, G. J., J. H. Stear, T. L. Noetzel, J. Al-Bassam, K. Kinoshita, S. C. Harrison, J. Howard and A. A. Hyman (2008). "XMAP215 is a processive microtubule polymerase." Cell **132**(1): 79-88.

Budczies, J., F. Klauschen, B. V. Sinn, B. Győrffy, W. D. Schmitt, S. Darb-Esfahani and C. Denkert (2012). "Cutoff Finder: a comprehensive and straightforward Web application enabling rapid biomarker cutoff optimization." PloS one **7**(12): e51862.

Burgess, S. G., I. Peset, N. Joseph, T. Cavazza, I. Vernos, M. Pfuhl, F. Gergely and R. Bayliss (2015). "Aurora-A-Dependent Control of TACC3 Influences the Rate of Mitotic Spindle Assembly." PLoS Genet **11**(7): e1005345.
Capelletti, M., M. E. Dodge, D. Ercan, P. S. Hammerman, S.-I. Park, J. Kim, H. Sasaki, D. M. Jablons, D. Lipson and L. Young (2014). "Identification of recurrent FGFR3–TACC3 fusion oncogenes from lung adenocarcinoma." Clinical cancer research **20**(24): 6551-6558.
Carmody, L. C., A. J. Baucum, M. A. Bass and R. J. Colbran (2008). "Selective targeting of the γ1 isoform of protein phosphatase 1 to F-actin in intact cells requires multiple domains in spinophilin and neurabin." The FASEB Journal **22**(6): 1660-1671.
Cerami, E., J. Gao, U. Dogrusoz, B. E. Gross, S. O. Sumer, B. A. Aksoy, A. Jacobsen, C. J. Byrne, M. L. Heuer and E. Larsson (2012). The cBio cancer genomics portal: an open platform for exploring multidimensional cancer genomics data, AACR.
Ceulemans, H., W. Stalmans and M. Bollen (2002). "Regulator-driven functional diversification of protein phosphatase-1 in eukaryotic evolution." Bioessays **24**(4): 371-381.
Cheeseman, L. P., D. G. Booth, F. E. Hood, I. A. Prior and S. J. Royle (2011). "Aurora A kinase activity is required for localization of TACC3/ch-TOG/clathrin inter-microtubule bridges." Communicative & integrative biology **4**(4): 409-412.
Chen, J.-R., L. I. Plotkin, J. I. Aguirre, L. Han, R. L. Jilka, S. Kousteni, T. Bellido and S. C. Manolagas (2005). "Transient versus sustained phosphorylation and nuclear accumulation of ERKs underlie anti-versus pro-apoptotic effects of estrogens." Journal of Biological Chemistry **280**(6): 4632-4638.
Choy, M. S., M. Hieke, G. S. Kumar, G. R. Lewis, K. R. Gonzalez-DeWhitt, R. P. Kessler, B. J. Stein, M. Hessenberger, A. C. Nairn and W. Peti (2014). "Understanding the antagonism of retinoblastoma protein dephosphorylation by PNUTS provides insights into the PP1 regulatory code." Proceedings of the National Academy of Sciences **111**(11): 4097-4102.
Cohen, P. T. (1997). "Novel protein serine/threonine phosphatases: variety is the spice of life." Trends Biochem Sci **22**(7): 245-251.
Cohen, P. T. (2002). "Protein phosphatase 1--targeted in many directions." J Cell Sci **115**(Pt 2): 241-256.
Cohen, P. T., N. D. Brewis, V. Hughes and D. J. Mann (1990). "Protein serine/threonine phosphatases; an expanding family." FEBS Lett **268**(2): 355-359.
Cohen, P. T. W. (2002). "Protein phosphatase 1 - targeted in many directions." Journal of Cell Science **115**(2): 241-256.
Conte, N., B. Delaval, C. Ginestier, A. Ferrand, D. Isnardon, C. Larroque, C. Prigent, B. Séraphin, J. Jacquemier and D. Birnbaum (2003). "TACC1-chTOG-Aurora A protein complex in breast cancer." Oncogene **22**(50): 8102.
Crooks, G. E., G. Hon, J. M. Chandonia and S. E. Brenner (2004). "WebLogo: a sequence logo generator." Genome Res **14**(6): 1188-1190.
Dephoure, N., K. L. Gould, S. P. Gygi and D. R. Kellogg (2013). "Mapping and analysis of phosphorylation sites: a quick guide for cell biologists." Molecular biology of the cell **24**(5): 535-542.
Dephoure, N., C. Zhou, J. Villen, S. A. Beausoleil, C. E. Bakalarski, S. J. Elledge and S. P. Gygi (2008). "A quantitative atlas of mitotic phosphorylation." Proc Natl Acad Sci U S A **105**(31): 10762-10767.

Ding, Z. M., C. J. Huang, X. F. Jiao, D. Wu and L. J. Huo (2017). "The Role of TACC3 in Mitotic Spindle Organization." Cytoskeleton.
Doxsey, S., W. Zimmerman and K. Mikule (2005). "Centrosome control of the cell cycle." Trends in cell biology **15**(6): 303-311.
Du, Y., L. Liu, C. Wang, B. Kuang, S. Yan, A. Zhou, C. Wen, J. Chen, Y. Wu and X. Yang (2016). "TACC3 promotes colorectal cancer tumourigenesis and correlates with poor prognosis." Oncotarget **7**(27): 41885.
Egloff, M. P., D. F. Johnson, G. Moorhead, P. T. Cohen, P. Cohen and D. Barford (1997). "Structural basis for the recognition of regulatory subunits by the catalytic subunit of protein phosphatase 1." EMBO J **16**(8): 1876-1887.
Enserink, J. M. and R. D. Kolodner (2010). "An overview of Cdk1-controlled targets and processes." Cell division **5**(1): 11.
Ezkurdia, I., D. Juan, J. M. Rodriguez, A. Frankish, M. Diekhans, J. Harrow, J. Vazquez, A. Valencia and M. L. Tress (2014). "Multiple evidence strands suggest that there may be as few as 19 000 human protein-coding genes." Human molecular genetics **23**(22): 5866-5878.
Fischer, E. H., H. Charbonneau and N. K. Tonks (1991). "Protein tyrosine phosphatases: a diverse family of intracellular and transmembrane enzymes." Science **253**(5018): 401-406.
Foraker, A. B., S. M. Camus, T. M. Evans, S. R. Majeed, C.-Y. Chen, S. B. Taner, I. R. Corrêa, S. J. Doxsey and F. M. Brodsky (2012). "Clathrin promotes centrosome integrity in early mitosis through stabilization of centrosomal ch-TOG." J Cell Biol **198**(4): 591-605.
Fuda, N. J., M. S. Buckley, W. Wei, L. J. Core, C. T. Waters, D. Reinberg and J. T. Lis (2012). "Fcp1 dephosphorylation of the RNA polymerase II C-terminal domain is required for efficient transcription of heat shock genes." Molecular and cellular biology **32**(17): 3428-3437.
Fullwood, M. J., W. Zhou and S. Shenolikar (2011). "Targeting phosphorylation of eukaryotic initiation factor-2α to treat human disease." Progress in molecular biology and translational science **106**: 75-106.
Gao, J., B. A. Aksoy, U. Dogrusoz, G. Dresdner, B. Gross, S. O. Sumer, Y. Sun, A. Jacobsen, R. Sinha and E. Larsson (2013). "Integrative analysis of complex cancer genomics and clinical profiles using the cBioPortal." Science signaling **6**(269): pl1.
Gergely, F. (2002). "Centrosomal TACCtics." Bioessays **24**(10): 915-925.
Gergely, F., V. M. Draviam and J. W. Raff (2003). "The ch-TOG/XMAP215 protein is essential for spindle pole organization in human somatic cells." Genes & development **17**(3): 336-341.
Gergely, F., C. Karlsson, I. Still, J. Cowell, J. Kilmartin and J. W. Raff (2000). "The TACC domain identifies a family of centrosomal proteins that can interact with microtubules." Proceedings of the National Academy of Sciences **97**(26): 14352-14357.
Gharbi-Ayachi, A., J.-C. Labbe, A. Burgess, S. Vigneron, J.-M. Strub, E. Brioudes, A. Van-Dorsselaer, A. Castro and T. Lorca (2010). "The Substrate of Greatwall Kinase, Arpp19, Controls Mitosis by Inhibiting Protein Phosphatase 2A." Science **330**(6011): 1673-1677.
Gibbons, J. A., D. C. Weiser and S. Shenolikar (2005). "Importance of a surface hydrophobic pocket on protein phosphatase-1 catalytic subunit in recognizing cellular regulators." Journal of Biological Chemistry **280**(16): 15903-15911.
Goldberg, J., H. B. Huang, Y. G. Kwon, P. Greengard, A. C. Nairn and J. Kuriyan (1995). "3-DIMENSIONAL STRUCTURE OF THE CATALYTIC SUBUNIT OF PROTEIN SERINE/THREONINE PHOSPHATASE-1." Nature **376**(6543): 745-753.

Guan, K. L. and J. E. Dixon (1991). "Evidence for protein-tyrosine-phosphatase catalysis proceeding via a cysteine-phosphate intermediate." J Biol Chem **266**(26): 17026-17030.
Gutiérrez-Caballero, C., S. G. Burgess, R. Bayliss and S. J. Royle (2015). "TACC3–ch-TOG track the growing tips of microtubules independently of clathrin and Aurora-A phosphorylation." Biology open: BIO201410843.
Ha, G.-H., J.-L. Kim and E.-K. Y. Breuer (2013). "TACC3 is essential for EGF-mediated EMT in cervical cancer." PloS one **8**(8): e70353.
Hanahan, D. and R. A. Weinberg (2000). "The Hallmarks of Cancer." Cell **100**(1): 57-70.
Harrington, D. (2005). "Linear rank tests in survival analysis." Encyclopedia of biostatistics.
Hartwell, L. H. and T. A. Weinert (1989). "Checkpoints: controls that ensure the order of cell cycle events." Science **246**(4930): 629-634.
He, J.-c., W. Yao, J.-m. Wang, P. Schemmer, Y. Yang, Y. Liu, Y.-w. Qian, W.-p. Qi, J. Zhang and Q. Shen (2016). "TACC3 overexpression in cholangiocarcinoma correlates with poor prognosis and is a potential anti-cancer molecular drug target for HDAC inhibitors." Oncotarget **7**(46): 75441.
Hendrickx, A., M. Beullens, H. Ceulemans, T. Den Abt, A. Van Eynde, E. Nicolaescu, B. Lesage and M. Bollen (2009). "Docking motif-guided mapping of the interactome of protein phosphatase-1." Chem Biol **16**(4): 365-371.
Holmfeldt, P., S. Stenmark and M. Gullberg (2004). "Differential functional interplay of TOGp/XMAP215 and the KinI kinesin MCAK during interphase and mitosis." The EMBO journal **23**(3): 627-637.
Honkanen, R. E. and T. Golden (2002). "Regulators of serine/threonine protein phosphatases at the dawn of a clinical era?" Curr Med Chem **9**(22): 2055-2075.
Hood, F. E. and S. J. Royle (2011). "Pulling it together: The mitotic function of TACC3." Bioarchitecture **1**(3): 105-109.
Hubner, N. C., A. W. Bird, J. Cox, B. Splettstoesser, P. Bandilla, I. Poser, A. Hyman and M. Mann (2010). "Quantitative proteomics combined with BAC TransgeneOmics reveals in vivo protein interactions." The Journal of cell biology **189**(4): 739-754.
Hunt, T. (2002). "Nobel Lecture. Protein synthesis, proteolysis, and cell cycle transitions." Biosci Rep **22**(5-6): 465-486.
Hurley, T. D., J. Yang, L. Zhang, K. D. Goodwin, Q. Zou, M. Cortese, A. K. Dunker and A. A. DePaoli-Roach (2007). "Structural basis for regulation of protein phosphatase 1 by inhibitor-2." J Biol Chem **282**(39): 28874-28883.
Ingebritsen, T. S. and P. Cohen (1983). "Protein phosphatases: properties and role in cellular regulation." Science **221**(4608): 331-338.
Jeng, J.-C., Y.-M. Lin, C.-H. Lin and H.-M. Shih (2009). "Cdh1 controls the stability of TACC3." Cell Cycle **8**(21): 3537-3544.
Jiang, F., B. Kuang, Y. Que, Z. Lin, L. Yuan, W. Xiao, R. Peng, X. Zhang and X. Zhang (2016). "The clinical significance of transforming acidic coiled-coil protein 3 expression in non-small cell lung cancer." Oncology reports **35**(1): 436-446.
Karsenti, E. and I. Vernos (2001). "The mitotic spindle: a self-made machine." Science **294**(5542): 543-547.
Kerk, D., G. Templeton and G. B. Moorhead (2008). "Evolutionary radiation pattern of novel protein phosphatases revealed by analysis of protein data from the completely sequenced genomes of humans, green algae, and higher plants." Plant Physiol **146**(2): 351-367.

Kettenbach, A. N., D. K. Schweppe, B. K. Faherty, D. Pechenick, A. A. Pletnev and S. A. Gerber (2011). "Quantitative phosphoproteomics identifies substrates and functional modules of Aurora and Polo-like kinase activities in mitotic cells." Sci Signal **4**(179): rs5.
Khandelwal, R. L. and J. H. Wang (2012). Reversible Protein Phosphorylation in Cell Regulation, Springer Science & Business Media.
Khoury, G. A., R. C. Baliban and C. A. Floudas (2011). "Proteome-wide post-translational modification statistics: frequency analysis and curation of the swiss-prot database." Scientific reports **1**: 90.
Kinoshita, K., T. L. Noetzel, L. Pelletier, K. Mechtler, D. N. Drechsel, A. Schwager, M. Lee, J. W. Raff and A. A. Hyman (2005). "Aurora A phosphorylation of TACC3/maskin is required for centrosome-dependent microtubule assembly in mitosis." J Cell Biol **170**(7): 1047-1055.
Klammer, M., M. Kaminski, A. Zedler, F. Oppermann, S. Blencke, S. Marx, S. Müller, A. Tebbe, K. Godl and C. Schaab (2012). "Phosphosignature predicts dasatinib response in non-small cell lung cancer." Molecular & Cellular Proteomics **11**(9): 651-668.
Kollman, J. M., J. K. Polka, A. Zelter, T. N. Davis and D. A. Agard (2010). "Microtubule nucleating γTuSC assembles structures with 13-fold microtubule-like symmetry." Nature **466**(7308): 879.
Krenn, V. and A. Musacchio (2015). "The Aurora B Kinase in Chromosome Bi-Orientation and Spindle Checkpoint Signaling." Front Oncol **5**: 225.
Lauffart, B., M. M. Vaughan, R. Eddy, D. Chervinsky, R. A. DiCioccio, J. D. Black and I. H. Still (2005). "Aberrations of TACC1 and TACC3 are associated with ovarian cancer." BMC women's health **5**(1): 8.
Lee, M. J., F. Gergely, K. Jeffers, S. Y. Peak-Chew and J. W. Raff (2001). "Msps/XMAP215 interacts with the centrosomal protein D-TACC to regulate microtubule behaviour." Nature cell biology **3**(7): 643.
LeRoy, P. J., J. J. Hunter, K. M. Hoar, K. E. Burke, V. Shinde, J. Ruan, D. Bowman, K. Galvin and J. A. Ecsedy (2007). "Localization of human TACC3 to mitotic spindles is mediated by phosphorylation on Ser558 by Aurora A: a novel pharmacodynamic method for measuring Aurora A activity." Cancer research **67**(11): 5362-5370.
Lesage, B., J. Qian and M. Bollen (2011). "Spindle checkpoint silencing: PP1 tips the balance." Curr Biol **21**(21): R898-903.
Li, J., C. Yen, D. Liaw, K. Podsypanina, S. Bose, S. I. Wang, J. Puc, C. Miliaresis, L. Rodgers and R. McCombie (1997). "PTEN, a putative protein tyrosine phosphatase gene mutated in human brain, breast, and prostate cancer." science **275**(5308): 1943-1947.
Li, Q., L. Ye, W. Guo, M. Wang, S. Huang and X. Peng (2017). "Overexpression of TACC3 is correlated with tumor aggressiveness and poor prognosis in prostate cancer." Biochemical and Biophysical Research Communications **486**(4): 872-878.
Lin, C.-H., C.-K. Hu and H.-M. Shih (2010). "Clathrin heavy chain mediates TACC3 targeting to mitotic spindles to ensure spindle stability." The Journal of cell biology **189**(7): 1097-1105.
Lindqvist, A., V. Rodriguez-Bravo and R. H. Medema (2009). "The decision to enter mitosis: feedback and redundancy in the mitotic entry network." Journal of Cell Biology **185**(2): 193-202.
Liu, D., M. Vleugel, C. B. Backer, T. Hori, T. Fukagawa, I. M. Cheeseman and M. A. Lampson (2010). "Regulated targeting of protein phosphatase 1 to the outer kinetochore by KNL1 opposes Aurora B kinase." J Cell Biol **188**(6): 809-820.

Liu, Y., A. Beyer and R. Aebersold (2016). "On the dependency of cellular protein levels on mRNA abundance." Cell **165**(3): 535-550.
Ma, M. P., P. J. Robinson and M. Chircop (2013). "Sorting nexin 9 recruits clathrin heavy chain to the mitotic spindle for chromosome alignment and segregation." PloS one **8**(7): e68387.
Mann, M. and O. N. Jensen (2003). "Proteomic analysis of post-translational modifications." Nature biotechnology **21**(3): 255-261.
McManus, J., Z. Cheng and C. Vogel (2015). "Next-generation analysis of gene expression regulation–comparing the roles of synthesis and degradation." Molecular BioSystems **11**(10): 2680-2689.
Mertins, P., D. Mani, K. V. Ruggles, M. A. Gillette, K. R. Clauser, P. Wang, X. Wang, J. W. Qiao, S. Cao and F. Petralia (2016). "Proteogenomics connects somatic mutations to signaling in breast cancer." Nature **534**(7605): 55.
Mertins, P., J. W. Qiao, J. Patel, N. D. Udeshi, K. R. Clauser, D. Mani, M. W. Burgess, M. A. Gillette, J. D. Jaffe and S. A. Carr (2013). "Integrated proteomic analysis of post-translational modifications by serial enrichment." Nature methods **10**(7): 634-637.
Mertins, P., F. Yang, T. Liu, D. Mani, V. A. Petyuk, M. A. Gillette, K. R. Clauser, J. W. Qiao, M. A. Gritsenko and R. J. Moore (2014). "Ischemia in tumors induces early and sustained phosphorylation changes in stress kinase pathways but does not affect global protein levels." Molecular & cellular proteomics **13**(7): 1690-1704.
Miller, M. L., S. Brunak, J. Olsen, M. Vermeulen, A. Santamaria, C. Kumar, L. Jensen, F. Gnad, J. Cox and T. S. Jensen (2010). "Quantitative phosphoproteomics reveals widespread full phosphorylation site occupancy during mitosis." Science Signaling **3**(104).
Mochida, S., S. L. Maslen, M. Skehel and T. Hunt (2010). "Greatwall Phosphorylates an Inhibitor of Protein Phosphatase 2A That Is Essential for Mitosis." Science **330**(6011): 1670-1673.
Mollapour, M., S. Tsutsumi, A. W. Truman, W. Xu, C. K. Vaughan, K. Beebe, A. Konstantinova, S. Vourganti, B. Panaretou and P. W. Piper (2011). "Threonine 22 phosphorylation attenuates Hsp90 interaction with cochaperones and affects its chaperone activity." Molecular cell **41**(6): 672-681.
Moorhead, G., R. W. MacKintosh, N. Morrice, T. Gallagher and C. MacKintosh (1994). "Purification of type 1 protein (serine/threonine) phosphatases by microcystin-Sepharose affinity chromatography." FEBS Lett **356**(1): 46-50.
Moorhead, G. B., V. De Wever, G. Templeton and D. Kerk (2009). "Evolution of protein phosphatases in plants and animals." Biochemical Journal **417**(2): 401-409.
Moorhead, G. B., L. Trinkle-Mulcahy and A. Ulke-Lemee (2007). "Emerging roles of nuclear protein phosphatases." Nat Rev Mol Cell Biol **8**(3): 234-244.
Morgan, D. O. (1995). "Principles of CDK regulation." Nature **374**(6518): 131-134.
Morgan, D. O. (1997). "Cyclin-dependent kinases: engines, clocks, and microprocessors." Annual review of cell and developmental biology **13**(1): 261-291.
Morgan, D. O. (2007). The cell cycle: principles of control, New Science Press.
Morgan, N. G. (1989). Cell signalling, Open University Press Milton Keynes.
Mori, D., Y. Yano, K. Toyo-Oka, N. Yoshida, M. Yamada, M. Muramatsu, D. Zhang, H. Saya, Y. Y. Toyoshima and K. Kinoshita (2007). "NDEL1 phosphorylation by Aurora-A kinase is essential for centrosomal maturation, separation, and TACC3 recruitment." Molecular and cellular biology **27**(1): 352-367.

Mueller, P. R., T. R. Coleman, A. Kumagai and W. G. Dunphy (1995). "Myt1: a membrane-associated inhibitory kinase that phosphorylates Cdc2 on both threonine-14 and tyrosine-15." Science **270**(5233): 86-90.
Nigg, E. A. (2001). "Mitotic kinases as regulators of cell division and its checkpoints." Nature Reviews Molecular Cell Biology **2**(1): 21-32.
Nixon, F. M., C. Gutiérrez-Caballero, F. E. Hood, D. G. Booth, I. A. Prior and S. J. Royle (2015). "The mesh is a network of microtubule connectors that stabilizes individual kinetochore fibers of the mitotic spindle." Elife **4**: e07635.
Nogales, E. and V. H. Ramey (2009). "Structure-function insights into the yeast Dam1 kinetochore complex." J Cell Sci **122**(21): 3831-3836.
Nogales, E., M. Whittaker, R. A. Milligan and K. H. Downing (1999). "High-resolution model of the microtubule." Cell **96**(1): 79-88.
Nousiainen, M., H. H. Sillje, G. Sauer, E. A. Nigg and R. Korner (2006). "Phosphoproteome analysis of the human mitotic spindle." Proc Natl Acad Sci U S A **103**(14): 5391-5396.
Nwagbara, B. U., A. E. Faris, E. A. Bearce, B. Erdogan, P. T. Ebbert, M. F. Evans, E. L. Rutherford, T. B. Enzenbacher and L. A. Lowery (2014). "TACC3 is a microtubule plus end-tracking protein that promotes axon elongation and also regulates microtubule plus end dynamics in multiple embryonic cell types." Mol Biol Cell **25**(21): 3350-3362.
O'Brien, L. L., A. J. Albee, L. Liu, W. Tao, P. Dobrzyn, S. B. Lizarraga and C. Wiese (2005). "The Xenopus TACC homologue, maskin, functions in mitotic spindle assembly." Molecular biology of the cell **16**(6): 2836-2847.
O'Connell, C. B. and A. L. Khodjakov (2007). "Cooperative mechanisms of mitotic spindle formation." Journal of cell science **120**(10): 1717-1722.
O'Connell, N., S. R. Nichols, E. Heroes, M. Beullens, M. Bollen, W. Peti and R. Page (2012). "The molecular basis for substrate specificity of the nuclear NIPP1: PP1 holoenzyme." Structure **20**(10): 1746-1756.
O'Connor, C. (2008). "Cell division: Stages of mitosis." Nature Education **1**(1): 188.
O'Farrell, P. H. (2001). "Triggering the all-or-nothing switch into mitosis." Trends in Cell Biology **11**(12): 512-519.
O'Regan, L., J. Sampson, M. W. Richards, A. Knebel, D. Roth, F. E. Hood, A. Straube, S. J. Royle, R. Bayliss and A. M. Fry (2015). "Hsp72 is targeted to the mitotic spindle by Nek6 to promote K-fiber assembly and mitotic progression." J Cell Biol **209**(3): 349-358.
Obaya, A. J. and J. M. Sedivy (2002). "Regulation of cyclin-Cdk activity in mammalian cells." Cell Mol Life Sci **59**(1): 126-142.
Olsen, J. V., B. Blagoev, F. Gnad, B. Macek, C. Kumar, P. Mortensen and M. Mann (2006). "Global, in vivo, and site-specific phosphorylation dynamics in signaling networks." Cell **127**(3): 635-648.
Olsen, J. V., M. Vermeulen, A. Santamaria, C. Kumar, M. L. Miller, L. J. Jensen, F. Gnad, J. Cox, T. S. Jensen, E. A. Nigg, S. Brunak and M. Mann (2010). "Quantitative phosphoproteomics reveals widespread full phosphorylation site occupancy during mitosis." Sci Signal **3**(104): ra3.
Parker, B. C., M. J. Annala, D. E. Cogdell, K. J. Granberg, Y. Sun, P. Ji, X. Li, J. Gumin, H. Zheng and L. Hu (2013). "The tumorigenic FGFR3-TACC3 gene fusion escapes miR-99a regulation in glioblastoma." The Journal of clinical investigation **123**(2): 855.

Peset, I., J. Seiler, T. Sardon, L. A. Bejarano, S. Rybina and I. Vernos (2005). "Function and regulation of Maskin, a TACC family protein, in microtubule growth during mitosis." J Cell Biol **170**(7): 1057-1066.
Peset, I. and I. Vernos (2008). "The TACC proteins: TACC-ling microtubule dynamics and centrosome function." Trends in cell biology **18**(8): 379-388.
Peters, D. G., D. M. Kudla, J. A. DeLoia, T. J. Chu, L. Fairfull, R. P. Edwards and R. E. Ferrell (2005). "Comparative gene expression analysis of ovarian carcinoma and normal ovarian epithelium by serial analysis of gene expression." Cancer Epidemiology and Prevention Biomarkers **14**(7): 1717-1723.
Petersen, B. O., J. Lukas, C. S. Sørensen, J. Bartek and K. Helin (1999). "Phosphorylation of mammalian CDC6 by cyclin A/CDK2 regulates its subcellular localization." The EMBO Journal **18**(2): 396-410.
Petschnigg, J., M. Kotlyar, L. Blair, I. Jurisica, I. Stagljar and R. Ketteler (2017). "Systematic identification of oncogenic EGFR interaction partners." Journal of molecular biology **429**(2): 280-294.
Piekorz, R. P., A. Hoffmeyer, C. D. Duntsch, C. McKay, H. Nakajima, V. Sexl, L. Snyder, J. Rehg and J. N. Ihle (2002). "The centrosomal protein TACC3 is essential for hematopoietic stem cell function and genetically interfaces with p53-regulated apoptosis." The EMBO journal **21**(4): 653-664.
Pinheiro, A. S., J. A. Marsh, J. D. Forman-Kay and W. Peti (2010). "Structural Signature of the MYPT1− PP1 Interaction." Journal of the American Chemical Society **133**(1): 73-80.
Pinsky, B. A., C. R. Nelson and S. Biggins (2009). "Protein phosphatase 1 regulates exit from the spindle checkpoint in budding yeast." Curr Biol **19**(14): 1182-1187.
Potapova, T. A., S. Sivakumar, J. N. Flynn, R. Li and G. J. Gorbsky (2011). "Mitotic progression becomes irreversible in prometaphase and collapses when Wee1 and Cdc25 are inhibited." Molecular biology of the cell **22**(8): 1191-1206.
Reimand, J., O. Wagih and G. D. Bader (2013). "The mutational landscape of phosphorylation signaling in cancer." Scientific reports **3**: 2651.
Rosenberg, J. S., F. R. Cross and H. Funabiki (2011). "KNL1/Spc105 recruits PP1 to silence the spindle assembly checkpoint." Curr Biol **21**(11): 942-947.
Royle, S. J. (2006). "The cellular functions of clathrin." Cellular and molecular life sciences **63**(16): 1823-1832.
Royle, S. J. (2012). "The role of clathrin in mitotic spindle organisation." J Cell Sci **125**(1): 19-28.
Royle, S. J., N. A. Bright and L. Lagnado (2005). "Clathrin is required for the function of the mitotic spindle." Nature **434**(7037): 1152.
Royle, S. J. and L. Lagnado (2006). "Trimerisation is important for the function of clathrin at the mitotic spindle." Journal of cell science **119**(19): 4071-4078.
Russell, P. and P. Nurse (1986). "cdc25+ functions as an inducer in the mitotic control of fission yeast." Cell **45**(1): 145-153.
Saxton, W. M., D. L. Stemple, R. J. Leslie, E. D. Salmon, M. Zavortink and J. R. McIntosh (1984). "Tubulin dynamics in cultured mammalian cells." The Journal of cell biology **99**(6): 2175-2186.

Schneider, L., F. Essmann, A. Kletke, P. Rio, H. Hanenberg, K. Schulze-Osthoff, B. Nürnberg and R. Piekorz (2008). "TACC3 depletion sensitizes to paclitaxel-induced cell death and overrides p21WAF-mediated cell cycle arrest." Oncogene **27**(1): 116.
Schneider, L., F. Essmann, A. Kletke, P. Rio, H. Hanenberg, W. Wetzel, K. Schulze-Osthoff, B. Nürnberg and R. P. Piekorz (2007). "The transforming acidic coiled coil 3 protein is essential for spindle-dependent chromosome alignment and mitotic survival." Journal of Biological Chemistry **282**(40): 29273-29283.
Schrodinger, LLC (2015). The PyMOL Molecular Graphics System, Version 1.8.
Sharma, K., R. C. D'Souza, S. Tyanova, C. Schaab, J. R. Wisniewski, J. Cox and M. Mann (2014). "Ultradeep human phosphoproteome reveals a distinct regulatory nature of Tyr and Ser/Thr-based signaling." Cell Rep **8**(5): 1583-1594.
Sharrocks, A. D., S.-H. Yang and A. Galanis (2000). "Docking domains and substrate-specificity determination for MAP kinases." Trends in biochemical sciences **25**(9): 448-453.
Shi, Y. G. (2009). "Serine/Threonine Phosphatases: Mechanism through Structure." Cell **139**(3): 468-484.
Sievers, F., A. Wilm, D. Dineen, T. J. Gibson, K. Karplus, W. Li, R. Lopez, H. McWilliam, M. Remmert and J. Söding (2011). "Fast, scalable generation of high-quality protein multiple sequence alignments using Clustal Omega." Molecular systems biology **7**(1): 539.
Singh, D., J. M. Chan, P. Zoppoli, F. Niola, R. Sullivan, A. Castano, E. M. Liu, J. Reichel, P. Porrati and S. Pellegatta (2012). "Transforming fusions of FGFR and TACC genes in human glioblastoma." Science **337**(6099): 1231-1235.
Singh, P., G. E. Thomas, K. K. Gireesh and T. K. Manna (2014). "TACC3 protein regulates microtubule nucleation by affecting γ-tubulin ring complexes." Journal of Biological Chemistry **289**(46): 31719-31735.
Spruance, S. L., J. E. Reid, M. Grace and M. Samore (2004). "Hazard ratio in clinical trials." Antimicrobial agents and chemotherapy **48**(8): 2787-2792.
StatisticsCanada. (March 19, 2017). "The 10 leading causes of death, 2013." Retrieved October, 26, 2017, from http://www.statcan.gc.ca/pub/82-625-x/2017001/article/14776-eng.htm.
Stewart, J. P., A. Thompson, M. Santra, B. Barlogie, T. R. Lappin and J. Shaughnessy (2004). "Correlation of TACC3, FGFR3, MMSET and p21 expression with the t (4; 14)(p16· 3; q32) in multiple myeloma." British journal of haematology **126**(1): 72-76.
Still, I. H., M. Hamilton, P. Vince, A. Wolfman and J. K. Cowell (1999). "Cloning of TACC1, an embryonically expressed, potentially transforming coiled coil containing gene, from the 8p11 breast cancer amplicon." Oncogene **18**(27).
Still, I. H., A. K. Vettaikkorumakankauv, A. DiMatteo and P. Liang (2004). "Structure-function evolution of the transforming acidic coiled coil genes revealed by analysis of phylogenetically diverse organisms." BMC evolutionary biology **4**(1): 16.
Still, I. H., P. Vince and J. K. Cowell (1999). "The third member of the transforming acidic coiled coil-containing gene family, TACC3, maps in 4p16, close to translocation breakpoints in multiple myeloma, and is upregulated in various cancer cell lines." Genomics **58**(2): 165-170.
Suhail, T. V., P. Singh and T. K. Manna (2015). "Suppression of centrosome protein TACC3 induces G1 arrest and cell death through activation of p38–p53–p21 stress signaling pathway." European journal of cell biology **94**(2): 90-100.
Sun, Y., Y. Tian, G.-Z. Wang, S.-H. Zhao, B. Han, Y.-L. Li and C.-L. Jiang (2017). "Overexpression of Transforming Acidic Coiled Coil-Containing Protein 3 Reflects Malignant

Characteristics and Poor Prognosis of Glioma." International journal of molecular sciences **18**(3): 235.
Tanenbaum, M. E., T. Vallenius, E. F. Geers, L. Greene, T. P. Mäkelä and R. H. Medema (2010). "Cyclin G-associated kinase promotes microtubule outgrowth from chromosomes during spindle assembly." Chromosoma **119**(4): 415-424.
Templeton, G. W., M. Nimick, N. Morrice, D. Campbell, M. Goudreault, A.-C. Gingras, A. Takemiya, K.-i. Shimazaki and G. B. Moorhead (2011). "Identification and characterization of AtI-2, an Arabidopsis homologue of an ancient protein phosphatase 1 (PP1) regulatory subunit." Biochemical Journal **435**(1): 73-83.
Terrak, M., F. Kerff, K. Langsetmo, T. Tao and R. Dominguez (2004). "Structural basis of protein phosphatase 1 regulation." Nature **429**(6993): 780-784.
Thakur, H. C., M. Singh, L. Nagel-Steger, D. Prumbaum, E. K. Fansa, L. Gremer, H. Ezzahoini, A. Abts, L. Schmitt and S. Raunser (2013). "Role of centrosomal adaptor proteins of the TACC family in the regulation of microtubule dynamics during mitotic cell division." Biological chemistry **394**(11): 1411-1423.
Trinkle-Mulcahy, L., J. Chusainow, Y. W. Lam, S. Swift and A. Lamond (2007). "Visualization of intracellular PP1 targeting through transiently and stably expressed fluorescent protein fusions." Methods Mol Biol **365**: 133-154.
Uhrig, R. G., A.-M. Labandera and G. B. Moorhead (2013). "Arabidopsis PPP family of serine/threonine protein phosphatases: many targets but few engines." Trends in plant science **18**(9): 505-513.
Ulisse, S., E. Baldini, M. Toller, J.-G. Delcros, A. Gueho, F. Curcio, E. De Antoni, L. Giacomelli, F. S. Ambesi-Impiombato and S. Bocchini (2007). "Transforming acidic coiled-coil 3 and Aurora-A interact in human thyrocytes and their expression is deregulated in thyroid cancer tissues." Endocrine-related cancer **14**(3): 827-837.
Wakula, P., M. Beullens, H. Ceulemans, W. Stalmans and M. Bollen (2003). "Degeneracy and function of the ubiquitous RVXF motif that mediates binding to protein phosphatase-1." Journal of Biological Chemistry **278**(21): 18817-18823.
Walczak, C. E. and R. Heald (2008). "Chapter Three-Mechanisms of Mitotic Spindle Assembly and Function." International review of cytology **265**: 111-158.
Wang, B., P. Zhang and Q. Wei (2008). "Recent progress on the structure of Ser/Thr protein phosphatases." Sci China C Life Sci **51**(6): 487-494.
Wilson, H. (1969). "Arms and bridges on microtubules in the mitotic apparatus." The Journal of cell biology **40**(3): 854.
Wittmann, T., A. Hyman and A. Desai (2001). "The spindle: a dynamic assembly of microtubules and motors." Nature cell biology **3**(1): E28.
Wu, J. Q., J. Y. Guo, W. Tang, C. S. Yang, C. D. Freel, C. Chen, A. C. Nairn and S. Kornbluth (2009). "PP1-mediated dephosphorylation of phosphoproteins at mitotic exit is controlled by inhibitor-1 and PP1 phosphorylation." Nat Cell Biol **11**(5): 644-651.
Yanagida, M., N. Kinoshita, E. M. Stone and H. Yamano (1992). "Protein phosphatases and cell division cycle control." Ciba Found Symp **170**: 130-140; discussion 140-136.
Yao, R., Y. Kondoh, Y. Natsume, H. Yamanaka, M. Inoue, H. Toki, R. Takagi, T. Shimizu, T. Yamori and H. Osada (2014). "A small compound targeting TACC3 revealed its different spatiotemporal contributions for spindle assembly in cancer cells." Oncogene **33**(33): 4242.

Yao, R., Y. Natsume and T. Noda (2007). "TACC3 is required for the proper mitosis of sclerotome mesenchymal cells during formation of the axial skeleton." Cancer science **98**(4): 555-562.
Yu, L.-R., Z. Zhu, K. C. Chan, H. J. Issaq, D. S. Dimitrov and T. D. Veenstra (2007). "Improved titanium dioxide enrichment of phosphopeptides from HeLa cells and high confident phosphopeptide identification by cross-validation of MS/MS and MS/MS/MS spectra." Journal of proteome research **6**(11): 4150-4162.
Yuan, L., Z.-H. Liu, Z.-R. Lin, L.-H. Xu, Q. Zhong and M.-S. Zeng (2014). "Recurrent FGFR3-TACC3 fusion gene in nasopharyngeal carcinoma." Cancer biology & therapy **15**(12): 1613-1621.
Yun, M., J. Rong, Z.-R. Lin, Y.-L. He, J.-X. Zhang, Z.-W. Peng, L.-Q. Tang, M.-S. Zeng, Q. Zhong and S. Ye (2015). "High expression of transforming acidic coiled coil-containing protein 3 strongly correlates with aggressive characteristics and poor prognosis of gastric cancer." Oncology reports **34**(3): 1397-1405.
Zheng, Y., M. L. Wong, B. Alberts and T. Mitchison (1995). "Nucleation of microtubule assembly by a gamma-tubulin-containing ring complex." Nature **378**(6557): 578.